FEDERAL UNIVERSITY OF ESPÍRITO SANTO

TECHNOLOGICAL CENTER

ENVIRONMENTAL ENGINEERING GRADUATE PROGRAM

Evaluation of nanotechnological processes applied to the harvesting of microalgae biomass

Vitória – ES

2023

FEDERAL UNIVERSITY OF ESPÍRITO SANTO

TECHNOLOGICAL CENTER

ENVIRONMENTAL ENGINEERING GRADUATE PROGRAM

Evaluation of nanotechnological processes applied to the harvesting of microalgae biomass

ANA CAROLINA DE LIMA BARIZÃO

Thesis presented to the Environmental Engineering Graduate Program, from the Technological Center of the Federal University of Espírito Santo, as a requirement for obtaining the title of Doctor in Environmental Engineering.

Advisor: Prof. Dr. Sérvio Túlio Alves Cassini
Co-advisor: Prof. Dr. Jairo Pinto de Oliveira

Vitória – ES

2023

Ficha catalográfica disponibilizada pelo Sistema Integrado de Bibliotecas - SIBI/UFES e elaborada pelo autor

---

de Lima Barizão, Ana Carolina, 1993-
D278e Evaluation of nanotechnological processes applied to the harvesting of microalgae biomass / Ana Carolina de Lima Barizão. - 2023.
131 f. : il.

Orientador: Sérvio Túlio Alves Cassini.
Coorientador: Jairo Pinto de Oliveira.
Tese (Doutorado em Engenharia Ambiental) - Universidade Federal do Espírito Santo, Centro Tecnológico.

1. Biotecnologia. 2. Nanotecnologia. 3. Nanopartículas. 4. Magnetismo. 5. Taninos. 6. Ferro. I. Alves Cassini, Sérvio Túlio. II. Pinto de Oliveira, Jairo. III. Universidade Federal do Espírito Santo. Centro Tecnológico. IV. Título.

CDU: 628

UNIVERSIDADE FEDERAL DO ESPÍRITO SANTO
CENTRO TECNOLÓGICO
PROGRAMA DE PÓS-GRADUAÇÃO EM ENGENHARIA AMBIENTAL

Ata da Septuagésima (70ª) Sessão de Defesa de Tese de Doutorado do Programa de Pós-Graduação em Engenharia Ambiental (PPGEA) do Centro Tecnológico (CT) da Universidade Federal do Espírito Santo (UFES), da aluna **Ana Carolina de Lima Barizão**, candidata ao grau de Doutora em Engenharia Ambiental.

Às catorze horas do dia vinte e cinco de julho de dois mil e vinte e três (25/07/2023), por videoconferência, Universidade Federal do Espírito Santo. O Prof. Dr. Sérvio Túlio Alves Cassini, presidindo a Sessão, deu início aos trabalhos apresentando ao público presente à candidata **Ana Carolina de Lima Barizão** e a banca examinadora da tese, composta pelos seguintes membros: Prof. Dr. Jairo Oliveira – Coorientador – PPGBIOTEC/UFES, Prof.ª Dr. ª Regina Pinho Keller – Examinadora Interna – PPGEA/CT/UFES, Prof.ª Dr.ª Laura Marina Pinotti – Examinadora Interna – PPGEN/UFES, Prof. Dr. André Romero da Silva – Examinador Externo – EDUCIMAT/IFES e Prof. Dr. Paulo Wagnner Pereira Antunes – Examinador Externo – BIOGEN. O Senhor Presidente da Banca Examinadora, Prof. Dr. Sérvio Túlio Alves Cassini passou em seguida a palavra à discente que em quarenta minutos apresentou a Tese intitulada: **"AVALIAÇÃO DE PROCESSOS NANOTECNOLÓGICOS APLICADOS À COLHEITA DE BIOMASSA DE MICROALGAS"**. Dando prosseguimento aos trabalhos de defesa da tese, o Senhor Presidente convidou os membros titulares da Banca Examinadora a tomarem assento à mesa, passando a palavra aos membros da Banca, um a um, iniciando os comentários de arguição da candidata com os examinadores externos. Após, o Senhor Presidente teceu comentários sobre o trabalho da candidata e franqueou a palavra ao público presente. Findada a arguição, o Senhor Presidente convidou a Banca Examinadora se reunir em separado, para deliberação. Ao retornar, o Senhor Presidente informou ao público presente a decisão da banca que resultou na APROVAÇÃO da examinada. Por fim, o presidente da sessão alertou que a aprovada somente terá direito ao título de Doutora em Engenharia Ambiental após entrega da versão final de sua tese em meio digital à Secretária do Programa com as correções apontadas pela banca, cumpridos todos os trâmites exigidos pelo Regimento do PPGEA e da homologação do resultado da defesa pelo Colegiado Acadêmico do PPGEA. Por fim, declarou encerrada a sessão, e eu, Sérvio Túlio Alves Cassini, Professor do Programa de Pós-Graduação em Engenharia Ambiental, do Centro Tecnológico, lavrei a presente ata, que irá assinada pelos membros da Banca Examinadora e pela doutoranda.

Prof. Dr. Sérvio Túlio Alves Cassini
Orientador - PPGEA/CT/UFES

Prof. Dr. Jairo Oliveira
Coorientador – PPGBIOTEC/UFES

Prof.ª Dr. ª Regina Pinho Keller
Examinadora Interna – PPGEA/CT/UFES

Prof.ª Dr. ª Laura Marina Pinotti
Examinadora Interna – PPGEN/ UFES

Prof. Dr. André Romero da Silva
Examinador – EDUCIMAT/IFES

Prof. Dr. Paulo Wagnner Pereira Antunes
Examinador Externo – BIOGEN

Ana Carolina de Lima Barizão
Doutoranda

Vitória/ES, 25 de julho de 2023

UNIVERSIDADE FEDERAL DO ESPÍRITO SANTO
CENTRO TECNOLÓGICO
PROGRAMA DE PÓS-GRADUAÇÃO EM ENGENHARIA AMBIENTAL

AVALIAÇÃO DE PROCESSOS NANOTECNOLÓGICOS APLICADOS À COLHEITA DE BIOMASSA DE MICROALGAS

Ana Carolina de Lima Barizão

Banca Examinadora:

_____
Prof. Dr. Sérvio Túlio Alves Cassini
Orientador - PPGEA/CT/UFES

_____
Prof. Dr. Jairo Oliveira
Coorientador – PPGBIOTEC/UFES

_____
Prof.ª Dr. ª Regina Pinho Keller
Examinadora Interna – PPGEA/CT/UFES

_____
Prof.ª Dr. ª Laura Marina Pinotti
Examinadora Interna – PPGEN/UFES

_____
Prof. Dr. André Romero da Silva
Examinador Externo – EDUCIMAT/IFES

_____
Prof. Dr. Paulo Wagnner Pereira Antunes
Examinador Externo – BIOGEN

Elisa Valentim Goulart
Coordenadora do Programa de Pós-Graduação em Engenharia Ambiental
UNIVERSIDADE FEDERAL DO ESPÍRITO SANTO

Vitória/ES, 25 de julho de 2023

Datas e horários baseados em Brasília, Brasil
Sincronizado com o NTP.br e Observatório Nacional (ON) em 03/08/2023 às 19:47:50

DOCS DEFESA ANACAROLINA BARIZÃO PPGEA

Data e Hora de Criação: 01/08/2023 às 12:49:38

Documentos que originaram esse envelope:
- DOCS DEFESA ANA CAROLINA BARIZÃO PPGEA.pdf (Arquivo PDF) - 2 página(s)

Hashs únicas referente à esse envelope de documentos

[SHA256]: 3c4cb3414c3d7235522fb5be3be628d8211c45f2e85f4b84582e538c4f0ed705
[SHA512]: 25a49e408fde034c3103804d45088f9dc0756a22ecc26b7dae1b8534022a53c1631906ab024c173fc0e4da71d3a8e7465e5995de11cb76d6b8bbe05c73c51355

Lista de assinaturas solicitadas e associadas à esse envelope

ASSINADO - Servio Tulio Alves Cassini (servio.cassini@ufes.br)
Data/Hora: 01/08/2023 - 13:01:41, IP: 187.36.165.250, Geolocalização: [-20.330949, -40.295709]
[SHA256]: 77864c4804aa2482e5c994202bf4db225a87a8157f98c3756e84ac13cc657cbe

ASSINADO - aromero@ifes.edu.br
Data/Hora: 01/08/2023 - 20:47:06, IP: 200.150.65.166, Geolocalização: [-25.516650, -54.585805]
[SHA256]: 7139d72b414a717337cded575272decad8dd2f394a6450422666e2db7d961be2

ASSINADO - laura.pinotti@ufes.br
Data/Hora: 01/08/2023 - 21:53:38, IP: 177.174.198.184
[SHA256]: d49057d095f149d01181bb80b24fdf3c111a289c8fd03bec43b977fda1ca5667

ASSINADO - kellygtr@gmail.com
Data/Hora: 02/08/2023 - 16:53:02, IP: 189.40.107.192, Geolocalização: [-7.3324158, -47.473416]
[SHA256]: a13254b2897551b750b8a94d29caf905f28629c9e3859247da2e4646d1c3d482

ASSINADO - pwpantunes@yahoo.com.br
Data/Hora: 03/08/2023 - 19:18:10, IP: 179.241.19.194, Geolocalização: [-23.007383, -47.149922]
[SHA256]: dccf21e0d470f090248ee555db31e5bdcf915582e55dd8063707ca26385aaf1f

ASSINADO - Jairo Pinto De Oliveira (jairo.oliveira@ufes.br)
Data/Hora: 03/08/2023 - 19:47:50, IP: 185.220.89.67, Geolocalização: [51.4857935, -0.1990392]
[SHA256]: 1221470b2de84bacac9627a3d30d62a0d10fc04e3ce1591ac03a35c6500ccc8a

Histórico de eventos registrados neste envelope

03/08/2023 19:47:50 - Envelope finalizado por jairo.oliveira@ufes.br, IP 185.220.89.67
03/08/2023 19:47:50 - Assinatura realizada por jairo.oliveira@ufes.br, IP 185.220.89.67
03/08/2023 19:47:48 - Envelope visualizado por jairo.oliveira@ufes.br, IP 185.220.89.67
03/08/2023 19:18:10 - Assinatura realizada por pwpantunes@yahoo.com.br, IP 179.241.19.194
03/08/2023 19:18:06 - Envelope visualizado por pwpantunes@yahoo.com.br, IP 179.241.19.194
02/08/2023 16:53:02 - Assinatura realizada por kellygtr@gmail.com, IP 189.40.107.192
01/08/2023 21:53:38 - Assinatura realizada por laura.pinotti@ufes.br, IP 177.174.198.184
01/08/2023 20:47:06 - Assinatura realizada por aromero@ifes.edu.br, IP 200.150.65.166
01/08/2023 20:46:52 - Envelope visualizado por aromero@ifes.edu.br, IP 200.150.65.166
01/08/2023 13:01:41 - Assinatura realizada por servio.cassini@ufes.br, IP 187.36.165.250
01/08/2023 13:01:30 - Envelope visualizado por servio.cassini@ufes.br, IP 187.36.165.250
01/08/2023 12:57:52 - Envelope registrado na Blockchain por servio.cassini@ufes.br, IP 187.36.165.250
01/08/2023 12:57:50 - Envelope encaminhado para assinaturas por servio.cassini@ufes.br, IP 187.36.165.250
01/08/2023 12:49:40 - Envelope criado por servio.cassini@ufes.br, IP 187.36.165.250

DEDICATION

I dedicate to my dear son Noah Gomes Barizão.

ACKNOWLEDGMENT

First of all, I would like to thank God for life and also for the people He has placed by my side.

To my family (father, mother, Camila, Gabriel, Luiz, and my dear son Noah), I want to dedicate my sincerest and most heartfelt gratitude. Thank you for all the support and love that have always sustained me on my journey.

I am immensely grateful to my advisor, Prof. Sérvio Túlio, and co-advisor, Prof. Jairo, for their guidance, advice, and knowledge exchange over the past four years. You have been essential to my development as a researcher.

I would also like to thank all the researchers and friends from LACAR and the Laboratory of Functional Nanomaterials (UFES), where I conducted mostly part of my research. Your daily support, assistance in the development of experiments, and the friendships we have built over the years have contributed to my education and made my days happier.

I am grateful to all the partner laboratories that provided their physical space, equipment, and researchers to contribute to the development of this work. Therefore, I especially thank the LUCCAR Laboratory (UFES), LABSAN Laboratory (UFES), Laboratory of Carbonaceous Materials (LMC), and the Nanomedicine and Nanotoxicology Group at the Institute of Physics of UFSCAR.

I would also like to express my gratitude to the members of my evaluation committee, Prof. Dr. André Romero da Silva, Dr. Paulo Wagnner Pereira Antunes, Prof. Dr.ª Laura Marina Pinotti, and Prof. Dr.ª Regina de Pinho Keller, for their availability to evaluate and contribute to my work. It is a pleasure to have your participation.

Finally, I would also like to thank the funding agencies, Coordenação de Aperfeiçoamento de Pessoal de Nível Superior (CAPES), Fundação Estadual de Amparo à Pesquisa do Estado do Espírito Santo (156/2018) and Conselho Nacional de Desenvolvimento Científico e Tecnológico (Cnpq) who financially supported this project, contributing to scholarships, improvement of laboratories and purchase of equipment.

EPIGRAPH

Isso de querer ser exatamente aquilo que a gente é,
ainda vai nos levar além. (P. LEMINSKI).

Contents

ABSTRACT

Microalgae have garnered significant interest due to the diverse applications in the production of biofuels, functional foods, cosmetics, and pharmaceuticals. However, one of the challenges encountered during their production is the harvesting stage, which is often laborious and inefficient. In this context, harvesting using magnetic nanoparticles emerges as a promising technique to overcome these difficulties. Nanoparticles can attach to the cell walls of microalgae, allowing their recovery through the application of a magnetic field. Some particles can even be utilized to functionalize these nanoparticles, enhancing their characteristics and optimizing their application. Thus, this study provided a comprehensive overview of the various potential applications of microalgae, emphasizing their potential in wastewater treatment, CO_2 fixation, and bioproduct production, seeking to solve the limiting step through innovative approaches that include the selection and analysis of nanoparticles derived from different sources and their optimized use in the harvesting of *Chlorella sp*. According to the characterization results, the nanoparticles from two sources used were magnetite. The experiments were optimized by factorial design, where the magnetic nanoparticles (MNPs) synthesized in laboratory (functionalized by *Rhizophora mangle*'s tannin) and applied in the harvesting of *Chlorella sp*, achieved a harvesting efficiency (HE%) of 92.6% ((MNP-TNs concentration =1,000 mg. L^{-1}; q_{exp}= 1.39 g. mg^{-1}; pH=4), maintaining this efficiency during 5 reuse cycles. Even at pH 10.4 (pH at end of cultivation), the MNP-TNs were able to maintain a HE%= 63% (qexp= 0.96 g. mg^{-1}) Satisfactorily, when nanoparticles obtained from an alternative source were used (particulate material) both MNPs (naked) and MNP-TAN (functionalized with commercial tannin) presented great harvesting efficiency, being that MNPs (naked) obtained higher harvesting efficiency (HE%=86%; MNPs concentration=1,250 mg. L^{-1}; pH=3) than functionalized nanoparticles (HE%=77%; MNP-TANs concentration=1,100 mg. L^{-1}; pH=3.5). However, for this it was necessary a higher MNPs concentration in a lower pH. The functionalization contributed to particle stabilization increasing its reuse cycles from 3 (MNSs) to 7 cycles (MNP-TANs). Although in this case the harvest efficiencies were a little lower, it is interesting to verify that a material obtained in natural ways, with a low cost and applied for the first time on this goal can also be considered highly promising for this purpose.

Keywords: Biotechnology, nanotechnology, *n*anoparticles, magnetism, tannins, Ferro.

Palavras-chave: Biotecnologia, nanotecnologia, nanopartículas, magnetismo, taninos, Ferro.

1. INTRODUCTION

Non-renewable energy sources have been depleting every year. In addition, the use of fossil fuels is considered one of the hugest world sources of CO_2 emissions globally, with NOx and SOx, contributing to the increase in global temperature. Due to this, renewable energy sources are widely recognized as invaluable for global health (Razzak *et al.*, 2022). In this way, microalgae biomass has been considered a promising energy source, while capturing high concentrations of CO_2 during their photosynthesis process, and resulting in rich biomass (Li, P. *et al.*, 2023). Microalgae are one of the most ancient photosynthetic organisms found in all aquatic ecosystems and their high valuable biomolecules content can be used not only in biofuel production but also in the composition of cosmetics (Zhuang *et al.*, 2022), drugs (Parameswari and Lakshmi, 2022), food, and feed (Ahmad and Ashraf, 2023).

In general, microalgae production consists of three steps: cultivation, harvesting, and processing. The cultivation can be done in different forms (opened and closed) and culture mediums. Apart from cultivation in synthetic mediums, such as BG11, it can easily grow in wastewater, due to the high nutrient concentration, especially Nitrogen and Phosphorus (Chen, J. *et al.*, 2022). If cultivated in wastewater, microalgae play two roles, improve the wastewater quality by incorporating nutrients and, use of these nutrients in their growth, and transforming a residue into of highly valuable molecules (Devi *et al.*, 2023).

The harvesting step is considered a bottleneck to microalgae industrial-scale production. Different harvesting methods (physical, chemical, biological, and magnetic methods) have been studied to solve this problem. Among them, the magnetic method stands out due to its high harvesting efficiency (HE%) obtained in a short time. However, the cost of the method, mainly related to the production of magnetite nanoparticles (a type of iron oxide), is a limiting factor for their application on large scales (Barizão *et al.*, 2021). Given this, the search for alternative sources of iron at the nanoscale can be an alternative to make the process cheaper. Brazil is considered one of the largest iron producers in the world, with the state of Espírito Santo refining most of the national iron (AGÊNCIA NACIONAL DE MINERAÇÃO – ANM, 2021). The intense industrial activity of iron processing results in part of these particles being dissipated by the air, making them a reasonable source of particulate material on nanoscale.

The use of functionalizers can also contribute to increasing harvest efficiency by providing functional groups that have a greater affinity with microalgae cell wall. In addition, functionalizers often significantly increase particle stability by increasing their recyclability for several cycles and consequently reducing the number of applied nanoparticles, which can also directly reflect on the costs involved. Tannin is a well-known organic flocculant used in microalgae flocculation, capable of reaching HE% greater than 90%. Commercial tannins from *Acacia decurrens* are already produced on large scales, however, little is known about the efficiency of tannins from *Rhizophora mangle*, a species-rich in tannins and widely available in mangroves worldwide (Ibrahim, Yaser and Lamaming, 2021a). Nevertheless, the efficiency of the method is dependent on several variables including nanoparticle characteristics, temperature, biomass concentration, agitation, and others (Dai *et al.*, 2023; Zheng *et al.*, 2015).

Thus, this thesis investigated the influence of the source and functionalization of nanoparticles on the harvesting efficiency of *Chlorella sp*. Other variables involved in the system (e.g., temperature, agitation, pH) were also considered, aiming to find optimal magnetic harvesting conditions. In this way, this work was structured into 4 Chapters. The first and second ones are reviews of the literature that support the third and fourth chapters, providing the main characteristics and multiple applications of microalgae, and in sequence, focusing on the harvesting step, the main limiting of the production, specifically in the magnetic harvesting method, including synthesis routes, functionalization methods, variables interfering with HE%, viability, and future perspectives.

Chapter 3 presented the optimization of the magnetic harvesting process from the application of Fe_3O_4 nanoparticles synthesized in a controlled environment and functionalized with tannin (from *Rhizophora mangle*, also extracted in the lab.) an efficient flocculant applied to water and wastewater treatment. While in the fourth chapter, the focus was to achieve a similar harvest efficiency, however using an alternative source of nanoparticles and comparing both in its naked and functionalized (commercial tannin) form (the publication status of the articles is in the Appendix III.).

2. OBJECTIVE

Evaluate the harvesting of *Chlorella sp*. by magnetic nanoparticles obtained from different sources.

2.1 Specific objectives

- Select and evaluate possible sources of magnetic nanoparticles;
- Identify the morphological and molecular characteristics of selected magnetic nanoparticles;
- Modify magnetic nanoparticles in order to increase their interaction with microalgae;
- Optimize the magnetic harvesting process by magnetic nanoparticles application in their both forms, naked and functionalized with tannin.

Chapter 1

Microalgae as tertiary wastewater treatment: Energy production, carbon neutrality, and high-value products

ABSTRACT

In general, wastewater treatment plants (WWTPs) use basic effluent treatment (primary and secondary). However, including a tertiary treatment may enhance the quality of the treated effluent, making it reusable for different purposes. Several tertiary treatment techniques are available in the literature (e.g., coagulation, flocculation, filtration, and oxidation), but they are mainly focused on nutrients and contaminants remove (e.g., trace metals). However, when microalgae cultivation is applied as tertiary treatment, other possibilities could be explored. During the growth, microalgae incorporate nutrients present in the effluent in their biomass that could generate further high-value products such as biofuel, biochar, and carotenoids. In addition, during photosynthesis process they can fixed high CO_2 rates, playing an important role in global climate mitigation under a carbon neutrality perspective. In this sense, we identified the potential of microalgae cultivation as a tertiary treatment, emphasizing its capacity of removal nutrients and also their potential reduce the WWTP's carbon footprint; while generating other high-value products.

Keywords: Bioenergy, nature-based solution, carbon, net-zero, cultivation, biological system.

1. Introduction

The consumption of fossil fuels over the last few decades is fostering global climate change. By this, the Paris signature and other national to international agreements are limiting global greenhouse gas (GHG) emissions to reduce worldwide the temperature increase by 2° C (Gielen *et al.*, 2019). However, the increase in the world population has enhanced the energy demand and related GHG emissions. Thus, the replacement of traditional energy source by a low-carbon emission energy is key to achieving this objective (Antar *et al.*, 2021; Wang *et al.*, 2022). Wastewater Treatment Plants (WWTP) are one of the largest consumers of energy in the world, being responsible for 26% of GHG emissions throughout the water supply chain (Vasilaki *et al.*, 2019). However, the application of the NEXUS concept in this context could look at WWTPs as refineries where is possible to harness water, energy, and materials (Behera *et al.*, 2020; Guven *et al.*, 2023).

The energy production in WWTPs occurs commonly in the anaerobic digestion step. During this process is possible to take advantage of the chemical energy of organic

matter digestion to produce biogas. Additionally, the transesterification of sludge coming from anaerobic digestors can result in biodiesel production (Zarei, 2020). A great example is the Louhasakul *et al.* work's that achieved a biogas production of 280 ml/g- COD (Chemical Oxygen Demand) from palm oil mill wastewater, which represented 74% of the theoretical yield (Louhasakul *et al.*, 2021). While Zarei et. al. obtained a yielded 18.81wt% of crude lipid, using activated sludge from milk. However, it is important to highlight that the biodiesel production potential can vary according to the lipid content of each effluent (Zarei, 2020). Despite being highly efficient in the degradation of organic matter and energy production, as a secondary treatment, anaerobic digestion often doesn´t be able to remove the nutrients and toxicity of effluent, requiring a polishing step (Li, X. *et al.*, 2023).

Several tertiary treatment technologies have been applied in the polishing of effluents. The combination of coagulation and synchronized oxidation-adsorption treatments increased COD removal, and also reduced the toxicity of effluent for zebrafish (Louhasakul *et al.*, 2021). However, these technologies usually present high energy costs, reaching 66.59%, which can increase WWTPs operating costs and environmental impacts (Li, X. *et al.*, 2023). In this context, studies applying microalgae as tertiary treatment have been highlighted.

Microalgae as a tertiary treatment, although usually consume energy, are highly efficient in polishing effluents (Li, X. *et al.*, 2023) removing high amounts of nutrients and converting them into biomass. The biomass from microalgae is a versatile feedstock, used in biofuel production and as a source of high-added value biomolecules. In addition, they have other associated benefits, such as high CO_2 fixation rates, and do not require arable lands for cultivation (Bundschuh *et al.*, 2014). In this way, this work sought to identify the state of the art regarding the use of microalgae as a tertiary treatment of effluents and their contribution to achieving net-zero WWTPs objective, self-supply of energy, and high-added value biomolecule production.

2. Microalgae cultivation applied as tertiary treatment in WWTP

In general, WWTPs include two stages in their treatments, primary (physical) treatment including bar screening and sedimentation basins, and secondary (biological) treatment which is related to activated sludge and biological filter process. The tertiary treatment is applied by a huge of WWTPs, including techniques such as disinfection, sand

filtration, constructed wetland, and soil aquifer treatment for deeper water purification. The tertiary treatment has the function of effluent polishing to eliminate high concentrations of nutrients, mostly Nitrogen (N; mainly ammonia, nitrate, and nitrite), and Phosphorus (P; mainly phosphate), the main responsible for water bodies eutrophication, and recalcitrant carbon (Gupta, Pawar and Pandey, 2019; Liu, X. *et al.*, 2020). But the high cost, GHG emissions and sludge production make it difficult for several WWTPs to include this treatment in their scope (Acién *et al.*, 2016). By this, nature-based solution (NBS) associated with tertiary treatment is increasing in the last few years. Microalgae cultivation associated with the treatment of effluents is considered a sustainable tertiary treatment alternative, with low GHG emissions (compared to other technologies), and the biomass produced, can still be converted into energy, favoring the circular economy (Morais *et al.*, 2022).

The bioreactors design used can vary, but each option present positive and negative points. Currently, microalgae growth associated with wastewater treatment systems is mainly developed in open ponds (ElFar *et al.*, 2021). Open ponds vary in configuration but essentially consist of a circular adductor channel with a shallow depth and propeller system to promote water circulation and aeration. This cultivation system has a reduced cost compared to other systems, especially due to low energy requirements, however, it may suffer from high contamination risk and space needed. The control of light intensity and temperature is very dependent on the weather, making it difficult to have high precision. Another option is the cultivation in photobioreactors (closed system) that can minimize the contamination risk, producing a high amount of biomass with fewer losses of CO_2 during the process. The control of growth parameters can also be considered more accurate, however, disadvantages such as high energy consumption and maintenance costs can limit their utilization (Bhatt *et al.*, 2022).

As in all biological systems, there is a high degree of expertise in different effluents (e.g., certain strains have very different performances in different wastewater). Many types of effluents (e.g., tobacco wastewater, raw sewage, primary, secondary effluents, and sludge dewatering liquid) can be used for microalgae cultivation (Hao *et al.*, 2022). Effluents from anaerobic treatment have been considered a prominent source, while raw sewage and effluents with high turbidity are not suitable as a growth medium for microalgae due to low light penetration (Li, G. *et al.*, 2022). The increase in antimicrobials and other xenobiotics discharge is a real problem in the treatment of effluents and also in microalgae cultivation (Wang *et al.*, 2021). In this sense, the balance

and dilution of inhibitory substances by mixing different types of wastewater are suggested (You, X. *et al.*, 2022). The dilution can lead to nutrient depletion, creating a condition of nutritional stress and further lipid synthesis, and triglyceride accumulation, reduced protein content and increased carotenogenesis (Chen *et al.*, 2011; Shahid *et al.*, 2020) as well as, the increase in biomass of some microalgae strains (Hernández-García *et al.*, 2019). The potential strategies and approaches for a viable integration of microalgae biomass production in WWTP is the centralization of domestic wastewater and CO_2 as a systemic bioremediation mechanism in a biorefinery (Do *et al.*, 2022); pre-treatment (settlement process) in order to reduce effluent turbidity and thus increase photosynthetic activity; supplementation with ferric citrate K_2HPO_4, (Li, G. *et al.*, 2022) and additional concentrations of the photosynthetic cofactor magnesium (Hanifzadeh, Garcia an Viamajala, 2018) to increase microalgae metabolic rates.

The treatment of WWTPs effluents is normally carried out outdoors under physiological temperatures and pH (Ali *et al.*, 2021; Wollmann *et al.*, 2019) demonstrating the importance of new strains of microalgae, the use of mixed cultures and consortia of microalgae and bacteria in order to increase biomass production and removal of contaminants (Chen *et al.*, 2021; González-González and De-Bashan, 2021). By this, the application of microalgal assemblages and bacterial consortia in the treatment of effluent systems is more vigorous than pure cultures (Craggs, Sutherland e Campbell, 2012). The most used taxa of microalgae are *Chlorella*, *Scenedesmus*, *Desmodesmus*, *Neochloris*, *Chlamydomonas*, *Nitzschia* e *Cosmarium*,(Wang, Y. *et al.*, 2016) being the species *Chlorella vulgaris* considered as a model by their high growth rates, non-production of toxins, resilience to many types of wastewater, efficient removal of pollutants and metabolic diversity - mixotrophy, heterotrophy and autotrophy (Nguyen *et al.*, 2019; Rosli *et al.*, 2019; Suparmaniam *et al.*, 2020). Mixotrophic and heterotrophic cultures have some advantages in the treatment of domestic effluents due to their ability to grow in high carbon load and produce high amounts of biomass, (Aggarwal *et al.*, 2021; Gao *et al.*, 2021) enhancing biomass downstream, that often does not reach 1 g. L^{-1} in photoautotroph.

For N removal using *Chlorella* (*Trebouxiophyceae*) is recommended to do: any pre-treatment different from anaerobic, while avoiding domestic wastewater uses, concentration of N< 527 mg. L^{-1}, temperature< 24.2 ºC, and photoperiod< 20h. For phosphorus removal, the best condition are: $CO_2 \geq 0.045$ % (v/v), pH< 8.35, and P initial concentration< 12.43 mg. L^{-1}. For biomass production are: initial inoculum≥ 0.0151 mg.

L^{-1}, temperature ≥ 18.25 ºC, pH< 7.88, and light intensity < 83.75 μmol. m^{-2}. s^{-1}. If using *Scenedesmus* (Chlorophyceae), the best conditions for their cultivation to remove N are: CO_2 concentrations< 0.52 % (v/v), photoperiod< 15h and light intensity< 112 μmol. m^{-2}. s^{-1}. For phosphorus removal: wastewater (other than industrial), autoclaving as a pre-treatment method, pH< 7.75, and light intensity ≥ 0.04 μmol. m^{-2}. s^{-1}; while for biomass production: light intensity≥ 0.0104 g. L^{-1}, initial phosphorus concentration ≥ 7.105 mg. L^{-1}, light intensity from 30.64 to 1925 m^{-2}. s^{-1}, and initial N concentration < 748.1 mg. L^{-1} (Singh and Mishra, 2022). Depending on the type of crop, yield, harvesting, and processing method, the energy input may exceed output; but studies are still needed prior to using microalgae for wastewater treatment (e.g., testing microalgae activity performance and their high rates of growth and removal of pollutants) (Gonçalves *et al.*, 2020; Losa *et al.*, 2020).

Biomass final composition can favor or disfavor its applications. For example, biomass with high protein content can decrease the performance of anaerobic digestion (Vargas-Estrada *et al.*, 2021) as a result of their degradation into ammonia which inhibits the activity of anaerobic microorganisms (Mahdy *et al.*, 2015). However, lipid-rich biomasses are excellent for biogas production due to their greater methanogenic potential (Vargas-Estrada *et al.*, 2021). As a result, the entire effluent treatment process end after the water with chemical indices below discharge limits, with the conversion of biomass into products that enable a positive return on investment (ROI) (Do *et al.*, 2022; Purba *et al.*, 2022).

3. Bioenergy from microalgae

Microalgae are versatile for different biofuel production; being able to produce liquid fuels (biodiesel), gaseous fuels (syngas, bio-methane, bio-hydrogen), and solid fuels (flakes and coal)(Ebhodaghe, Imanah and Ndibe, 2022). Biodiesel has been the most studied biofuel from microalgae in the last few years. It is considered a sustainable fuel due to its smaller polluting potential, emitting fewer particles, sulfur, and other greenhouse gases than petroleum-based biodiesel (Ahmad *et al.*, 2022; Ahn *et al.*, 2022). Through nutrients obtained from wastewater, microalgae are able to produce a high amount of lipids. Triacylglycerides (TAG) are the most desirable lipids type in biodiesel production. TAG could be extracted by alcoholic reaction and converted into diglycerides, in sequence into monoglycerides, and finally into glycerol

(transesterification) (Ahmad *et al.*, 2022; Arutselvan *et al.*, 2022). The transesterification process also reduces the viscosity of oil, making their use in motors possible. Fuels deriving microalgae that have a greater acid oleic content frequently result in fuel with more oxidative stability. Bioethanol is another successful biofuel from microalgae. In this case, are desirable high carbohydrate levels in biomass, especially starch and cellulose. Usually, a pre-treatment is necessary to release the cell content. Thus, through the hydrolysis process is possible to decompose carbohydrates into monosaccharides, such as glucose. These sugars will ferment in anaerobic fermentation, normally induced by yeasts of the genus Saccharomyces resulting in bioethanol (third-generation) (Ahn *et al.*, 2022; Gondi *et al.*, 2022).

Microalgae are considered excellent feedstock for biogas production due to high concentrations of polysaccharides, small amounts of cellulose, and the absence of lignin. The biogas is produced by anaerobic digestion of microalgae biomass and is composed mostly of methane (from 55 to 75%) and CO_2 (from 25 to 45%) (Budiman and Wu, 2018). CO_2 can be reintegrated into the system and biomethane to industry. Another important gaseous fuel is biohydrogen. It can be produced in both types of reactions; light-dependent (biophotolysis of water and photofermentation) and light-independent (dark fermentation using anaerobic bacteria). The last one is the cheapest and most ecological method of production; while producing profitable by-products such as organic acids and alcohols. Also, biohydrogen is considered a fuel with superior characteristics with low density, high energetic potential, and does not emit greenhouse gases (Ahmad *et al.*, 2022a; Gondi *et al.*, 2022; Nagarajan, Chang and Lee, 2020).

Other fuels also could be produced from microalgae, such as biocrude and biochar. Biocrude is a fuel produced from a hydrothermal liquefaction process. Due to the difficulties and high costs involved in drying microalgae biomass, this fuel production process has been attractive, to be carried out in wet ways and generate a lot of high-added value products (natural gas, biochar, and others) (Hossain *et al.*, 2022; Islam *et al.*, 2022; Mishra and Mohanty, 2020).

Biochar is a vegetable coal with high carbon content, produced from the hydrothermal decomposition of any type of biomass under the absence of oxygen and mild temperatures (Gan *et al.*, 2018; Yu *et al.*, 2017). Also, biocoal can act as a long-term sink of carbon dioxide in the atmosphere, being able to reduce up to 84% of wetlands treatment emissions (Yu *et al.*, 2017). Microalgae biochar is considered more efficient

than lignocellulosic biomass, with pre-treatment simpler and more economical (Law *et al.*, 2022).

Although highly versatile, microalgae biomass could have high production costs, even when associated with wastewater treatment, and the energetic balance could end up being negative. In this way, the selection of species and technologies applied must be done carefully. Comparing different microalgae and drying technologies, Even et. al. concluded that using microalgae biofilms and solar drying beds is possible achieve a net production of heat of +0.48 MJ. Unlike when using planktonic microalgae and a ring dryer that resulted in a negative net heat produced (−1.32 MJ). This may be related to the higher productivity of microalgae biofilms, almost twice as high as that of planktonic microalgae, and also to the reduced energy expenditure in biomass drying (Even *et al.*, 2022). It is important to highlight that even when the liquid energy was positive, the value was very close to 0. Thus, if just this microalgae function were considered, their application could not be so interesting. However, another important ecosystem service is performed by them. The microalgae can be also considered an indirect carbon capture and storage, a negative emission technology.

4. Carbon capture and balance towards carbon neutrality at WWTP

Carbon capture and utilization and/or storage technologies have been used to mitigate the increasing anthropogenic emission of CO_2 in the last decades. However, most of the methods applied have high energy consumption and use highly toxic products. By this, microalgae cultivation has been considered a promising nature-based solution for carbon sequestration (CO_2 biofixation occurs during photosynthesis), and their biomass can be used for the production of biofuels and products with high added value (Leflay and Pandhal Brown, 2021).

The efficiency of microalgae to biofix CO_2 is species-specific and variable according to CO_2 sources (Table 1). However, environmental variables, such as temperature, pH, and others will influence biofixation rates. In general, moderate light intensity and temperature favor carboxylation process (photosynthesis). During the day pH levels rise due to the use of CO_2 in this process. However, high temperatures and light intensities favor oxygenation and pH toward lower levels (Barsanti and Cualtieri, 2010; Bartley *et al.*, 2013). At low pH (3 up to 5) the CO2 is the most abundant specie dissolved, while in neutral pH (between 6 and 8) is HCO_3^- and in basic pH the dominant specie is

HCO_3^{2-} (Espinosa-Carreón and Escobedo-Urías, 2017). Also, the assimilation of inorganic carbon can be different according to microalgae species. Mainly three pathways are possible, direct CO_2 assimilation (via plasmatic membrane), conversion of HCO_3^- to CO_2 by enzyme carbonic anhydrase, and direct transport of bicarbonate via the plasmatic membrane (Klinthong *et al.*, 2015).

Table 1. Global microalgae species-specific carbon dioxide (CO_2) sources and concentration for fixation rates aiming their biomass productivity.

Microalgae	**Source of CO_2**	**CO_2 concentration (%)**	**CO_2 sequestration (g. L^{-1}) or CO_2 fixation rate**	**Productivity or concentration of biomass**	**Ref.**
Chlorella sp.	Air	5	287 ± 7 mg CO_2. d^{-1} for 0.5 L	0.314 ± 0.004 g. L^{-1}. d^{-1}	(Yadav *et al.*, 2015)
Chlorella sp.	Flue gas	5	250 ± 13 mg. CO_2^{-1}. d^{-1} for 0.5 L	0.273 ± 0.012 g. L^{-1}. d^{-1}	(Yadav *et al.*, 2015)
Chlorella sp.	Air	10	249 ± 11 mg. CO_2^{-1}. d^{-1} for 0.5 L	0.271 ± 0. 067 g. L^{-1}. d^{-1}	(Yadav *et al.*, 2015)
Chlorella sp.	Flue gas	100	175 ± 10 mg. CO_2^{-1}. d^{-1} for 0.5 L	0.191 ± 0.11 g. L^{-1}. d^{-1}	(Yadav *et al.*, 2015a)
Chlorella vulgaris	Air	10	***	104.76 ± 10.73 mg dw. L^{-1}. d^{-1}	(Yoo *et al.*, 2010)
Chlorella vulgaris	Air	6.5	2.29 g. L^{-1}. d^{-1}	***	(Anjos *et al.*, 2013)
Chlorella PY-ZU1	Air	15	0.95 g. L^{-1}. d^{-1}	10.51 g. L^{-1}	(Cheng *et al.*, 2013)
Chlorella sorokiniana	Air	5	0.83 g. L^{-1}. d^{-1}	4.4 g. L^{-1}	(Kumar and Das, 2012)
Scenedesmus obliquus	Air	6	0.188 g. L^{-1}. d^{-1}	0.1 g. L^{-1}.d^{-1}	(Morais, de and Costa, 2007)
Scenedesmus sp.	Air	10	***	217.50 ± 11.24 mg dw. L^{-1}. d^{-1}	(Yoo *et al.*, 2010)
	Flue gas	5.5	***	203 mg. L^{-1}. d^{-1}	(Yoo *et al.*, 2010)
Spirulina **sp.**	Air	6	0.376 g. L^{-1}. d^{-1}	0.2 g. L^{-1}.d^{-1}	(Morais, de and Costa, 2007)

Botryococcus braunii	Air	10	***	26,55 mg dw. L^{-1}. d^{-1}	(Yoo *et al.*, 2010)
	Flue gas	5.5	***	77 mg. L^{-1}. d^{-1}	(Yoo *et al.*, 2010)

Microalgae can obtain CO_2 for biofixation from two different sources: atmospheric CO_2 and flue gas. Most of the atmospheric CO_2 is from diffuse sources (50%), becoming difficult to use in microalgae cultivation. But flue gas has high concentrations of CO_2 (400-fold higher than in the atmosphere) (Kong *et al.*, 2021). The ideal CO_2 concentrations in flue gas for the cultivation of most microalgae species are around 5 and 10 % (Ho, Chen and Chang, 2010; Sydney *et al.*, 2010). Although some species are able to support different ranges, including very high concentrations. *Anabaena sp*. CH_1 demonstrated excellent CO_2 tolerance even at 15% of CO_2, fixing 33.1%, almost the same fixation got at 10% CO_2 level. However, the chlorophyll content was much higher at 15% of CO_2 (2.08+_0.11%), where growth was inhibited. *Scenedesmus spp.* also demonstrated the ability to withstand high levels of CO_2 in its growth. At 40% of CO_2. In addition, the purity degree of the gas is important to avoid impacts on cell growth; while high levels of SO_x and nitrogen oxides (NO_x) can make cell growth unfeasible. In the case of SO_x, its excess leads to the increase of hydrogen ions during the hydrolysis of sulfur dioxide (SO_2), acidifying the medium. About the NO_x, depending on the amount, its conversion into nitrite can serve as a supply of nutrients, however, the excess will also limit microalgae cultivation (Vale *et al.*, 2020).

Despite the harmful effect of NO_x, SO_x, and CO in flue gas over microalgae, some works demonstrated that under some conditions (such as using prior filtration of particles, changes in initial cell concentration, pH, and others). It is possible to obtain higher growth, as evidenced by the microalgae *Chlorella sp.* which was cultivated with 10% of CO_2 in the flue gas. Also, major flue gas concentrations resulted in higher CO_2 fixation, the most suited initial cell density was observed to be 0.15 g L^{-1} resulting in the highest biomass concentration and CO_2 fixation rate of 2.13 ± 0.01 g. L^{-1} and 0.259 ± 0.01 g. CO_2^{-1}. day^{-1}, respectively (Yadav *et al.*, 2015).

Furthermore, the source of CO_2 can influence the cellular composition of microalgae and favor certain types of biofuel. For example, the application of oil-burning flue gas increased by 1.9 folds (39.44 mg. L^{-1}. d^{-1}) and about 4-folds (20.65 mg. L^{-1}. d^{-}

[1]) the lipid productivity of *Scenedesmus* sp. and *B. braunii*. For *B. braunni*, a high concentration of oleic acid (55%) was identified among the fatty acids, which are the main component of biodiesel, demonstrating their potential for biofuel production (Yoo *et al.*, 2010).

Microalgae cultivation associated with WWTP has the capacity to reduce WWTP's carbon footprint due to their high capacity of carbon sequestration within their biomass. But as a result of the huge amount of energy needed during entire wastewater treatment, it is not feasible to use a net-zero carbon perspective. Under the Net-Zero perspective, the company does not emit carbon during its activities, so, it is not necessary to compensate for carbon emissions). Furthermore, a carbon-neutral action is widely recommended in the WWTP case (balancing out the greenhouse gas (GHG) emitted using carbon capture strategies and/or replacing fossil fuels with nature-based fuels). As a result, the carbon offset produced by the chosen nature-based solution can be used to reach climate goals and signatures due to the generation of carbon credits (the total carbon credits are the sum of carbon removal credits minus carbon emissions (Patel, Joun and Sim, 2020; Xin *et al.*, 2018).

In general, in a WWTP the wastewater will pass through sand or gravel filters prior to the lagoon storage, where the wastewater will be decanted to generate sludge and nutrient-rich treated effluent [1]. The nutrient-rich effluent will be used at reactors for the cultivation of high-productive microalgae assemblages. After that, the produced microalgae will be [2] transferred to the processing unit [3] to be converted to produce biofuels (e.g., biogas, bioethanol, and biochar), as well as the [4] sludge produced in the lagoons (e.g., production of biogas, and biochar). [5] The produced biofuels (except biochar) can return to the system to partially offset WWTPs carbon footprint due to the generation of carbon credits (carbon removal credits due to biofuel replacing petroleum-based fuels; see Etter *et al.*, 2022 (Etter *et al.*, 2021). [6] Furthermore, microalgae production can be enhanced using flue gas from nearby industries. [7] In addition, both microalgae and sludge can produce other nature-based products that can be associated with climate/pollution mitigation efforts (e.g., biochar applied to enhance soils carbon stocks, and non-soil applications such as cement, asphalt, and plastics. Furthermore, it is invaluable to demonstrate that biochar store carbon in the long-term (Etter *et al.*, 2021).

In this sense, it is essential to include microalgae cultivation in the scope of wastewater treatment, as a tertiary treatment, to reach WWTP carbon neutrality; while reducing energy consumption during their production. The produced microalgae can be

converted to biofuels and other bioproducts applied as nature-based solutions that will enhance their carbon offset potential (Figure 1). In addition, we highlight that the use of the sludge produced due to WWTP activities can support the carbon offset from microalgae, as well as the production of nature-based solutions (e.g., bio-asphalt). By another hand, the cultivated microalgae can be used to produce other bioproducts not related to carbon neutrality (e.g., pigments); but these activities cannot generate carbon credits or reach carbon neutrality goals (Etter *et al.*, 2021; Lu *et al.*, 2018; Slade and Bauen, 2013).

In addition, it is invaluable to integrate microalgae and sludges bio-products with WWTP to promote more sustainable actions, while lower the environmental impact of wastewater treatment. For this, is urgent the development of a methodology focused on NBS applied to WWTP to reach carbon neutrality. Creating a methodology focused on this topic will increment their carbon credits generation, enhance project reliability, and make possible monitoring, reporting, and verification (MRV) regulations in the long term (see CDM, Gold Standard, and VERRA methodologies).

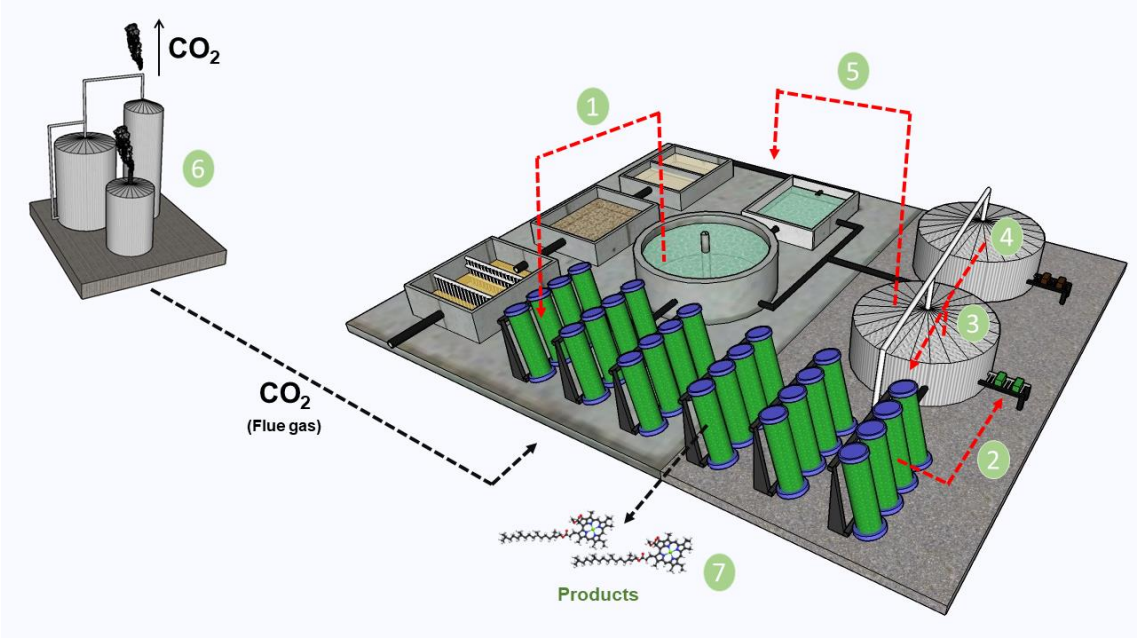

Figure 1. Wastewater treatment plants coupling microalgae and the sludge produced during the process to generate energy, carbon-rich materials and other co-products.

5. Other bioproducts from microalgae biomass

In addition to biofuels, other high- value molecules can be extracted from microalgae, including exopolysaccharides (EPS), carotenoids, fucoxanthin, sterols, peptides, polyunsaturated Fatty (Pufas), diterpenes and other (Fawcett *et al.*, 2022a). These molecules are greatly effective as antibacterial (Najdenski *et al.*, 2013) immunomodulatory (Riccio and Lauritano, 2019) and antiviral (Yim *et al.*, 2003). However, cultivation using non-sterile medium can present the growth of unknown microorganisms and build up heavy metal, which limits biomass application for human purposes (Goswami *et al.*, 2022). In this way, the viable applications of microalgae biomass cultivated in wastewater effluent are mainly for biofertilizers, animal feedstock, and bioplastic production. However, even in this case, microalgae cultivation is indicated to be conducted in wastewater from food, such as from beer or palm oil industry due to the lower number of harmful microorganisms compared to other wastewater mediums (Ahmad *et al.*, 2022; Goswami *et al.*, 2022).

The microalgae-based biofertilizer can be considered similar or better than inorganic fertilizers, for being rich in micronutrients, such as natural trace elements and phytohormones that are essential for the proper growth and development of plants (Lorentz *et al.*, 2020; Nayak, Swain and Sen, 2019). In addition, contribute to soil water retention and aggregate stability (Khan *et al.*, 2019; Nayak, Swain and Sen, 2019). The whole biomass from other processes can be used in biofertilizer production, for example, residual biomass from biodiesel production, that corresponds to approximately 65% of all biomass applied, thus reducing the costs of the process (Nayak, Swain and Sen, 2019).

Oilseed production takes around 23% of cultivated land (6% for human food production, and 17% is used for feedstock production). About 27% of the animal feedstock consists of oilseed flours, their main function is the supplied protein to maximize animal production (Fawcett *et al.*, 2022). In this way, microalgae have proven to have more protein than some oilseeds, such as soybean. In addition, microalgae present a high percentage of carbohydrates and have antimicrobial properties that aid the animal's intestinal tract, in addition to its superior fatty acid profile, vitamins, minerals, and aminoacids, which reduce the need for expensive synthetic supplements (Catone *et al.*, 2021; Fawcett *et al.*, 2022).

However, it is important to analyze the digestibility of the biomass before applying it on larger scales. as microalgae are rarely used as the only source of nutrients,

but rather as a part of the feed composition. Inclusion rates vary according to the animal, in general, birds (10% of microalgae inclusion) are more tolerant than swine (5.51% of microalgae inclusion) and cattle (1.18% of microalgae inclusion) (Fawcett *et al.*, 2022). Gratell *et al.* found that 16% inclusion of *Nannochloropsis oceanica* in the diet of commercial birds resulted in hypertrophy of vital organs and increased water intake, however, at 8% the biomass could be used without adverse effects. Thus, it is worth highlighting the adequate percentage of supplementation (Catone *et al.*, 2021; Fawcett *et al.*, 2022).

Despite non-conventional, biofertilizers, animal feedstock and biochar from microalgae biomass can be used as NBS for carbon neutrality to be implemented by the buyer of these products. It works similarly to the carbon neutrality strategies highlighted on topic 5. In general, the buyer could generate carbon credits by the difference between NBS-managed emissions and non-managed emissions. In this sense, the animal feedstock can be used to reduce the enteric methane emissions from ruminants' diets by suppressing or inhibiting methanogenesis (Sünkel *et al.*, 2021); while decreasing nitrous oxide (N_2O) emissions from agriculture can be developed using biofertilizers with lower amounts of N, where some species of microalgae can be useful raw material (Michigan State University, 2013); in this case, it is invaluable to develop a carbon neutrality methodology as those foreseen in VERRA and Gold Standards methodologies. Furthermore, biochar is the most prominent NBS strategy from microalgae cultivation in WWTP. Besides their use in biodiesel production, biochar can be buried in agricultural and forest management systems to increase soil carbon stocks and sink in the long term as a result of carbon stability over time (Etter *et al.*, 2021).

Also, some microalgae taxa, such as *Chlorella spp.* and Cyanobacteria, are able to synthesize biodegradable polymers called Polyhydroxyalkanoates (PHA), which production is directly influenced by factors, such as light-dark cycles, nutrient availability, temperature, pH, among others. Its accumulation takes place in the form of glycogen inside the microalgae and occurs when the cells are under conditions of limited nutrients, such as nitrogen and phosphorus (Ahmad *et al.*, 2022; Goswami *et al.*, 2022). In a sterile medium, microalgae can be used as a substitute for absorbable sutures and synthetic skins, however, when using wastewater, their applications are limited to avoid contamination, Furthermore, PHA has polymeric properties compared to plastic (Ahmad *et al.*, 2022; Goswami *et al.*, 2022) making possible their application as a raw material for GHG (CO_2 and/or CH_4) capture and utilization in plastic materials to produce useful

plastic for sale in the plastics market. By this, the produced bioplastic will mitigate traditional plastic production and needs to provide carbon immobilization in the long term. If the bioplastic is biodegradable, it is necessary for the manufacturing plastic to be less emission-intensive than the business as usual (Newlight Technologies, 2019).

6. Conclusion and future perspectives

This study supports the efficiency of using microalgae cultivation as a tertiary treatment in WWTP. Many species of microalgae proved to be highly efficient in producing biomass from their cultivation in effluents. However, the quality and composition of the final biomass are variable according to the species and the type of effluent used, limiting the comparison between different methodologies. Although different cultivation systems proved their performance on a bench or pilot scale, data on the efficiency of the system (photobioreactors) on larger scales are scarce. Thus, it is urgent the development of methodology standardization for species-specific microalgae and the best effluents for each cultivation, which will provide high biomass production capacity, while contributing and encouraging microalgae application in large scale WWTP.

As a result, microalgae culture as a tertiary treatment will mitigate WWTPs carbon footprint under the scope of carbon neutrality through the generation of carbon credits from the reduction in GHG emissions; and/or the production of bioproducts with fewer climate impacts compared to the business as usual. Microalgae have a high capacity for CO_2 fixation, especially when applying flue gas, as those produced by industries activity. However, it is important to highlight that the use of this type of tertiary treatment generates biomass rich in molecules that can be converted into different products, including biofuels that can help reduce the release of CO_2 from WWTP, unlike other treatment techniques that only remove the nutrients. Despite the promising scenario and solid data that prove the efficiency of this method, further studies are needed to validate the use of the technique on larger scales and to standardize the cultivation models, as mentioned above. In this sense, the use of microalgae as a tertiary treatment is highly recommended and has huge potential to be applied to reach carbon mitigation goals from local to international scales, but investments are still needed; while other climate mitigation methodologies could be developed to enhance microalgae and related

bioproducts efficiency to mitigate GHG emissions from WWTPs up to a Net-Zero perspective.

7. References

ACIÉN, F. G.; GÓMEZ-SERRANO, C.; MORALES-AMARAL, M. M.; FERNÁNDEZ-SEVILLA, J. M.; MOLINA-GRIMA, E. Wastewater treatment using microalgae: how realistic a contribution might it be to significant urban wastewater treatment? **Applied microbiology and biotechnology**, v. 100, n. 21, p. 9013–9022, 1 nov. 2016.

AGGARWAL, C.; SINGH, D.; SONI, H.; PAL, A. Heterotrophic Cultivation of Microalgae in Wastewater. *Em*: [s.l: s.n.]. p. 493–506.

AHMAD, A.; BANAT, F.; ALSAFAR, H.; HASAN, S. W. Algae biotechnology for industrial wastewater treatment, bioenergy production, and high-value bioproducts. **Science of The Total Environment**, v. 806, p. 150585, 1 fev. 2022.

AHN, Y.; PARK, S.; JI, M. K.; HA, G. S.; JEON, B. H.; CHOI, J. Biodiesel production potential of microalgae, cultivated in acid mine drainage and livestock wastewater. **Journal of Environmental Management**, v. 314, p. 115031, 15 jul. 2022.

ALI, S.; PAUL PETER, A.; CHEW, K. W.; MUNAWAROH, H. S. H.; SHOW, P. L. Resource recovery from industrial effluents through the cultivation of microalgae: A review. **Bioresource Technology**, v. 337, n. June, p. 125461, 2021.

ANJOS, M.; FERNANDES, B. D.; VICENTE, A. A.; TEIXEIRA, J. A.; DRAGONE, G. Optimization of CO2 bio-mitigation by Chlorella vulgaris. **Bioresource Technology**, v. 139, p. 149–154, 1 jul. 2013.

ANTAR, M.; LYU, D.; NAZARI, M.; SHAH, A.; ZHOU, X.; SMITH, D. L. Biomass for a sustainable bioeconomy: An overview of world biomass production and utilization. **Renewable and Sustainable Energy Reviews**, v. 139, 1 abr. 2021.

ARUTSELVAN, C.; SEENIVASAN, H. KUMAR; LEWIS OSCAR, F.; RAMYA, G.; THUY LAN CHI, N.; PUGAZHENDHI, A.; THAJUDDIN, N. Review on wastewater treatment by microalgae in different cultivation systems and its importance in biodiesel production. **Fuel**, v. 324, p. 124623, 15 set. 2022.

BARSANTI, L.; CUALTIERI, PAOLO. **Algae: Anatomy, Biochemistry and Biotechnology**. [s.l: s.n.].

BARTLEY, M. L.; BOEING, W. J.; DUNGAN, B. N.; HOLGUIN, F. O.; SCHAUB, T. pH effects on growth and lipid accumulation of the biofuel microalgae Nannochloropsis salina and invading organisms. **Journal of Applied Phycology 2013 26:3**, v. 26, n. 3, p. 1431–1437, 5 nov. 2013.

BEHERA, C. R.; AL, R.; GERNAEY, K. V.; SIN, G. A process synthesis tool for WWTP – An application to design sustainable energy recovery facilities. **Chemical Engineering Research and Design**, v. 156, p. 353–370, 1 abr. 2020.

BHATT, A.; KHANCHANDANI, M.; RANA, M. S.; PRAJAPATI, S. K. Techno-economic analysis of microalgae cultivation for commercial sustainability: A state-of-the-art review. **Journal of Cleaner Production**, v. 370, p. 133456, 10 out. 2022.

BUDIMAN, P. M.; WU, T. Y. Role of chemicals addition in affecting biohydrogen production through photofermentation. **Energy Conversion and Management**, v. 165, p. 509–527, 1 jun. 2018.

BUNDSCHUH, J.; YUSAF, T.; MAITY, J. P.; NELSON, E.; MAMAT, R.; INDRA MAHLIA, T. M. Algae-biomass for fuel, electricity and agriculture. **Energy**, v. 78, p. 1–3, 15 dez. 2014.

CATONE, C. M.; RIPA, M.; GEREMIA, E.; ULGIATI, S. Bio-products from algae-based biorefinery on wastewater: A review. **Journal of environmental management**, v. 293, 1 set. 2021.

CHEN, M.; TANG, H.; MA, H.; HOLLAND, T. C.; NG, K. Y. S.; SALLEY, S. O. Effect of nutrients on growth and lipid accumulation in the green algae Dunaliella tertiolecta. **Bioresource Technology**, v. 102, n. 2, p. 1649–1655, jan. 2011.

CHEN, Z.; LI, T.; YANG, B.; JIN, X.; WU, H.; WU, J.; LU, Y.; XIANG, W. Isolation of a novel strain of Cyanobacterium sp. with good adaptation to extreme alkalinity and high polysaccharide yield. **Journal of Oceanology and Limnology**, v. 39, n. 3, p. 1131–1142, 7 maio 2021.

CHENG, J.; HUANG, Y.; FENG, J.; SUN, J.; ZHOU, J.; CEN, K. Improving CO2 fixation efficiency by optimizing Chlorella PY-ZU1 culture conditions in sequential bioreactors. **Bioresource Technology**, v. 144, p. 321–327, 1 set. 2013.

CRAGGS, R.; SUTHERLAND, D.; CAMPBELL, H. Hectare-scale demonstration of high rate algal ponds for enhanced wastewater treatment and biofuel production. **Journal of Applied Phycology**, v. 24, n. 3, p. 329–337, 22 jun. 2012.

DO, C. V. T.; PHAM, M. H. T.; PHAM, T. Y. T.; DINH, C. T.; BUI, T. U. T.; TRAN, T. D.; NGUYEN, V. T. Microalgae and bioremediation of domestic wastewater. **Current Opinion in Green and Sustainable Chemistry**, v. 34, p. 100595, 2022.

EBHODAGHE, S. O.; IMANAH, O. E.; NDIBE, H. Biofuels from microalgae biomass: A review of conversion processes and procedures. **Arabian Journal of Chemistry**, v. 15, n. 2, p. 103591, 1 fev. 2022.

ELFAR, O. A.; CHANG, C.-K.; LEONG, H. Y.; PETER, A. P.; CHEW, K. W.; SHOW, P. L. Prospects of Industry 5.0 in algae: Customization of production and new advance technology for clean bioenergy generation. **Energy Conversion and Management: X**, v. 10, p. 100048, jun. 2021.

ESPINOSA-CARREÓN, T. L.; ESCOBEDO-URÍAS, D. South region of the Gulf of California large marine ecosystem upwelling, fluxes of CO2 and nutrients. **Environmental Development**, v. 22, p. 42–51, 1 jun. 2017.

ETTER, H.; VERA, A.; AGGARWAL, C.; DELANEY, M.; MANLEY, S. Methodology for biochar utilization in soil and non-soil applications. **VERRA VCS**, 2021. . Acesso em: 26 dez. 2022

EVEN, C.; HADROUG, D.; BOUMLAIK, Y.; SIMON, G. Microalgae-based Bioenergy with Carbon Capture and Storage quantified as a Negative Emissions Technology. **Energy Nexus**, v. 7, p. 100117, 1 set. 2022.

FAWCETT, C. A.; SENHORINHO, G. N. A.; LAAMANEN, C. A.; SCOTT, J. A. Microalgae as an alternative to oil crops for edible oils and animal feed. **Algal Research**, v. 64, p. 102663, 1 maio 2022.

GAN, Y. Y.; ONG, H. C.; SHOW, P. L.; LING, T. C.; CHEN, W. H.; YU, K. L.; ABDULLAH, R. Torrefaction of microalgal biochar as potential coal fuel and application as bio-adsorbent. **Energy Conversion and Management**, v. 165, p. 152–162, 1 jun. 2018.

GAO, F.; YANG, Z.-Y.; ZHAO, Q.-L.; CHEN, D.-Z.; LI, C.; LIU, M.; YANG, J.-S.; LIU, J.-Z.; GE, Y.-M.; CHEN, J.-M. Mixotrophic cultivation of microalgae coupled with anaerobic hydrolysis for sustainable treatment of municipal wastewater in a hybrid system of anaerobic membrane bioreactor and membrane photobioreactor. **Bioresource Technology**, v. 337, p. 125457, out. 2021.

GIELEN, D.; BOSHELL, F.; SAYGIN, D.; BAZILIAN, M. D.; WAGNER, N.; GORINI, R. The role of renewable energy in the global energy transformation. **Energy Strategy Reviews**, v. 24, p. 38–50, 1 abr. 2019.

GONÇALVES, R. F.; ASSIS, T. I.; MACIEL, G. B.; BORGES, R. M.; CASSINI, S. T. A. Co-digestion of municipal wastewater and microalgae biomass in an upflow anaerobic sludge blanket reactor. **Algal Research**, v. 52, p. 102117, dez. 2020.

GONDI, R.; KAVITHA, S.; YUKESH KANNAH, R.; KUMAR, G.; RAJESH BANU, J. Wastewater based microalgae valorization for biofuel and value-added products recovery. **Sustainable Energy Technologies and Assessments**, v. 53, p. 102443, 1 out. 2022.

GONZÁLEZ-GONZÁLEZ, L. M.; DE-BASHAN, L. E. Toward the Enhancement of Microalgal Metabolite Production through Microalgae–Bacteria Consortia. **Biology**, v. 10, n. 4, p. 282, 1 abr. 2021.

GOSWAMI, R. K.; MEHARIYA, S.; KARTHIKEYAN, O. P.; GUPTA, V. K.; VERMA, P. Multifaceted application of microalgal biomass integrated with carbon dioxide reduction and wastewater remediation: A flexible concept for sustainable environment. **Journal of Cleaner Production**, v. 339, p. 130654, 10 mar. 2022.

GUPTA, S.; PAWAR, S. B.; PANDEY, R. A. Current practices and challenges in using microalgae for treatment of nutrient rich wastewater from agro-based industries. **Science of The Total Environment**, v. 687, p. 1107–1126, 15 out. 2019.

GUVEN, H.; ERSAHIN, M. E.; OZGUN, H.; OZTURK, I.; KOYUNCU, I. Energy and material refineries of future: Wastewater treatment plants. **Journal of Environmental Management**, v. 329, p. 117130, 1 mar. 2023.

HANIFZADEH, M.; GARCIA, E. C.; VIAMAJALA, S. Production of lipid and carbohydrate from microalgae without compromising biomass productivities: Role of Ca and Mg. **Renewable Energy**, v. 127, p. 989–997, nov. 2018.

HAO, T.-B.; BALAMURUGAN, S.; ZHANG, Z.-H.; LIU, S.-F.; WANG, X.; LI, D.-W.; YANG, W.-D.; LI, H.-Y. Effective bioremediation of tobacco wastewater by microalgae at acidic pH for synergistic biomass and lipid accumulation. **Journal of Hazardous Materials**, v. 426, p. 127820, 15 mar. 2022.

HERNÁNDEZ-GARCÍA, A.; VELÁSQUEZ-ORTA, S. B.; NOVELO, E.; YÁÑEZ-NOGUEZ, I.; MONJE-RAMÍREZ, I.; ORTA LEDESMA, M. T. Wastewater-leachate treatment by microalgae: Biomass, carbohydrate and lipid production. **Ecotoxicology and Environmental Safety**, v. 174, p. 435–444, jun. 2019.

HO, S. H.; CHEN, W. M.; CHANG, J. S. Scenedesmus obliquus CNW-N as a potential candidate for CO2 mitigation and biodiesel production. **Bioresource Technology**, v. 101, n. 22, p. 8725–8730, 1 nov. 2010.

HOSSAIN, M. R.; KHALEKUZZAMAN, M.; KABIR, S. BIN; ISLAM, M. B.; BARI, Q. H. Production of light oil-prone biocrude through co-hydrothermal liquefaction of wastewater-grown microalgae and peat. **Journal of Analytical and Applied Pyrolysis**, v. 161, 1 jan. 2022.

ISLAM, M. B.; KHALEKUZZAMAN, M.; KABIR, S. BIN; HOSSAIN, M. R.; ALAM, M. A. Substituting microalgal biomass with faecal sludge for high-quality biocrude production through co-liquefaction: A sustainable biorefinery approach. **Fuel Processing Technology**, v. 225, 1 jan. 2022.

KHAN, S. A.; SHARMA, G. K.; MALLA, F. A.; KUMAR, A.; RASHMI; GUPTA, N. Microalgae based biofertilizers: A biorefinery approach to phycoremediate wastewater and harvest biodiesel and manure. **Journal of Cleaner Production**, v. 211, p. 1412–1419, 20 fev. 2019.

KLINTHONG, W.; YANG, Y. H.; HUANG, C. H.; TAN, C. S. A Review: Microalgae and their applications in CO2 capture and renewable energy. **Aerosol and Air Quality Research**, v. 15, n. 2, p. 712–742, 2015.

KONG, W.; SHEN, B.; LYU, H.; KONG, J.; MA, J.; WANG, Z.; FENG, S. Review on carbon dioxide fixation coupled with nutrients removal from wastewater by microalgae. **Journal of Cleaner Production**, v. 292, p. 125975, 10 abr. 2021.

KUMAR, K.; DAS, D. Growth characteristics of Chlorella sorokiniana in airlift and bubble column photobioreactors. **Bioresource Technology**, v. 116, p. 307–313, 1 jul. 2012.

LAW, X. N.; CHEAH, W. Y.; CHEW, K. W.; IBRAHIM, M. F.; PARK, Y. K.; HO, S. H.; SHOW, P. L. Microalgal-based biochar in wastewater remediation: Its synthesis, characterization and applications. **Environmental research**, v. 204, n. Pt A, 1 mar. 2022.

LEFLAY, H.; PANDHAL, J.; BROWN, S. Direct measurements of CO2 capture are essential to assess the technical and economic potential of algal-CCUS. **Journal of CO2 Utilization**, v. 52, p. 101657, 1 out. 2021.

LI, G.; HU, R.; WANG, N.; YANG, T.; XU, F.; LI, J.; WU, J.; HUANG, Z.; PAN, M.; LYU, T. Cultivation of microalgae in adjusted wastewater to enhance biofuel production and reduce environmental impact: Pyrolysis performances and life cycle assessment. **Journal of Cleaner Production**, v. 355, n. April, p. 131768, 2022.

LI, X.; HE, M.; SUN, G.; MA, C.; LI, Y.; LI, L.; LI, B.; YANG, M.; ZHANG, Y. Toxicological evaluation of industrial effluents using zebrafish: Efficacy of tertiary

treatment of coking wastewater. **Environmental Technology & Innovation**, v. 30, p. 103067, 1 maio 2023.

LIU, X.; CHEN, G.; TAO, Y.; WANG, J. Application of effluent from WWTP in cultivation of four microalgae for nutrients removal and lipid production under the supply of CO2. **Renewable Energy**, v. 149, p. 708–715, 1 abr. 2020.

LORENTZ, J. F.; CALIJURI, M. L.; ASSEMANY, P. P.; ALVES, W. S.; PEREIRA, O. G. Microalgal biomass as a biofertilizer for pasture cultivation: Plant productivity and chemical composition. **Journal of Cleaner Production**, v. 276, 10 dez. 2020.

LOSA, J. P.; SANTOS, F. M.; ALVIM-FERRAZ, M. C. M.; MARTINS, F. G.; PIRES, J. C. M. Dynamic Modeling of Microalgal Growth. *Em*: **Encyclopedia of Marine Biotechnology**. [s.l.] Wiley, 2020. p. 547–567.

LOUHASAKUL, Y.; TREU, L.; KOUGIAS, P. G.; CAMPANARO, S.; CHEIRSILP, B.; ANGELIDAKI, I. Valorization of palm oil mill wastewater for integrated production of microbial oil and biogas in a biorefinery approach. **Journal of Cleaner Production**, v. 296, p. 126606, 10 maio 2021.

LU, L.; GUEST, J. S.; PETERS, C. A.; ZHU, X.; RAU, G. H.; REN, Z. J. Wastewater treatment for carbon capture and utilization. **Nature Sustainability 2018 1:12**, v. 1, n. 12, p. 750–758, 14 dez. 2018.

MAHDY, A.; MENDEZ, L.; BALLESTEROS, M.; GONZÁLEZ-FERNÁNDEZ, C. Protease pretreated Chlorella vulgaris biomass bioconversion to methane via semi-continuous anaerobic digestion. **Fuel**, v. 158, p. 35–41, 15 out. 2015.

MICHIGAN STATE UNIVERSITY, E. P. R. I. Quantifying N2O Emissions Reductions in Agricultural Crops through Nitrogen Fertilizer. **VERRA VCS**, 2013. . Acesso em: 26 dez. 2022

MISHRA, S.; MOHANTY, K. Co-HTL of domestic sewage sludge and wastewater treatment derived microalgal biomass – An integrated biorefinery approach for sustainable biocrude production. **Energy Conversion and Management**, v. 204, 15 jan. 2020.

MORAIS, E. G. DE; AMARO MARQUES, J. C.; CERQUEIRA, P. R.; DIMAS, C.; SOUSA, V. S.; GOMES, N.; RIBAU TEIXEIRA, M.; NUNES, L. M.; VARELA, J.; BARREIRA, L. Tertiary urban wastewater treatment with microalgae natural consortia in novel pilot photobioreactors. **Journal of Cleaner Production**, v. 378, p. 134521, 10 dez. 2022.

MORAIS, M. G. DE; COSTA, J. A. V. Biofixation of carbon dioxide by Spirulina sp. and Scenedesmus obliquus cultivated in a three-stage serial tubular photobioreactor. **Journal of Biotechnology**, v. 129, n. 3, p. 439–445, 1 maio 2007.

NAGARAJAN, D.; CHANG, J. S.; LEE, D. J. Pretreatment of microalgal biomass for efficient biohydrogen production – Recent insights and future perspectives. **Bioresource Technology**, v. 302, p. 122871, 1 abr. 2020.

NAJDENSKI, H. M.; GIGOVA, L. G.; ILIEV, I. I.; PILARSKI, P. S.; LUKAVSKÝ, J.; TSVETKOVA, I. V.; NINOVA, M. S.; KUSSOVSKI, V. K. Antibacterial and antifungal activities of selected microalgae and cyanobacteria. **International Journal of Food Science & Technology**, v. 48, n. 7, p. 1533–1540, 1 jul. 2013.

NAYAK, M.; SWAIN, D. K.; SEN, R. Strategic valorization of de-oiled microalgal biomass waste as biofertilizer for sustainable and improved agriculture of rice (Oryza sativa L.) crop. **The Science of the Total Environment**, v. 682, p. 475–484, 16 maio 2019.

NEWLIGHT TECHNOLOGIES. **VCS Methodology VM0040 Methodology for Greenhouse Gas Capture and Utilization in Plastic MaterialsVERRA VCS**, 2019. . Acesso em: 26 dez. 2022

NGUYEN, T. D. P.; NGUYEN, D. H.; LIM, J. W.; CHANG, C.-K.; LEONG, H. Y.; TRAN, T. N. T.; VU, T. B. H.; NGUYEN, T. T. C.; SHOW, P. L. Investigation of the Relationship between Bacteria Growth and Lipid Production Cultivating of Microalgae Chlorella Vulgaris in Seafood Wastewater. **Energies**, v. 12, n. 12, p. 2282, 14 jun. 2019.

PATEL, A. K.; JOUN, J.; SIM, S. J. A sustainable mixotrophic microalgae cultivation from dairy wastes for carbon credit, bioremediation and lucrative biofuels. **Bioresource Technology**, v. 313, p. 123681, 1 out. 2020.

PURBA, L. D. A.; OTHMAN, F. S.; YUZIR, A.; MOHAMAD, S. E.; IWAMOTO, K.; ABDULLAH, N.; SHIMIZU, K.; HERMANA, J. Enhanced cultivation and lipid production of isolated microalgae strains using municipal wastewater. **Environmental Technology & Innovation**, v. 27, p. 102444, 2022.

Quantifying N2O Emissions Reductions in Agricultural Crops through Nitrogen Fertilizer Rate Reduction Approved VCS Methodology VM0022 Sectoral Scope 14 Quantifying N2O Emissions Reductions in Agricultural Crops through Nitrogen Fertilizer Rate Reduction. [s.d.].

RICCIO, G.; LAURITANO, C. Microalgae with Immunomodulatory Activities. **Marine Drugs 2020, Vol. 18, Page 2**, v. 18, n. 1, p. 2, 18 dez. 2019.

ROSLI, S.-S.; LIM, J.-W.; JUMBRI, K.; LAM, M.-K.; UEMURA, Y.; HO, C.-D.; TAN, W.-N.; CHENG, C.-K.; KADIR, W.-N.-A. Modeling to enhance attached microalgal biomass growth onto fluidized beds packed in nutrients-rich wastewater whilst simultaneously biofixing CO2 into lipid for biodiesel production. **Energy Conversion and Management**, v. 185, p. 1–10, abr. 2019.

SHAHID, A.; MALIK, S.; ZHU, H.; XU, J.; NAWAZ, M. Z.; NAWAZ, S.; ASRAFUL ALAM, MD.; MEHMOOD, M. A. Cultivating microalgae in wastewater for biomass production, pollutant removal, and atmospheric carbon mitigation; a review. **Science of The Total Environment**, v. 704, p. 135303, fev. 2020.

SINGH, V.; MISHRA, V. Evaluation of the effects of input variables on the growth of two microalgae classes during wastewater treatment. **Water Research**, v. 213, n. February, p. 118165, 2022.

SLADE, R.; BAUEN, A. Micro-algae cultivation for biofuels: Cost, energy balance, environmental impacts and future prospects. **Biomass and Bioenergy**, v. 53, p. 29–38, 1 jun. 2013.

SÜNKEL, M.; KAND, D.; VRANCKEN, H.; MILLER, M.; RIEDE, O. Methodology for the reduction of enteric methane emissions from ruminants through the use of feed ingredients**. VERRA VCS**, 2021. . Acesso em: 26 dez. 2022

SUPARMANIAM, U.; LAM, M. K.; UEMURA, Y.; SHUIT, S. H.; LIM, J. W.; SHOW, P. L.; LEE, K. T.; MATSUMURA, Y.; LE, P. T. K. Flocculation of Chlorella vulgaris by shell waste-derived bioflocculants for biodiesel production: Process optimization, characterization and kinetic studies. **Science of The Total Environment**, v. 702, p. 134995, fev. 2020.

SYDNEY, E. B.; STURM, W.; CARVALHO, J. C. DE; THOMAZ-SOCCOL, V.; LARROCHE, C.; PANDEY, A.; SOCCOL, C. R. Potential carbon dioxide fixation by industrially important microalgae. **Bioresource Technology**, v. 101, n. 15, p. 5892–5896, 1 ago. 2010.

VALE, M. A.; FERREIRA, A.; PIRES, J. C. M.; GONÇALVES, A. L. CO2 capture using microalgae. *Em*: **Advances in Carbon Capture**. [s.l.] Elsevier, 2020. p. 381–405.

VARGAS-ESTRADA, L.; LONGORIA, A.; OKOYE, P. U.; SEBASTIAN, P. J. Energy and nutrients recovery from wastewater cultivated microalgae: Assessment of the

impact of wastewater dilution on biogas yield. **Bioresource Technology**, v. 341, p. 125755, 1 dez. 2021.

VASILAKI, V.; MASSARA, T. M.; STANCHEV, P.; FATONE, F.; KATSOU, E. A decade of nitrous oxide (N2O) monitoring in full-scale wastewater treatment processes: A critical review. **Water Research**, v. 161, p. 392–412, 15 set. 2019.

WANG, S.; JI, B.; ZHANG, M.; GU, J.; MA, Y.; LIU, Y. Tetracycline-induced decoupling of symbiosis in microalgal-bacterial granular sludge. **Environmental Research**, v. 197, p. 111095, jun. 2021.

WANG, X. *et al.* A combined light regime and carbon supply regulation strategy for microalgae-based sugar industry wastewater treatment and low-carbon biofuel production to realise a circular economy. **Chemical Engineering Journal**, v. 446, p. 137422, 15 out. 2022.

WANG, Y.; HO, S.-H.; CHENG, C.-L.; GUO, W.-Q.; NAGARAJAN, D.; REN, N.-Q.; LEE, D.-J.; CHANG, J.-S. Perspectives on the feasibility of using microalgae for industrial wastewater treatment. **Bioresource Technology**, v. 222, p. 485–497, dez. 2016.

WOLLMANN, F.; DIETZE, S.; ACKERMANN, J.; BLEY, T.; WALTHER, T.; STEINGROEWER, J.; KRUJATZ, F. Microalgae wastewater treatment: Biological and technological approaches. **Engineering in Life Sciences**, v. 19, n. 12, p. 860–871, 7 dez. 2019.

XIN, C.; ADDY, M. M.; ZHAO, J.; CHENG, Y.; MA, Y.; LIU, S.; MU, D.; LIU, Y.; CHEN, P.; RUAN, R. Waste-to-biofuel integrated system and its comprehensive techno-economic assessment in wastewater treatment plants. **Bioresource Technology**, v. 250, p. 523–531, 1 fev. 2018.

YADAV, G.; KAREMORE, A.; DASH, S. K.; SEN, R. Performance evaluation of a green process for microalgal CO2 sequestration in closed photobioreactor using flue gas generated in-situ. **Bioresource Technology**, v. 191, p. 399–406, 1 set. 2015.

YIM, J. H.; KIM, S. J.; AHN, S. H.; LEE, C. K.; RHIE, K. T.; LEE, H. K. Antiviral Effects of Sulfated Exopolysaccharide from the Marine Microalga Gyrodinium impudicum Strain KG03. **Marine Biotechnology 2003 6:1**, v. 6, n. 1, p. 17–25, 29 set. 2003.

YOO, C.; JUN, S. Y.; LEE, J. Y.; AHN, C. Y.; OH, H. M. Selection of microalgae for lipid production under high levels carbon dioxide. **Bioresource Technology**, v. 101, n. 1, p. S71–S74, 1 jan. 2010.

YOU, X.; YANG, L.; ZHOU, X.; ZHANG, Y. Sustainability and carbon neutrality trends for microalgae-based wastewater treatment: A review. **Environmental Research**, v. 209, n. December 2021, p. 112860, 2022.

YU, K. L.; SHOW, P. L.; ONG, H. C.; LING, T. C.; CHI-WEI LAN, J.; CHEN, W. H.; CHANG, J. S. Microalgae from wastewater treatment to biochar – Feedstock preparation and conversion technologies. **Energy Conversion and Management**, v. 150, p. 1–13, 2017.

ZAREI, M. Wastewater resources management for energy recovery from circular economy perspective. **Water-Energy Nexus**, v. 3, p. 170–185, 1 jan. 2020.

Chapter 2

Nanomagnetic approach applied to microalgae biomass harvesting: advances, gaps, and perspectives

ABSTRACT

Microalgae biomass is a versatile option for a myriad of purposes, as it does not require farmable land for cultivation and due of its high CO_2 fixation efficiency during growth. However, biomass harvesting is considered a bottleneck in the process because of its high cost. Magnetic harvesting is a promising method on account of its low cost, high harvesting speed, and efficiency, which can be used to improve the results of other harvesting methods. Here, we present the state of the art of the magnetic harvesting method. Detailed approaches involving different nanomaterials are described, including types, route of synthesis, and functionalization, variables that interfere with harvesting, recycling methods of nanoparticles and medium. In addition to discussing the overall perspectives of the method, we provide a guideline for future research.

Keywords: Nanomaterials; nanoparticles; magnetism; iron oxide; synthesis route; functionalized nanoparticles.

1. Introduction

Microalgae biomass is a versatile production resource through its high lipid content (up to 57% of dry biomass) (Liu, Wang and Zhou, 2008). This feature makes it useful for the generation of fuels ranging from liquids, such as biodiesel and bioethanol, to solid flakes (Phukan *et al.*, 2011). In addition, microalgae biomass does not require farmable lands, otherwise used for food production, generating from 30 to 100-folds more energy per hectare than any terrestrial plant and fixing high rates of CO_2 during the growth process (Bundschuh *et al.*, 2014).

Microalgae biomass production consists of three steps: cultivation, harvesting, and processing, with harvesting being a limiting factor for the process. In general, the microalgae small size (< 30 μm) (Molina Grima *et al.*, 2003) and low-density increase operational costs and energy consumption, which represents up to 30% of total production value (Wang, H. *et al.*, 2013). Among the harvesting methods studied, promising results were obtained with the chemical flocculation process (efficiency greater than 80%) (Gutiérrez *et al.*, 2016). However, the use of chemicals contaminates the biomass, making its application unfeasible in some cases, such as food supplements (Gobi *et al.*, 2021). In

this sense, new approaches for microalgae harvesting are being developed, such as magnetic separation (Liu, P. *et al.*, 2020).

Magnetic methods, which are among the main options to optimize the harvesting process, employ magnetic agents, such as nanoparticles (NPs). NPs have specific properties, such as high surface area, making them highly reactive, promoting their adsorption processes, and altering their magnetic properties (Gehrke, Geiser e Somborn-Schulz, 2015). Furthermore, nanoparticles can adhere to microalgae walls, enhancing harvesting and lowering operational costs and energy consumption (Wang *et al.*, 2015), with up to 95% efficiency (Abo Markeb *et al.*, 2019). Recently, different kinds of nanomaterials have been studied for microalgae harvesting (Zhao *et al.* 2019); (Toh *et al.* 2014), applying a considerable range of culture media (Abo Markeb *et al.*, 2019) and conditions (Wang *et al.*, 2015). This review provides an overview of microalgae biomass harvesting with emphasis on synthesis, functionalization, and the effect of variables (pH, temperature, among others) on the harvesting process, along with the challenges and perspectives for the use of magnetic nanomaterials in this research area.

2. Microalgae: Morphology and cultivation

Microalgae are ancient photosynthetic organisms found in all aquatic ecosystems (Brennan and Owende 2010). Although only 100,000 species had been described in the literature by 2016, about 200,000 to 800,000 species are estimated to occur around the world (Suparmaniam *et al.*, 2019). These microorganisms are divided into six classes: Chlorophyta (green), Phaeophyta (brown), Pyrrophyta (dinoflagellates), Chrysophyta (diatoms), Rhodophyta (red), and Euglenophyta (euglenoids) (Enamala *et al.*, 2018).

Structurally, microalgae cells comprise a nucleus, chloroplasts, endoplasmic reticulum, vacuoles, Golgi body, and cytoplasm protected by a negatively charged cell wall (-7.5 to -40 mV)(Okoro *et al.*, 2019). As for the chemical composition, microalgae contain mainly carbohydrates (20% dry matter), proteins (45% dry matter), lipids (20% dry matter), and pigments (*e.g.*, lutein, carotenoids, and beta-carotene). Although the type and concentration of microalgae components vary across species (Table 1), these parameters can be adjusted by medium and cultivation conditions (Phukan *et al.*, 2011).

Table 1. Main molecular content of major microalgae species studied in recent years.

Species	**Carbohydrates (% dry matter)**	**Proteins (% dry matter)**	**Lipids (% dry matter)**	**Ref.**
Chlorella vulgaris	23.43	45.23	18.12	(Alagawany *et al.*, 2021)
Nannochloropsis sp.	12.4	36.4	27.8	(Wang, Sheng and Yang, 2017)
Pavlova sp.	26.0	43.0	20.0	(Aysu *et al.*, 2017)
Scenedesmus obliquus	11.5	65.1	10.6	(Amorim *et al.*, 2020)
Tetraselmis sp.	15.0	42.0	14.0	(Khatoon *et al.*, 2014)
Arthrospira platensis	37.4	56.2	6.4	(Ranganathan *et al.*, 2017)
Dunaliella Salina	15.0	57.0	6.0	(Bhattacharya and Goswami 2020)
Haematococcus pluvialis	27.0	48.0	15.0	(Bhattacharya and Goswami 2020)

In general, microalgae can be cultivated in several ways, through different types of system (open or closed), operation modes (batch, semi-continuous, or continuous), and energy and carbon supply to the cell (autotrophic, heterotrophic, or mixotrophic) (Yin *et al.*, 2020). Raceway ponds are the most popular type of open system. They are simple, inexpensive, and can be operated using natural or wastewater. However, long ponds increase evaporation rates and the possibility of contamination (Brennan and Owende 2010). In contrast, these problems hardly occur in closed systems (*e.g.*, tubular design), which are enclosed by glass or plastic structures and have spargers that improve mixing. As a result, biomass production is much higher and the probability of contamination is lower (Figure 1) (Baharuddin *et al.* 2016; Seo *et al.* 2015).

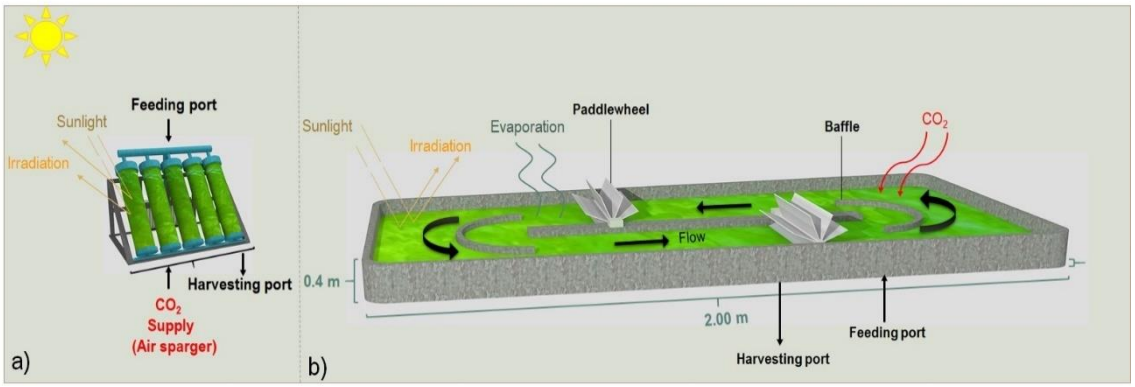

Figure 1. Main systems of microalgae cultivation. a) PBRs (closed systems) and b) Raceway ponds (open systems)

As to operate modes, the batch mode is more efficient when the focus is nutrient removal, such as in wastewater treatment. However, the volumetric production of biomass is lower compared with that of continuous operation (Bernardes, 2011; Mohammadi *et al.*, 2018). Thus, semi-continuous and continuous modes are the most desirable for large-scale production, because of high productivity, control of growth rate, and better-quality biomass. In the semi-continuous mode, biomass harvesting is intermittent, while in the continuous mode the input of culture medium and removal of nutrients is continuous (Yin *et al.*, 2020).

Regarding metabolic pathways, the physiological and biochemical responses of different species to different metabolisms are usually very significant. Heterotrophic cultivation, which uses organic carbon (*e.g.*, glucose and acetate) and low light, has gained attention because of higher biomass production rates (Wang *et al.*, 2017) compared with autotrophic cultivation, which uses inorganic carbon (CO_2). On the other hand, there are mixotrophic species capable of combining mechanisms that use organic and inorganic carbon (Kim, S. *et al.*, 2013). However, the molecular physiology of mixotrophic microalgae is not fully understood yet (Vidotti *et al.*, 2020). Some species can adapt to all three metabolic pathways, such as *Chlorella sorokiniana* (Kim, S. *et al.*, 2013), *Chlorella zofingiensis* (Liu *et al.*, 2011), and *Chlorella vulgaris* (Vidotti *et al.*, 2020).

3. Harvesting

The harvesting process entails removing the excess water of microalgae biomass through a sequence of steps. Microalgae can be harvested through four methods (Figure 2): physical (gravity sedimentation, centrifugation, membrane filtration, and flotation), chemical (flocculation and coagulation), biological (autoflocculation and bioflocculation), and magnetic methods (mainly magnetic nanoparticles (MNPs)) (Figure 2).

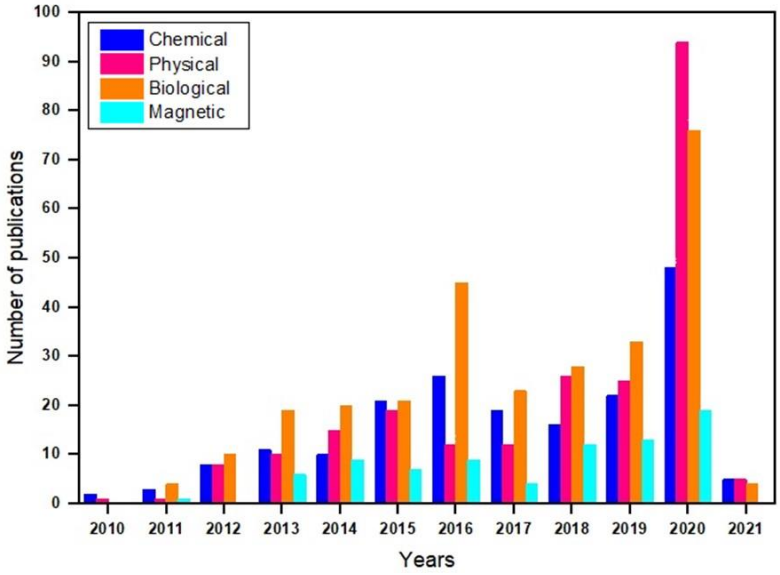

Figure 2. Number of publications related to the four harvesting methods from 2010 to December 6, 2020. The search was conducted on the Scopus platform using the search string: Topic = (microalgae* OR microalgae biomass) AND topic = (harvesting* OR recovery OR harvest) AND topic = (autofloculation* OR bioflocculation* OR coagulation* OR flocculation* OR centrifugation* OR bioflocculation* OR flotation* OR “gravity sedimentation”* OR “magnetic methods”* OR “chemical methods”* OR “physical methods”* OR “biological methods”* OR “magnetic nanoparticle”* OR nanoparticle*). Papers using more than one harvest method have been computed for each method.

Physical methods, which are less complex than the other methods, are based on the use of physical properties of the material, medium, or environment for dewatering (solid/liquid), and are often associated with biological and chemical methods. This, in

turn, justifies the increase in publications along the timescale evaluated (Figure 2). A harvesting efficiency HE> 89% was obtained through gravity sedimentation using *Golenkinia* SDEC-16; however, as sedimentation is time-consuming, this method is suitable for microalgae of high cytoplasmatic density (Nie *et al.*, 2018). Centrifugation is also yet another efficient method to harvest microalgae, with HE> 95% (13,000 xg) having been reported (Xu *et al.*, 2015). Nevertheless, as high shear rates can disrupt the microalgae cell wall, it is not recommended when soluble metabolites (*e.g.*, β-carotene) must be recovered (Molina Grima *et al.*, 2003). Physical methods have some negative points, such as high energy consumption, expensive implantation and maintenance, besides fouling (*e.g.*, membrane application) (Mathimani and Mallick 2018).

In chemical flocculation, the microalgae can interact with the flocculant through four mechanisms, individually or combined: I) charge neutralization; II) electrostatic patch; III) polymer bridge; and IV) sweeping flocculation (precipitation of minerals and microalgae) (Vandamme, Foubert anfd Muylaert, 2013). Main chemical flocculants include $Fe_2(SO_4)_3$, $FeCl_3$, $Al_2(SO_4)_3$, and inorganic polymers (polyaluminium chloride (PACl) and polyacrylamide (PAM)) (Ahmad *et al.*, 2011). The impossibility of separating the chemical flocculant from the harvested microalgae causes the harvested biomass to potentially contain high rates of metal, making the use of microalgae unfeasible in some applications, *e.g.*, as medicines (Gerardo *et al.*, 2015). *Chlorella sp.* KR-1 was harvested by $FeCl_3$ (560 mg L^{-1}) and $Fe_2(SO_4)_3$ (1,060 mg L^{-1}); in both cases HE was higher than 99% (Kim *et al.*, 2015). In the harvesting of *Microcystis aeruginosa* induced by pH, $FeCl_3$, $AlCl_3$, and chitosan, the best performance was obtained using 3.75 mg L^{-1} of $FeCl_3$ (HE= 92%) (Geada *et al.*, 2019).

Biological harvesting methods employ natural characteristics of microalgae (such as autoflocculation) or the association between plant compounds and microorganisms (bioflocculation). It is noteworthy that, although highly efficient, autoflocculation is not a usual process, as the presence of negatively charged functional groups on the cell surface, such as carboxyl and sulfate, promote electrostatic repulsion (Salim *et al.*, 2013). A limited carbon dioxide supply for long periods of time increases the pH, inducing autoflocculation mediated by the precipitation of carbonate salts. Alkaline pH values can occur in the exponential growth phase due to high CO_2 consumption during photosynthesis, as in the case of *Phaeodactylum tricornutum* (Şirin *et al.*, 2012). Bioflocculation, on the other hand, includes polysaccharides and proteins that can form bridges between cells, resulting in larger and more stable flakes (Jung *et al.* 2015);

(Ummalyma *et al.* 2017). Extracellular polymeric substances (EPS) are an example of a macromolecular compound that induces bioflocculation. (Aljuboori *et al.* 2016) showed that EPS associated with Zn^{2+}; which neutralizes the residual charge of EPS functional groups, acting as a bridge between microalgae cells; was efficient, flocculating up to 86.7% of the microalgae *Scenedesmus quadricauda*. Mung bean protein (MBP) is yet another efficient compound, having induced a robust bioflocculation of *Nannochloropsis* sp. (HE> 92%; flocculant dosage 20 mL L^{-1}). A strong bond between MBP and microalgae cells was formed, resulting in firm flakes (Kandasamy and Shaleh 2017). Other examples of bioflocculation agents are tannin (Fuad *et al.*, 2018), chitosan (Farid *et al.*, 2013), and *Moringa oleifera* (Baharuddin *et al.*, 2016). References to biological harvesting methods have increased in the last few years because these are low-cost, environmentally friendly methods. Moreover, the harvested biomass is purer than that from chemical methods (Shurair *et al.*, 2019).

4. Magnetic method

The magnetic method is the most recently developed harvesting method, featuring an increasing number of studies (Figure 2). This relatively new method has characteristics that stand out compared with the other methods. As in most physical methods (centrifugation, filtration, and sedimentation), it yields pure, high-quality biomass, albeit with much lower energy expenditure. Also, the possibility to recycle nanoparticles several times is one of the unique strengths of the magnetic method. In the other techniques, such as flocculation and bioflocculation, the flocculant remains in the biomass for downstream processes (Yin *et al.* 2020). However, some concerns such as the separation between biomass and nanoparticles after harvest can be a challenge and should be considered (Okoro *et al.*, 2019).

The magnetic method requires the interaction between microalgae and selective magnetic adsorbents (magnetic nanoparticles), what makes them sensitive to an external magnetic field. Nanomaterials are materials in which at least one dimension is within nanoscale (from 1 to 100 nm), and can be classified into several types (Das *et al.*, 2020). The main properties of nanomaterials include electrical, mechanical, optical, and magnetic properties, the latter being the most exploited to harvest microalgae. Zero-dimensional species (0D) are the most commonly used (nanoparticles; mostly iron oxide) (Abo Markeb *et al.*, 2019b), although two-dimensional (2D) species are also employed

(graphene oxide) (Liu *et al.*, 2016). In magnetic harvesting methods, iron oxide nanoparticles (IONPs) play a key role. These include mainly Fe_3O_4 (magnetite) and γ-Fe_2O_3 (maghemite), due to attractive magnetic characteristics. Magnetic materials are divided into five groups: diamagnetic, paramagnetic, ferromagnetic, antiferromagnetic, and ferrimagnetic (Petry *et al.*, 2019). In diamagnetic materials, atoms are not unpaired; thus, a weak repulsion occurs after being exposed to an applied magnetic field, with the alignment of the atoms' magnetic moments being lost upon the removal of the external field. In ferromagnetic materials, permanent and aligned magnetic moments occur regardless of the presence of a magnetic field (similar magnet behavior). However, antiferromagnetic materials have a null magnetic moment because the spins align in opposite directions, despite having the same magnitude. Ferrimagnetic materials, on the other hand, have different magnitudes and antiparallel magnetic moments, resulting in spontaneous magnetism (Figure 3) (Petry *et al.* 2019); (Arruebo *et al.* 2007).

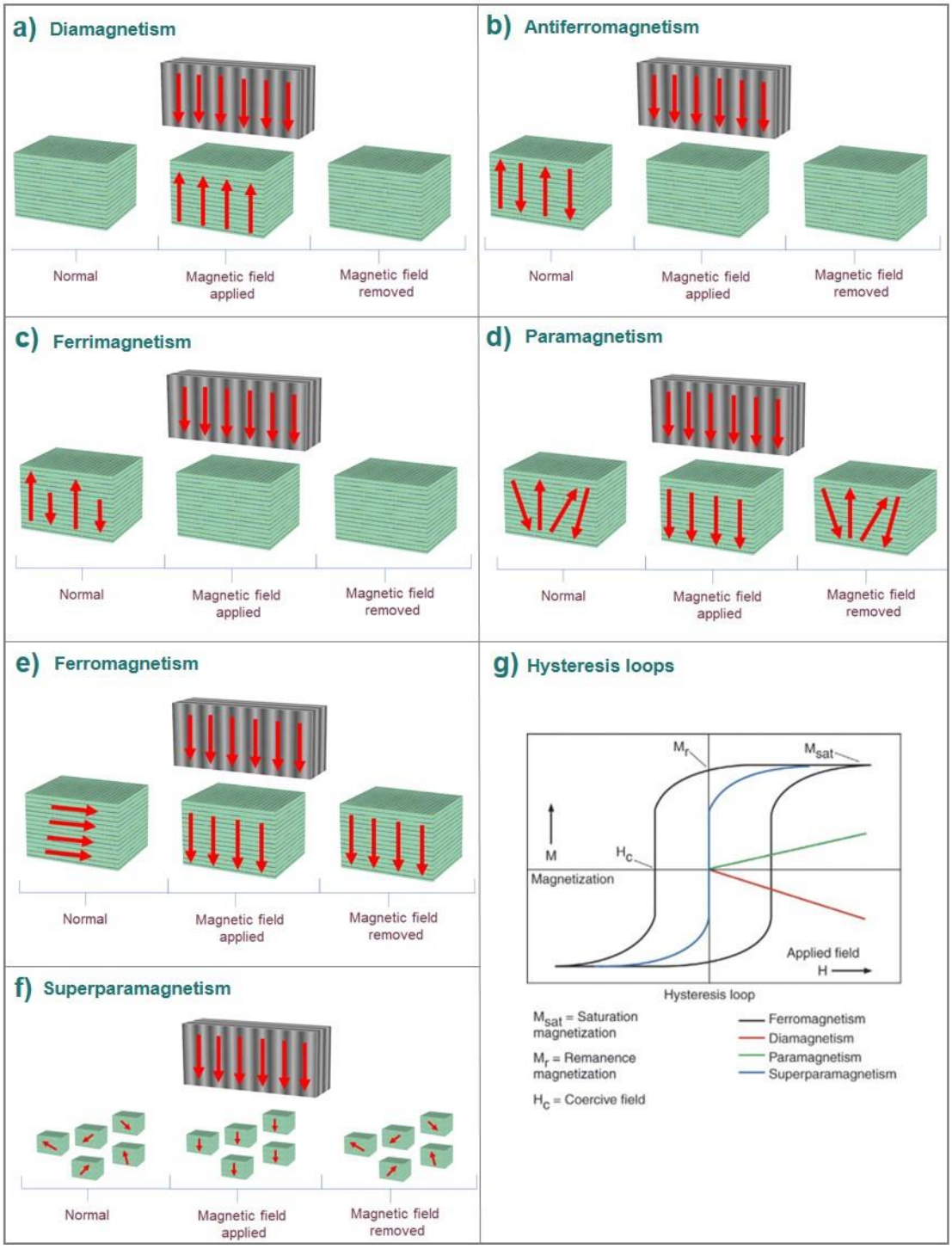

Figure 3. The main types of magnetism in nanomaterials and their respective hysteresis loops (based on (Petry *et al.* 2019); (Arruebo *et al.* 2007) (License numbers: 5017650713190; 5017641458639)).

Superparamagnetism can occur in nanoparticles (< 30 nm), especially when thermal energy exceeds anisotropy energy (Singh *et al.*, 2015). Superparamagnetic nanoparticles are used mostly because of their potential to be magnetized up to saturation

through an external magnetic field. However, if the magnetic field is removed, the spins assume their previous organization. Overall, both Fe_3O_4 and γ-Fe_2O_3 show superparamagnetism. However, Fe_3O_4 (bulk materials; 92-100 Am^2 kg^{-1}) has higher saturation magnetization than γ-Fe_2O_3 (60-80 Am^2 kg^{-1}) (Figure 3) (Cornell and Schwertmann 1996). All ferrite present high magnetization (Co, Cu, Ni), albeit with some disadvantages, such as oxidation, absence of biocompatibility, and high cost (Horák *et al.*, 2007). Notwithstanding, superparamagnetic NPs have many advantages, such as less agglomeration due to zero reminiscence, higher magnetization, and lower magnetic field application (Horák *et al.* 2007;Borlido *et al.* 2013). Also, magnetite is amphoteric: its surface charge ranges from positive (from acid to neutral pH) to negative (from pH 7 to alkaline pH) values, enabling the interaction with the microalgae negative cell wall in acid pH, thus improving harvesting through an electrostatic attraction mechanism (Hu *et al.*, 2013). (Bharte e Desai 2019) achieved a highly efficient harvesting of *Chlorella pyrenoidosa* (90% HE; 1 g L^{-1}) with 500 mg. L^{-1} iron oxide nanoparticles (IONPs), and of *Chlorella minutissima* (85% HE; 1 g. L^{-1}) using 600 mg L^{-1} IONPs, both without any surface modification.

Furthermore, γ-Fe_2O_3 are also superparamagnetic NPs and can be obtained through Fe_3O_4 oxidation. Color is a good indicator of change in the crystalline phase, Fe_3O_4 is naturally black, becoming reddish- brown in its oxidized state (Goss, 1988). This superparamagnetic NP yields considerable results in microalgae harvesting; *e.g.*, blooming microalgae predominantly *Microcystis aeruginosa,* but also *Pediastrum boryanum, Cymbella affinis,* and *Ulnaria ulna*, were harvested with 82.4% efficiency (Duman, Sahin and Atabani, 2019). Other materials have been applied to harvest microalgae and yielded satisfactory results. One such material is barium ferrite ($BaFe_{12}O_{19}$), especially in barium hexaferrite form, which presents a strong and unusual uniaxial anisotropic magnetic field. $BaFe_{12}O_{19}$ was employed to harvest *Chlorella* sp. KR-1 in two forms: naked NPs and NPs functionalized by (3-aminopropyl) triethoxysilane (APTES). Naked NPs have a slightly positive surface charge (< 10 mV) that decreases near the isoelectric point (pH ≈ 5.2), while functionalized NPs are highly positive at pH 5 (≈ 40 mV) (Seo *et al.*, 2014a) due to the protonation of the amine terminal (NH^{3+}) (Howarter e Youngblood 2006). The isoelectric point changed at pH 9.8, improving adsorption in the microalgae cell wall (99.5% HE, 3 min.) (Seo *et al.*, 2014b). Thus, barium ferrite is also considered a good option for harvesting microalgae.

4.1 Synthesis route of magnetic nanoparticles

Nanomaterials can be synthesized by three routes: physical, chemical, and biological. Some synthesis methods are listed in Table 2, along with general information on them.

Table 2. Metadata on different routes for the synthesis of nanomaterials.

Synthesis methods	**Precursors**	**Nanomaterial**	**Size**	**Additional characteristics**	**Ref.**
Ball milling method	$(Fe(NO_3)_3 \cdot 9H_2O)$ $(C_2H_6O_2)$ $(C_8H_{11}NO_2 \cdot HCl)$ Pot and ball (steel)	Carbon-encapsulated Fe_3O_4	13 nm, 9 nm, 7 nm, and 10 nm to 0.1, 0.2, 0.3 and 0.6 dopamine-dosage, respectively.	-Saturation magnetization is lower bulk Fe_3O_4	(Zhang and Wen 2020)
Laser ablation	-	Fe NPs	From 277 nm to 1090 nm.	-Low stability (it agglomerates)	(Kupracz *et al.*, 2020)
Coprecipitation	-Ferrous and ferric chlorides; -Ammonium hydroxide; -Glycerol.	Iron oxide NPs (mixed phase; Fe_3O_4 and γ-Fe_2O_3).	From 30 nm to 55 nm.	- Saturation magnetization of 56 emu g^{-1}; -Non-zero hysteresis; -Uniform and highly-crystalline NPs are synthesized at alkaline pH values; - Polydisperse nanoparticles are	(Smolkova *et al.*, 2015)

				formed when the pH ranges from acidic to alkaline during synthesis.	
Sol–gel	-Iron (II) chloride tetrahydrate (98%); -Propylene oxide (99%); -Absolute ethanol.	α-Fe_2O_3 γ-Fe_2O_3 Fe_3O_4	4.9 nm (γ-Fe_2O_3; Fe_3O_4); 10.1 nm (α-Fe_2O_3).	- γ-Fe_2O_3 and Fe_3O_4, narrow size distribution; -Higher average size.	(Cui, Liu and Ren, 2013)
Hydrothermal	$FeSO_4$ $CH_3(CH_2)_8COOH$ $CH_3(CH_2)_9NH_2$	α-Fe_2O_3/ Fe_3O_4	α-Fe_2O_3 (25 nm); Fe_3O_4 (14 nm).	-When $CH_3(CH_2)_8COOH$ was used for NPs modification, cubic NPs were obtained; -When $CH_3(CH_2)_9NH_2$ was used for NPs modification, spherical NPs were obtained.	(Takami *et al.*, 2007)
Green synthesis (plant extract)	-($Fe(NO_3)_3.9H_2O$ (98%); - Antioxidant from *Stevia* leaves extract.	Fe_3O_4	<25 nm	-High stability (zeta potential of −41.1 mV); - Saturation magnetization of 5.35 emu g^{-1}; -NPs have a shell made mainly of	(Khatami *et al.*, 2019)

				carbohydrate compounds.	
Extracellular biosynthesis	-Iron chloride; -Sodium dodecyl sulfate; -Sodium citrate; -Dimethyl sulfoxide; - Nutrient broth of *Bacillus cereus*.	Fe_3O_4	29.3 nm	- Saturation magnetization of 58.96 emu g^{-1}; - Different surface groups (hydroxyl, carboxyl, carbonyl and amine).	(Fatemi *et al.*, 2018)

4.1.1 Physical route

The physical route encompasses mechanical and vapor methods. Mechanical milling is always cited among mechanical techniques; it involves energy transfer from the balls to the sample powder, what changes the temperature of the process (Figure 4) (Tjong and Chen 2004). Despite extensively studied, this technique has some limitations, such as long milling times and aggregation of nanoparticles, which hinders the precise refining of crystals and the control of nanoparticle size. Thus, the addition of chemical components is common, and the method is now known as the mechanochemical method. In this method, chemical reagents such as reducing agents and surfactants can help stabilize NPs. Some factors can be combined to control particle size, such as type of mill, milling container, milling speed, chemical agent, and especially milling time, to (maintain a stable fracture state and welding of particles) (Ghorbani, 2014). Metallic NPs such as Ag, Cu, oxides, sulfides, and Fe_3O_4 are produced primarily by the mechanochemical method (Marinca *et al.*, 2016; Paskevicius *et al.*, 2009).

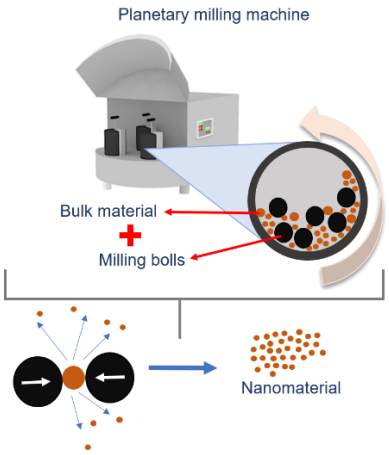

Figure 4. Mechanical milling synthesis of nanomaterials by a planetary milling machine.

On the other hand, the laser ablation technique, which produces nanoparticles with narrow size distribution (500 nm), have emerged as a very attractive, yet complex process. The method consists of heating a target surface to boiling point through laser pulses, what then generates a plasma plume containing the atoms of the target material. By expanding the plasma, condensation takes place and nanoparticles are formed (Ghorbani, 2014). (Muniz-Miranda *et al.* 2017) produced bimetallic Fe_3O_4/Ag NPs by laser ablation, with both magnetic and plasmonic characteristics. The laser ablation method is environmentally friendly, easy to execute, and useful for working with lasting, stable NPs (Dell'Aglio *et al.*, 2015).

4.1.2 Chemical route

As a whole, the chemical route includes a reduction reaction by organic and inorganic agents (Das *et al.*, 2020). Several methods use precipitation to produce nanoparticles, such as coprecipitation, sol-gel, and hydrothermal. The precipitation process involves the precipitation of substances dissolved in the medium by supersaturation. In coprecipitation nucleation, growth and agglomeration occur at the same time. Nucleation has a key role in this process and must happen slowly to yield uniform nanoparticles. It is considered a rapid and simple method that allows modification of the particle surface (Rane *et al.* 2018;Nam e Luong 2019). As a result, it is the main synthesis method adopted to produce NPs applied to microalgae harvesting (Figure 5) (Wang *et al.* 2016; Liu *et al.* 2019).

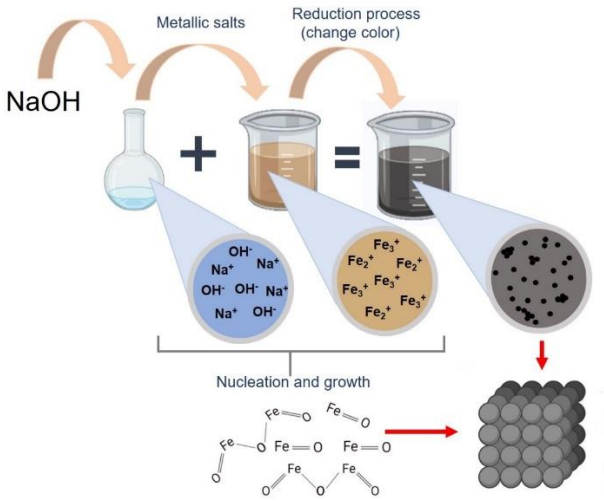

Figure 5. Synthesis of magnetite nanoparticles by coprecipitation.

On the other hand, in the sol-gel process, the transition between a liquid solution "sol" to a solid "gel" phase occurs through a series of hydrolysis and polymerization reactions (Pooyan, 2005). This method has some advantages: it requires relatively low temperatures, it has good stoichiometric control of the precursors, and it produces high purity materials (Kumar, 2020). The hydrothermal method, on the other hand, can be applied when the synthesis employs materials insoluble at normal temperature and pressure. In this case, the synthesis occurs by chemical reactions in a sealed heated solution above normal temperature and pressure. It is considered a success in the preparation of various solids such as magnetic materials, luminescence phosphors, fluorides, and others (Rane *et al.*, 2018). Some advantages of this technique include the use of relatively mild temperatures (< 300 °C), good dispersion, and environmentally friendly (Li and Liu, 2010).

4.1.3 Biological route

Biological methods are considered environmentally friendly, non-toxic, and low-cost. These methods are applied mainly in the production of metallic NPs such as Ag (silver) (Alkhalaf, Hussein and Hamza, 2020), CuO (copper oxide) (Velsankar *et al.*, 2020), zinc oxide (Bandeira *et al.*, 2020), Fe_3O_4 (Ruíz-Baltazar, 2020), among others. The synthesis can occur through the application of phytochemicals (*e.g.*, antioxidants and polyphenols) from several parts of the plant, such as leaves, roots, stems, and fruits, which work as stabilizing agents (Figure 6) (Khare *et al.*, 2019).

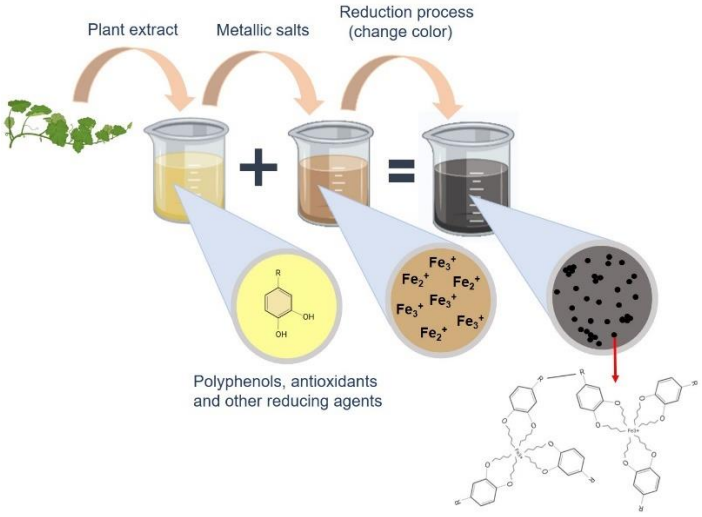

Figure 6. Synthesis of magnetite nanoparticles using molecules extracted from plants as reducing agents.

Despite being useful, this approach does not have a well-established reduction mechanism yet. The extracts are produced from different species at different concentrations, what can interfere with the characteristics of the nanoparticles. Other variables that interfere in the process are the concentration of metal salts, pH, temperature, and reaction time (Kumar and Yadav, 2009). The main problem with this method is the presence of impurities in the extracts, which can reduce saturation magnetization (Goss, 1988). Moreover, the presence of impurities generates nanomaterials with low crystallinity, which are common products of synthesis by natural reducing agents at mild temperatures (Barizão, *et al.*, 2020). However, that does not occur in some instances; maghemite, for example, was produced free of impurities in an environmentally friendly manner (Duman, Sahin and Atabani, 2019).

Reducing agents can also be provided by bacteria and fungi. In such cases, vital enzymes and proteins work as reducing agents and biocatalysts, rendering it a simple method owing to the ease of cultivation of such microorganisms (Fernández *et al.*, 2016). Synthesis can occur in two different ways: intracellularly, in which metal ions are absorbed by reducing enzymes and stored in the cytoplasm or cell wall, and extracellularly, in which the reducing agents are on the cell-free supernatant. Of these two methods, extracellular synthesis stands out because of the easy NP recovery step (Sadhasivam, Vinayagam and Balasubramaniyan, 2020).

The use of fungal culture supernatant is also common. *Manglicolous fungi* from Indian Sundarbans, for example, were tested in the synthesis of iron oxide nanoparticles. Different extracellular fungal enzymes, proteins, and other bioactive composts act as hydrolyzing agents, forming covalent, van der waals, or hydrogen bonds with dissociated iron ions (Fe^{3+} and Fe^{2+}). Very small NPs were produced this way, in the range of 2-16 nm. The bioactive compounds on the surface of the NPs (mainly proteins) generated diamagnetic hindrance. Thus, the resulting nanoparticles were considered paramagnetic at room temperature, although they did exhibit superparamagnetic characteristics at low temperatures (Mahanty *et al.*, 2019).

4.2 Methods of functionalization

Despite the successful results of naked NP applications, several studies suggest surface functionalization to optimize the process. Functionalization can change surface charge, size, magnetic properties, and other features of NPs, favoring an efficient microalga harvesting. There are some options for functionalization, including other nanomaterials. Polyamidoamine (PAMAM) is one of the most common dendrimers, especially because it ensures straightforward synthesis and surface functionalization (Sabín López *et al.*, 2020). In some cases, functionalization takes three steps. In the first stage, silane is inserted into Fe_3O_4NPs; in the second stage, NPs are grafted through Michael addition – a reaction between nucleophiles and olefins/alkynes in which the nucleophile is added across carbon-carbon multiple bonds (Pascault and Williams, 2012); in the last stage, an amination reaction takes place, resulting in highly positive NPs that did not aggregate because of strong electrostatic repulsion, thus favoring the adsorption between nanoparticles and algae cells. In addition, NPs stability increased over a much larger pH range, with the isoelectric point ranging from pH≈ 6 in naked NPs to pH≈ 9.2 in functionalized NPs (Figure 7). Although the saturation magnetization suffered a slight drop, from 62.7 emu g^{-1} to 66.7 emu g^{-1} (magnetization volume). However, it was sufficient to separate the microalgae from the culture medium, reaching 95% HE in 2 minutes (80 mg L^{-1} NPs at pH 8.0; natural pH of *Chlorella sp.* culture). For naked nanoparticles, 200 mg L^{-1} was required to ensure the same harvest efficiency of 95% at pH 8 (Wang, T. *et al.*, 2016).

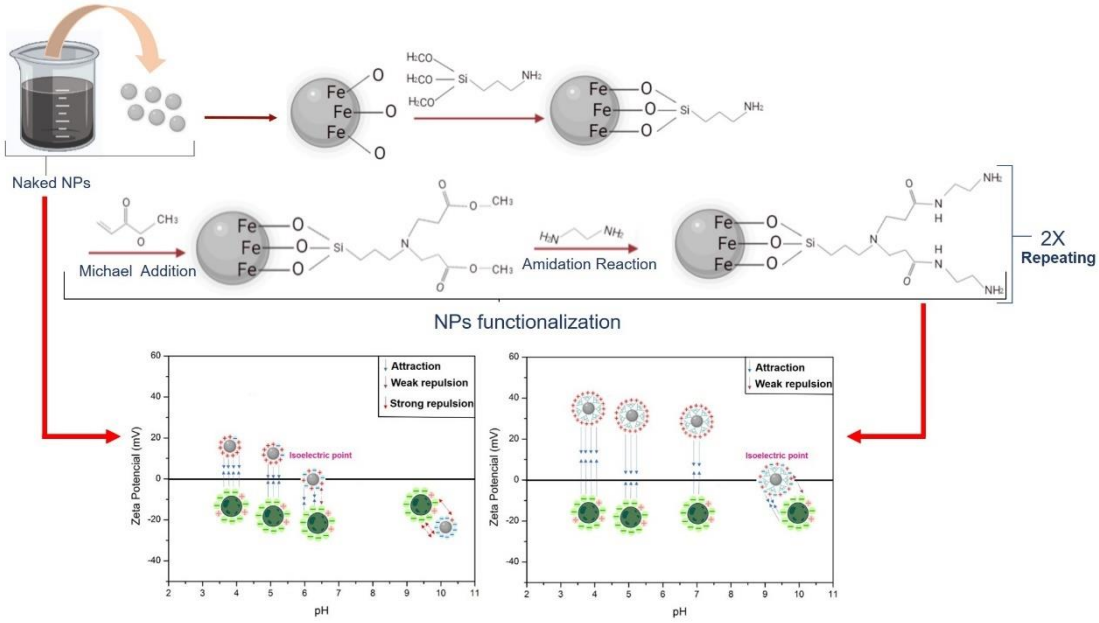

Figure. 7 Functionalization of Fe_3O_4-PAMAM NPs and interaction between microalgae and NPs at different pH values. a) *Chlorella sp.* and naked Fe_3O_4NPs; b) *Chlorella sp.* and Fe_3O_4NPs grafted with amino-rich dendrimers (based on (Wang, T. *et al.*, 2016) (License number: 5017660317864)).

Furthermore, magnetic graphene oxide (Fe_3O_4 + graphene oxide) was modified for microalgae harvesting. Modifications were required because, despite the super adsorbent surface, its functional groups are rich in oxygen, resulting in a negative charge. Studies associating magnetic graphene with a PDDA (diallyl dimethylammonium chloride) cationic polymer showed that the new material achieved a harvest efficiency of 95.35%, which is higher than that of magnetic graphene oxide application alone (80.14% HE for 70 mg NPs L^{-1} dose of algae cells in 5 min) (Liu *et al.*, 2016).

The use of synthetic and natural polymers for functionalization is common, with NPs assuming the shape of a magnetic core surrounded by a polymeric shell, which provides functional groups favorable for harvesting (Hu Yang and Bo Yuan, 2009). (Liu *et al.* 2019)) achieved harvest efficiencies of 98.92 ± 0.41% for *Chlorella pyrenoidosa* (0.5 g L^{-1}) in a 20 min flocculation time with 20 mL L^{-1} NPs, and of 45 ± 0.35% for *Scenedesmus obliquus* (0.4 g L^{-1}) in a 15 min flocculation time with 16 mL L^{-1} NPs, using Fe_3O_4NPs coated with polyethyleneimine (PEI; an organic polymer). Nevertheless, (Hu *et al.* 2014) used Fe_3O_4 NPs coated with PEI to harvest *Chlorella ellipsoidea*, achieving a 97% HE in 2 min using a nanocomposite dosage of 20 mg L^{-1}. This demonstrates that nanocomposites formed by the same material can have different harvesting capacities. As

to natural polymers, chitosan is the most frequently studied for microalgae harvesting. It has a high capacity to effectively destabilize the negative charge of microalgae (through polymer bridging or electrostatic patch effects) inducing larger flakes formation. The chitosan-based flocculant showed a harvesting efficiency of 46% in *Chlorella vulgaris*, a very small value compared to the magnetic chitosan's harvesting efficiency of 91.4% (Barekati-Goudarzi *et al.*, 2016). Several binders coated NPs are found in the extant literature, with highly significant HEs (Table 3).

Table 3**.** Some binders from literature data and their respective harvesting efficiency (HE) for different microalgae species.

Microalgae	**Nanoparticle**	**Binder**	**HE**	**Ref.**
Chlorella sp.	**Fe_3O_4**	Poly(diallyldimethylammonium chloride) (PDDA)	98%	(Toh *et al.*, 2014)
Chlorella sp.	**Fe_3O_4**	Chitosan	99%	(Toh *et al.*, 2014)
Chlorella sp.	**Fe_3O_4**	Carbon microparticles	99%	(Seo *et al.*, 2015)
Chlorella sp.	**Fe_3O_4** (10 mg L^{-1})	polyarginine (PA)	95%	(Liu *et al.*, 2017)
Chlorella vulgaris	**Fe_3O_4** (200 mg L^{-1})	Polyethyleneimine (PEI)	97%	(Gerulová *et al.*, 2018)
Botryococcus braunii	**Fe_3O_4** (200 mg L^{-1})	Polyethyleneimine (PEI)	68%	(Gerulová *et al.*, 2018)
Chlorella sp. TISTR8236	**Fe_3O_4** (500 mg L^{-1})	Cassava starch	98%	(Jangyubol *et al.*, 2018)
Chlorella vulgaris	**Fe_3O_4** (5 g L^{-1})	Quaternary ammonium (QPP)	91.0%	(Zhao *et al.*, 2019)
Chlorella vulgaris	**Fe_3O_4** (20 g L^{-1})	Natural polymer from *Larix gmelinii*	95.6%	(Wang *et al.*, 2018)
Chlorella vulgaris	**Fe_3O_4** (25 mg L^{-1})	Amine	>95%	(Almomani, 2020)

4.3 Variables that affect harvesting

The interaction levels between microalgae and nanoparticles change according to certain variables, such as pH, growth stage, NP dosage, and temperature. The electronegativity of the microalgae cell wall varies according to growth phases, with better harvesting rates being obtained on the exponential phase near the stationary phase, where the cell wall has a higher surface load. For *Chlorella sp.* the ideal moment to apply magnetic harvesting is on the 10^{th} day (maximum growth is reached at the 14^{th} day) (Lim *et al.*, 2012). Furthermore, studies on *Chlorella zofingiensis* report that the number of functional groups (carboxyl, phosphate, and mine/hydroxyl) is higher in the exponential phase, declining in the following phases. The surface charge went from -20.6 ± 0.9 mV (exponential phase) to -12.2 ± 0.5 mV (declining phase), reducing the stability of cells (Zhang *et al.*, 2012), as confirmed by the zeta potential. However, the process is specific to each microalga species.

Nanoparticle dosage is another important factor, as it also varies according to each species and other variables, and it can increase until saturation point. Naked Fe_3O_4 NPs at 0.12 g L^{-1} were applied to the harvesting of *Nannochloropsis maritima*, with 95% HE (Hu *et al.*, 2013). When the same nanoparticles were applied in the harvesting of *Botryococcus braunii* and *Chlorella ellipsoidea* at 75 and 300 mg L^{-1}, respectively, a slightly higher efficiency (< 98%) was achieved (Xu *et al.*, 2011a). Although the nanoparticles were the same, optimal concentrations varied considerably. Functionalized NPs can be strongly positive and, in that case, the concentration of NPs decreases dramatically. In order to achieve 95% HE for *B. braunii*, only 0.025 g L^{-1} of Fe_3O_4NPs coated with cationic polyacrylamide (CPAM) were used (Ge *et al.*, 2015). Mixing time and speed are also important variables that can improve the interaction between microalgae and NPs, favoring the formation of larger and more stable flakes. However, these variables are also quite divergent between studies. In general, low agitation speeds and long mixing times achieve higher HE, because these conditions prevent the desorption of molecules from the microalgae surface (Duman, Sahin and Atabani, 2019). This observation was confirmed by (Liu *et al.* 2019) for the harvest of *C. pyrenoidosa* (80.96%) and *S. obliquus* (94.10%), in which the increase in flocculation time up to 12 min led to an increase in efficiency. Regarding agitation speed, intermediate values are preferred, since low speeds reduce the contact between NPs and microalgae, while high speeds can cause excessive shear and break the flakes.

Adsorption and desorption of H^+ and OH^- on the surface of the metal oxide depend highly on pH, thus being the most important parameter of the system (Nascimento, do *et al.*, 2019). Fe_3O_4 is highly positive at pH 4 (<+30 mV) and highly negative at pH 10 (> -30 mV), whereas, at pH 7, it is practically neutral (isoelectric point). The harvesting of *B. braunii* was more efficient at low pH (pH 4≈ -15 mV) because of protonation, and of *C. ellipsoidea* at pH 7.0, in which both NPs and microalgae were practically neutral (Xu *et al.*, 2011a). There are some cases in which the best HE is obtained when both NPs and microalgae are negatively charged, with no electrostatic attraction. That is the case of *C. reinhardtii* (-43 mV at pH 8.8) and *P. tricornutum* (−13 mV at pH 8.8), harvested with naked Fe_3O_4NPs. Harvesting occurred through ion-exchange between protonated amino groups ($–NH^{3+}$) of surface glycoproteins and deprotonated hydroxyl groups ($–O^-$) on the magnetite surface at high pH (Cerff *et al.*, 2012). If the culture medium used is not the traditional BG11 medium, which contains suitable and known components for the cultivation of microalgae, other unknown variables may interfere in harvesting (*e.g.*, suspended solids and natural organic matter– NOM). That is the case when cultivation takes place in fish tanks. Suspended solids and NOM have negative charges and can bind to NPs, thus becoming competitive (Toh *et al.*, 2012).

In open systems, such as those exposed to the environment, monitoring the temperature is important because it can vary considerably. Increased temperatures can improve HE by reducing the viscosity of the medium and/or increasing the energy in the system, intensifying particle distribution and favoring NPs-microalgae adsorption (Wang *et al.* 2015b); (Nassar 2010). However, in some cases, wide temperature variations do not affect HE (Liu *et al.*, 2018). Regarding the magnetic gradient, it can be of two types: *i)* low-gradient magnetic separation (LGMS), which presents low energy consumption, is easy to design, and uses only permanent magnets, with its efficiency depending on the number of NPs that can induce magnetophoresis in labeled microalgae cells; *ii)* while the high gradient magnetic separation (HGMS), which is more expensive but viable, containing a magnetized matrix. Using IONPs to harvest *Scenedesmus* sp., *Spirulina sp*., *Chlorella* sp., *Tetraedron* sp., *Haematococcus* sp., and *Dictyosphaerium* sp. in a fish tank, both LGMS and HGMS showed satisfactory results, although HGMS was less dependent upon NP concentration (Toh *et al.* 2012); (Hirschbein *et al.* 1982). LGMS operated with a permanent magnet of N50 NdFeB (∼6000 G), while HGMS operated under a continuous flow with a magnetic field gradient >1000 T m^{-1}.

4.4 Nanoparticles and medium recycling methods

The recycling of nanoparticles has been investigated, as it reduces the use of expensive reagents necessary to prepare them. Recirculating the culture medium can also be a good option, as it reduces the copious volumes of water needed for cultivation. The main method employed to separate microalgae and NPs is changing the pH, mainly by dissolution in an acid medium. Fe_3O_4 regeneration through dissolution with HCl after harvesting of *C. ellipsoidea* was highly satisfactory (96.3%). However, not all microalgae adapt to this method, which can cause cell lysis, thus becoming unfeasible for some applications. Therefore, the selection of the particle regeneration process depends on its final applications. If the desired compound is intracellular, the NPs do not interfere with further processing technologies by remaining attached to the cell wall. Otherwise, if the cell will be processed as a whole, it is usually desirable to dissolve the NPs to avoid biomass contamination (Prochazkova, Safarik an Branyik, 2013). In this regard, microalgae go through previous treatments before being exposed to NPs. *B. braunii* was treated with 1,2-dimethoxyethane en-hexane to avoid the dissolution of some organic components of the cells. This treatment yielded an NPs-recovery rate of 95.4% after the harvesting of *B. braunii*. These NPs could be reused for up to five cycles while maintaining the same microalgae harvesting capacity (Xu *et al.*, 2011). When merely changing the pH does not yield the expected result, it is possible to modify other variables or apply a combination of methods. Demagnetization of *C. vulgaris* adsorbed in magnetic microparticles of iron oxide under acid treatment (10 vol.% H_2SO_4) was increased from 20% to 100% by introducing energy into the system via ultrasound, what increased the temperature up to 40°C (Prochazkova, Safarik and Branyik, 2013).

The NPs-microalgae separation can also be achieved by increasing the pH using NaOH. Fe_3O_4NPs grafted with starch were regenerated by combining the strong base method with ultrasonic treatment. Regenerated NPs were reused for five cycles, however, the harvesting efficiency decreased from 97.0% to 75.5% (Wang, T. *et al.*, 2016). The strong base method (pH 12) was also adopted in the regeneration of porous Fe_3O_4NPs functionalized with polyarginine associated with *Chlorella sp*. In this case, HE decreased from 95% to 61% after five cycles (Liu *et al.*, 2017). On the other hand, by using dH_2O at pH 12 associated with short ultrasonic time, 94-99% of Fe_3O_4NPs were recovered and it was possible to perform 10 cycles with 90-97% harvest efficiency. Without the ultrasonic process, the recovery of NPs was 90%, albeit with less energy cost (Lee *et al.*,

2014). The particle size can change the efficiency of demagnetization: the smaller the NP, the more complex the process. Smaller NPs tend to bind strongly to the surface of microalgae because of high surface area. Tests using barium ferrite ($BaFe_{12}O_{19}$) conjugated to *Chlorella* sp. demonstrated an increase in demagnetization efficiency from 12.5% to 85%, when the particle size increased from 108 nm to 1.17 μm (Seo *et al.*, 2014).

To support the recycling of the culture medium, studies provided evidence that some microalgae, such as *N. maritime*, were harvested using Fe_3O_4NPs and that the culture medium was reused for five consecutive occasions. No negative effect was found on the final biomass in any cycle (Hu *et al.*, 2013). However, tests carried out to predict the influence of residual nanomaterials in the culture medium revealed that the cells undergo an initial growth stimulus that tends to decay over time. This phenomenon can be associated with negative interactions between NPs and microalgae, such as damage and alteration in the permeability of the cell membrane, reduction of photosynthetic activity by shading effect, and biochemical destruction, among others (Liu *et al.*, 2018). Thus, further studies aiming to improve the quality of the medium recovered are necessary.

5. Economic viability, gaps, and perspectives

The harvesting method selection is directly linked to economic viability. This is considered the biggest challenge in the large-scale production of microalgae. However, several papers do not usually include production costs in their discussions. In most cases, the success of the method is defined only by HE. Nanoparticle concentration, harvesting time, and other variables are also discussed, but the relationship between each variable and their cost is not displayed. Nevertheless, some authors did prove the viability of magnetic harvesting even on prototype scales. (Wang *et al.* 2014) used a circular magnetic separator (2,000 G) in the harvesting of *B. braunni* (1.23 g L^{-1}) by Fe_3O_4 nanoparticles functionalized with cationic polyacrylamide. The authors reported a 90% HE at a cost of US$ 2.07 kg^{-1} of harvested microalgae. This low cost is mostly due to the cost of nanoparticles (US$ 0.73 kg^{-1} of harvested microalgae). Energy expenditure was also considered low (4.50 kWh m^{-3}), well below flotation (18 kWh m^{-3}), for example (Almomani, 2020).

Interesting results were also reported by (Almomani 2020) in the harvesting of a mixed algal culture (2.2 g L^{-1}) using two different NPs, naked Fe_3O_4 NPs and amine-

coated Fe_3O_4 NPs (25 mg L^{-1}). Both cases yielded 90% HE, although in naked Fe3O4 NPs the NPs cost was US$ 2.9 m^{-3}, while coated amine Fe_3O_4 NPs the cost was reduced by 19%. Applying five NPs-reuse cycles, the NP cost was reduced even further, to US$ 0.45 and 0.52 m^{-3}, respectively. The cost of functional magnetic nanocomposites based on graphene (GPF) for the harvesting of *Chlorella* sp. (191 mg L^{-1}) was also reported. High harvesting efficiency was obtained (HE> 95%) and the cost was US$ 7.27 Kg^{-1}, a sum slightly higher than that of Fe_3O_4 because of the high cost of graphene.

Although the cited examples demonstrate the economic viability of magnetic harvesting, most cases take only the NPs cost into account, excluding energy expenditure, labor, equipment, and maintenance. This is due to a high number of studies reporting only small-scale experiments, hindering the cost estimate of the harvesting process as a whole. Studies reporting simple and efficient magnetic separator designs, on a pilot scale, are still scarce (Wang *et al.*, 2014). Issues such as the best shape for the harvesting chamber and a viable source of magnetic field generation must be carefully investigated. A universal NPs production also needs more attention, for it is still difficult to find NPs that present high HE for several microalgae species. This happens due to very specific interactions between each NPs with each microalgae species, thus, the HE varies substantially in each case. The use of more stable NPs is also desirable. Naked NPs have been successfully applied, although their high instability can limit the recycling process, raising costs. One of the best options for more stable NPs production is the use of binders in functionalization. Some techniques can help in understanding these mechanisms of surface bonding such as as kinetic, isothermal, thermodynamic, and response surface methods (RSM) (Yin *et al.*, 2020).

We believe the magnetic harvesting method may be one of the most effective methods for harvesting microalgae on an industrial scale in a near future. Some applications of microalgae biomass are still unfeasible due to the high cost of production. According to (Ganesan *et al.* 2020), until the year 2020, the production of biofuels from microalgae corresponded to twice the value of first-generation biofuels. In this way, the viability of the harvest stage, one of the costliest, can contribute to reducing the cost of the entire production, thus furthering greater biomass application, mainly on major scales.

6. Conclusions

This review evidenced a myriad of positive results related to the application of the magnetic method to microalgae harvesting, especially by iron oxide NPs. Magnetite and maghemite are notably the most promising materials, due to their strong magnetic behavior. This method has as advantages low energy consumption, low cost, high harvesting efficiency in a short time, and the possibility to recycle both NPs and culture medium. Nevertheless, some points need to be improved. Naked NPs have been successfully applied, although their high instability can limit the recycling process. Regarding the more stable functionalized particles, these can have greater affinity for some microalga species than for others, limiting their application to pure cultures. Notwithstanding, in solving these issues, the magnetic method has the potential to become one of the most viable harvesting methods.

7. References

ABO MARKEB, A.; LLIMÓS-TURET, J.; FERRER, I.; BLÁNQUEZ, P.; ALONSO, A.; SÁNCHEZ, A.; MORAL-VICO, J.; FONT, X. The use of magnetic iron oxide based nanoparticles to improve microalgae harvesting in real wastewater. **Water Research**, v. 159, p. 490–500, 1 ago. 2019.

AHMAD, A. L.; MAT YASIN, N. H.; DEREK, C. J. C.; LIM, J. K. Optimization of microalgae coagulation process using chitosan. **Chemical Engineering Journal**, v. 173, n. 3, p. 879–882, 1 out. 2011.

ALAGAWANY, M.; TAHA, A. E.; NORELDIN, A.; EL-TARABILY, K. A.; ABD EL-HACK, M. E. Nutritional applications of species of Spirulina and Chlorella in farmed fish: A review. **Aquaculture**, v. 542, p. 736841, 15 set. 2021.

ALJUBOORI, A. H. R.; UEMURA, Y.; THANH, N. T. Flocculation and mechanism of self-flocculating lipid producer microalga Scenedesmus quadricauda for biomass harvesting. **Biomass and Bioenergy**, v. 93, p. 38–42, 1 out. 2016.

ALKHALAF, M. I.; HUSSEIN, R. H.; HAMZA, A. Green synthesis of silver nanoparticles by Nigella sativa extract alleviates diabetic neuropathy through anti-inflammatory and antioxidant effects. **Saudi Journal of Biological Sciences**, 8 maio 2020.

ALMOMANI, F. Algal cells harvesting using cost-effective magnetic nano-particles. **Science of the Total Environment**, v. 720, p. 137621, 10 jun. 2020.

AMORIM, M. L.; SOARES, J.; VIEIRA, B. B.; BATISTA-SILVA, W.; MARTINS, M. A. Extraction of proteins from the microalga Scenedesmus obliquus BR003 followed by lipid extraction of the wet deproteinized biomass using hexane and ethyl acetate. **Bioresource Technology**, v. 307, p. 123190, 1 jul. 2020.

ARRUEBO, M.; FERNÁNDEZ-PACHECO, R.; IBARRA, M. R.; SANTAMARÍA, J. Magnetic nanoparticles for drug delivery. **Nano Today**, v. 2, n. 3, p. 22–32, 1 jun. 2007.

AYSU, T.; OLA, O.; MAROTO-VALER, M. M.; SANNA, A. Effects of titania based catalysts on in-situ pyrolysis of Pavlova microalgae. **Fuel Processing Technology**, v. 166, p. 291–298, 1 nov. 2017.

BAHARUDDIN, N. N. D. E.; AZIZ, N. S.; SOHIF, H. N.; KARIM, W. A. A.; AL-OBAIDI, J. R.; BASIRAN, M. N. Marine microalgae flocculation using plant: The case of Nannochloropsis oculata and Moringa oleifera. **Pakistan Journal of Botany**, v. 48, n. 2, p. 831–840, 2016.

BANDEIRA, M.; GIOVANELA, M.; ROESCH-ELY, M.; DEVINE, D. M.; SILVA CRESPO, J. DA. Green synthesis of zinc oxide nanoparticles: A review of the synthesis methodology and mechanism of formation. **Sustainable Chemistry and Pharmacy**, v. 15, p. 100223, 1 mar. 2020.

BAREKATI-GOUDARZI, M.; REZA MEHRNIA, M.; POURASGHARIAN ROUDSARI, F.; BOLDOR, D. Rapid separation of microalga *Chlorella vulgaris* using magnetic chitosan: Process optimization using response surface methodology. **Particulate Science and Technology**, v. 34, n. 2, p. 165–172, 3 mar. 2016.

BERNARDES, M. A. S. **Biofuel's Engineering Process Technology - Google Livros**. Rijeka: [s.n.].

BHARTE, S.; DESAI, K. Harvesting Chlorella species using magnetic iron oxide nanoparticles. **PHYCOLOGICAL RESEARCH**, v. 67, n. 2, p. 128–133, 2019.

BHATTACHARYA, M.; GOSWAMI, S. Microalgae – A green multi-product biorefinery for future industrial prospects. **Biocatalysis and Agricultural Biotechnology**, v. 25, p. 101580, 1 maio 2020.

BORLIDO, L.; AZEVEDO, A. M.; ROQUE, A. C. A.; AIRES-BARROS, M. R. Magnetic separations in biotechnology. **Biotechnology Advances**, v. 31, n. 8, p. 1374–1385, 1 dez. 2013.

BRENNAN, L.; OWENDE, P. Biofuels from microalgae-A review of technologies for production, processing, and extractions of biofuels and co-products. **Renewable and Sustainable Energy Reviews**, v. 14, n. 2, p. 557–577, 1 fev. 2010.

BUNDSCHUH, J.; YUSAF, T.; MAITY, J. P.; NELSON, E.; MAMAT, R.; INDRA MAHLIA, T. M. Algae-biomass for fuel, electricity and agriculture. **Energy**, v. 78, p. 1–3, 15 dez. 2014.

CERFF, M.; MORWEISER, M.; DILLSCHNEIDER, R.; MICHEL, A.; MENZEL, K.; POSTEN, C. Harvesting fresh water and marine algae by magnetic separation: Screening of separation parameters and high gradient magnetic filtration. **Bioresource Technology**, v. 118, p. 289–295, 1 ago. 2012.

CORNELL. R. M.;; SCHWERTMANN, U. **The Iron Oxides: Structure, Properties, Reactions, Occurrences and Uses**. 2. ed. [s.l.] Wiley-VCH Verlag, 1996. v. 1

CUI, H.; LIU, Y.; REN, W. Structure switch between α-Fe2O3, γ-Fe2O3 and Fe3O4 during the large scale and low temperature sol-gel synthesis of nearly monodispersed iron oxide nanoparticles. **Advanced Powder Technology**, v. 24, n. 1, p. 93–97, 1 jan. 2013.

DAS, S.; MUKHERJEE, A.; SENGUPTA, G.; SINGH, V. K. Overview of nanomaterials synthesis methods, characterization techniques and effect on seed germination. *Em*: **Nano-Materials as Photocatalysts for Degradation of Environmental Pollutants**. [s.l.] Elsevier, 2020. p. 371–401.

DELL'AGLIO, M.; GAUDIUSO, R.; PASCALE, O. DE; GIACOMO, A. DE. Mechanisms and processes of pulsed laser ablation in liquids during nanoparticle production. **Applied Surface Science**, v. 348, p. 4–9, 1 set. 2015.

DUMAN, F.; SAHIN, U.; ATABANI, A. E. Harvesting of blooming microalgae using green synthetized magnetic maghemite (Γ-Fe2O3) nanoparticles for biofuel production. **Fuel**, v. 256, p. 115935, 15 nov. 2019.

ENAMALA, M. K.; ENAMALA, S.; CHAVALI, M.; DONEPUDI, J.; YADAVALLI, R.; KOLAPALLI, B.; ARADHYULA, T. V.; VELPURI, J.; KUPPAM, C. Production of biofuels from microalgae - A review on cultivation, harvesting, lipid extraction, and numerous applications of microalgae. **Renewable and Sustainable Energy Reviews**, v. 94, p. 49–68, 1 out. 2018.

FARID, M. S.; SHARIATI, A.; BADAKHSHAN, A.; ANVARIPOUR, B. Using nano-chitosan for harvesting microalga Nannochloropsis sp. **Bioresource Technology**, v. 131, p. 555–559, 1 mar. 2013.

FATEMI, M.; MOLLANIA, N.; MOMENI-MOGHADDAM, M.; SADEGHIFAR, F. Extracellular biosynthesis of magnetic iron oxide nanoparticles by Bacillus cereus strain HMH1: Characterization and in vitro cytotoxicity analysis on MCF-7 and 3T3 cell lines. **Journal of Biotechnology**, v. 270, p. 1–11, 20 mar. 2018.

FERNÁNDEZ, J. G.; FERNÁNDEZ-BALDO, M. A.; BERNI, E.; CAMÍ, G.; DURÁN, N.; RABA, J.; SANZ, M. I. Production of silver nanoparticles using yeasts and evaluation of their antifungal activity against phytopathogenic fungi. **Process Biochemistry**, v. 51, n. 9, p. 1306–1313, 1 set. 2016.

FUAD, N.; OMAR, R.; KAMARUDIN, S.; HARUN, R.; IDRIS, A.; WAN AZLINA, W. A. K. G. Effective use of tannin based natural biopolymer, AFlok-BP1 to harvest marine microalgae Nannochloropsis sp. **Journal of Environmental Chemical Engineering**, v. 6, n. 4, p. 4318–4328, 1 ago. 2018.

GANESAN, R.; MANIGANDAN, S.; SAMUEL, M. S.; SHANMUGANATHAN, R.; BRINDHADEVI, K.; LAN CHI, N. T.; DUC, P. A.; PUGAZHENDHI, A. A review on prospective production of biofuel from microalgae. **Biotechnology Reports**, v. 27, p. e00509, 1 set. 2020.

GE, S.; AGBAKPE, M.; ZHANG, W.; KUANG, L. Heteroaggregation between PEI-coated magnetic nanoparticles and algae: Effect of particle size on algal harvesting efficiency. **ACS Applied Materials and Interfaces**, v. 7, n. 11, p. 6102–6108, 25 mar. 2015.

GEADA, P.; OLIVEIRA, F.; LOUREIRO, L.; ESTEVES, D.; TEIXEIRA, J. A.; VASCONCELOS, V.; VICENTE, A. A.; FERNANDES, B. D. Comparison and optimization of different methods for Microcystis aeruginosa's harvesting and the role of zeta potential on its efficiency. **Environmental Science and Pollution Research**, v. 26, n. 16, p. 16708–16715, 1 jun. 2019.

GEHRKE, I.; GEISER, A.; SOMBORN-SCHULZ, A. Innovations in nanotechnology for water treatment. **Nanotechnology, Science and Applications**, v. 8, p. 1, 6 jan. 2015.

GERARDO, M. L.; HENDE, S. VAN DEN; VERVAEREN, H.; COWARD, T.; SKILL, S. C. Harvesting of microalgae within a biorefinery approach: A review of the

developments and case studies from pilot-plants. **Algal Research**, v. 11, p. 248–262, 1 set. 2015.

GERULOVÁ, K.; BARTOŠOVÁ, A.; BLINOVÁ, L.; BÁRTOVÁ, K.; DOMÁNKOVÁ, M.; GARAIOVÁ, Z.; PALCUT, M. Magnetic Fe3O4-polyethyleneimine nanocomposites for efficient harvesting of Chlorella zofingiensis, Chlorella vulgaris, Chlorella sorokiniana, Chlorella ellipsoidea and Botryococcus braunii. **Algal Research**, v. 33, p. 165–172, 1 jul. 2018.

GHORBANI, H. R. A Review of Methods for Synthesis of Al Nanoparticles : Oriental Journal of Chemistry. **Oriental Journal of Chemistry**, v. 30, n. 4, p. 1941–1949, 2014.

GOBI, S.; GOBI, K.; LEE, K. T.; VADIVELU, V. Self-flocculation of enriched mixed microalgae culture in a sequencing batch reactor. **Environmental Science and Pollution Research**, p. 1–11, 23 jan. 2021.

GOSS, C. Saturation Magnetisation, Coercivity and Lattice Parameter Changes in the System Fe304-yFe2O3, and Their Relationship to Structure. **Phys Chem Minerals**, v. 16, p. 164–171, 1988.

GUTIÉRREZ, R.; FERRER, I.; GONZÁLEZ-MOLINA, A.; SALVADÓ, H.; GARCÍA, J.; UGGETTI, E. Microalgae recycling improves biomass recovery from wastewater treatment high rate algal ponds. **Water Research**, v. 106, p. 539–549, 1 dez. 2016.

HIRSCHBEIN, B. L.; BROWN, D. W.; WHITESIDES, G. M. Magnetic separations in chemistry and biochemistry. **CHEMTECH**, v. 12, n. 3, p. 172–179, 1982.

HORÁK, D.; BABIČ, M.; MACKOVÁ, H.; BENEŠ, M. J. Preparation and properties of magnetic nano- and microsized particles for biological and environmental separations. **Journal of Separation Science**, v. 30, n. 11, p. 1751–1772, 1 jul. 2007.

HOWARTER, J. A.; YOUNGBLOOD, J. P. Optimization of silica silanization by 3-aminopropyltriethoxysilane. **Langmuir**, v. 22, n. 26, p. 11142–11147, 19 dez. 2006.

HU, Y. R.; GUO, C.; WANG, F.; WANG, S. K.; PAN, F.; LIU, C. Z. Improvement of microalgae harvesting by magnetic nanocomposites coated with polyethylenimine. **Chemical Engineering Journal**, v. 242, p. 341–347, 15 abr. 2014.

HU, Y. R.; WANG, F.; WANG, S. K.; LIU, C. Z.; GUO, C. Efficient harvesting of marine microalgae Nannochloropsis maritima using magnetic nanoparticles. **Bioresource Technology**, v. 138, p. 387–390, 1 jun. 2013.

HU YANG, BO YUAN, Y. L. & R. C. Preparation of magnetic chitosan microspheres and its applications in wastewater treatment. v. 52, n. 3, p. 249–256, 2009.

JANGYUBOL, K.; KASEMWONG, K.; CHAROENRAT, T.; CHITTAPUN, S. Magnetic–cationic cassava starch composite for harvesting Chlorella sp. TISTR8236. **Algal Research**, v. 35, p. 561–568, 1 nov. 2018.

JUNG, J. Y.; LEE, H.; SHIN, W. S.; SUNG, M. G.; KWON, J. H.; YANG, J. W. Utilization of seawater for cost-effective cultivation and harvesting of Scenedesmus obliquus. **Bioprocess and Biosystems Engineering**, v. 38, n. 3, p. 449–455, 26 fev. 2015.

KANDASAMY, G.; SHALEH, S. R. M. Harvesting of the Microalga Nannochloropsis sp. by Bioflocculation with Mung Bean Protein Extract. **Applied Biochemistry and Biotechnology**, v. 182, n. 2, p. 586–597, 2017.

KHARE, T.; OAK, U.; SHRIRAM, V.; VERMA, S. K.; KUMAR, V. Biologically synthesized nanomaterials and their antimicrobial potentials. *Em*: **Comprehensive Analytical Chemistry**. [s.l.] Elsevier B.V., 2019. v. 87p. 263–289.

KHATAMI, M.; ALIJANI, H. Q.; FAKHERI, B.; MOBASSERI, M. M.; HEYDARPOUR, M.; FARAHANI, Z. K.; KHAN, A. U. Super-paramagnetic iron oxide nanoparticles (SPIONs): Greener synthesis using Stevia plant and evaluation of its antioxidant properties. **Journal of Cleaner Production**, v. 208, p. 1171–1177, 20 jan. 2019.

KHATOON, H.; ABDU RAHMAN, N.; BANERJEE, S.; HARUN, N.; SULEIMAN, S. S.; ZAKARIA, N. H.; LANANAN, F.; ABDUL HAMID, S. H.; ENDUT, A. Effects of different salinities and pH on the growth and proximate composition of Nannochloropsis sp. and Tetraselmis sp. isolated from South China Sea cultured under control and natural condition. **International Biodeterioration and Biodegradation**, v. 95, n. PA, p. 11–18, 1 nov. 2014.

KIM, D. Y.; OH, Y. K.; PARK, J. Y.; KIM, B.; CHOI, S. A.; HAN, J. I. An integrated process for microalgae harvesting and cell disruption by the use of ferric ions. **Bioresource Technology**, v. 191, p. 469–474, 8 jun. 2015.

KIM, S.; PARK, J. EUN; CHO, Y. B.; HWANG, S. J. Growth rate, organic carbon and nutrient removal rates of Chlorella sorokiniana in autotrophic, heterotrophic and mixotrophic conditions. **Bioresource Technology**, v. 144, p. 8–13, 1 set. 2013.

KUMAR, A. Sol gel synthesis of zinc oxide nanoparticles and their application as nano-composite electrode material for supercapacitor. **Journal of Molecular Structure**, v. 1220, p. 128654, 15 jun. 2020.

KUMAR, V.; YADAV, S. K. Plant-mediated synthesis of silver and gold nanoparticles and their applications. **Journal of Chemical Technology and Biotechnology**, v. 84, n. 2, p. 151–157, 1 fev. 2009.

KUPRACZ, P.; COY, E.; GROCHOWSKA, K.; KARCZEWSKI, J.; RYSZ, J.; SIUZDAK, K. The pulsed laser ablation synthesis of colloidal iron oxide nanoparticles for the enhancement of TiO2 nanotubes photo-activity. **Applied Surface Science**, v. 530, p. 147097, 15 nov. 2020.

LEE, K.; LEE, S. Y.; PRAVEENKUMAR, R.; KIM, B.; SEO, J. Y.; JEON, S. G.; NA, J. G.; PARK, J. Y.; KIM, D. M.; OH, Y. K. Repeated use of stable magnetic flocculant for efficient harvest of oleaginous Chlorella sp. **Bioresource Technology**, v. 167, p. 284–290, 1 set. 2014.

LI, A. D.; LIU, W. C. Optical properties of ferroelectric nanocrystal/polymer composites. *Em*: **Physical Properties and Applications of Polymer Nanocomposites**. [s.l.] Elsevier Ltd, 2010. p. 108–158.

LIM, J. K.; CHIEH, D. C. J.; JALAK, S. A.; TOH, P. Y.; YASIN, N. H. M.; NG, B. W.; AHMAD, A. L. Rapid magnetophoretic separation of microalgae. **Small**, v. 8, n. 11, p. 1683–1692, 11 jun. 2012.

LIMA BARIZÃO, A. C. DE; SILVA, M. F.; ANDRADE, M.; BRITO, F. C.; GOMES, R. G.; BERGAMASCO, R. Green synthesis of iron oxide nanoparticles for tartrazine and bordeaux red dye removal. **Journal of Environmental Chemical Engineering**, v. 8, n. 1, p. 103618, 1 fev. 2020.

LIU, J.; HUANG, J.; SUN, Z.; ZHONG, Y.; JIANG, Y.; CHEN, F. Differential lipid and fatty acid profiles of photoautotrophic and heterotrophic Chlorella zofingiensis: Assessment of algal oils for biodiesel production. **Bioresource Technology**, v. 102, n. 1, p. 106–110, 1 jan. 2011.

LIU, P. R.; WANG, T.; YANG, Z. Y.; HONG, Y.; HOU, Y. L. Long-chain poly-arginine functionalized porous Fe3O4 microspheres as magnetic flocculant for efficient harvesting of oleaginous microalgae. **Algal Research**, v. 27, p. 99–108, 1 nov. 2017.

LIU, P. R.; YANG, Z. Y.; HONG, Y.; HOU, Y. L. An in situ method for synthesis of magnetic nanomaterials and efficient harvesting for oleaginous microalgae in algal culture. **Algal Research**, v. 31, p. 173–182, 1 abr. 2018.

LIU, P. R.; ZHANG, H. L.; WANG, T.; YANG, W. L.; HONG, Y.; HOU, Y. L. Functional graphene-based magnetic nanocomposites as magnetic flocculant for efficient harvesting of oleaginous microalgae. **Algal Research**, v. 19, p. 86–95, 1 nov. 2016.

LIU, P.; WANG, T.; YANG, Z.; HONG, Y.; XIE, X.; HOU, Y. Effects of Fe3O4 nanoparticle fabrication and surface modification on Chlorella sp. harvesting efficiency. **Science of the Total Environment**, v. 704, p. 135286, 20 fev. 2020.

LIU, Y.; JIN, W.; ZHOU, X.; HAN, S.-F.; TU, R.; FENG, X.; JENSEN, P. D.; WANG, Q. Efficient harvesting of Chlorella pyrenoidosa and Scenedesmus obliquus cultivated in urban sewage by magnetic flocculation using nano-Fe3O4 coated with polyethyleneimine. **Bioresource Technology**, v. 290, p. 121771, 2019.

LIU, Z. Y.; WANG, G. C.; ZHOU, B. C. Effect of iron on growth and lipid accumulation in Chlorella vulgaris. **Bioresource Technology**, v. 99, n. 11, p. 4717–4722, 1 jul. 2008.

MAHANTY, S.; BAKSHI, M.; GHOSH, S.; GAINE, T.; CHATTERJEE, S.; BHATTACHARYYA, S.; DAS, S.; DAS, P.; CHAUDHURI, P. Mycosynthesis of iron oxide nanoparticles using manglicolous fungi isolated from Indian sundarbans and its application for the treatment of chromium containing solution: Synthesis, adsorption isotherm, kinetics and thermodynamics study. **Environmental Nanotechnology, Monitoring and Management**, v. 12, p. 100276, 1 dez. 2019.

MARINCA, T. F.; CHICINAŞ, H. F.; NEAMŢU, B. V.; CHICINAŞ, I.; ISNARD, O.; POPA, F.; PĂŞCUŢĂ, P. Nanocrystalline/nanosized Fe3O4 obtained by a combined route ceramic-mechanical milling. Effect of milling on the chemical composition, formation of phases and powder characteristics. **Advanced Powder Technology**, v. 27, n. 4, p. 1588–1596, 1 jul. 2016.

MATHIMANI, T.; MALLICK, N. **A comprehensive review on harvesting of microalgae for biodiesel - Key challenges and future directionsRenewable and Sustainable Energy Reviews**Elsevier Ltd, , 1 ago. 2018.

MOHAMMADI, M.; MOWLA, D.; ESMAEILZADEH, F.; GHASEMI, Y. Cultivation of microalgae in a power plant wastewater for sulfate removal and biomass production: A batch study. **Journal of Environmental Chemical Engineering**, v. 6, n. 2, p. 2812–2820, 1 abr. 2018.

MOLINA GRIMA, E.; BELARBI, E. H.; ACIÉN FERNÁNDEZ, F. G.; ROBLES MEDINA, A.; CHISTI, Y. Recovery of microalgal biomass and metabolites: Process options and economics. **Biotechnology Advances**, v. 20, n. 7–8, p. 491–515, 1 jan. 2003.

MUNIZ-MIRANDA, M.; GELLINI, C.; GIORGETTI, E.; MARGHERI, G. Bifunctional Fe3O4/Ag nanoparticles obtained by two-step laser ablation in pure water. **Journal of Colloid and Interface Science**, v. 489, p. 100–105, 1 mar. 2017.

NAM, N. H.; LUONG, N. H. Nanoparticles: Synthesis and applications. *Em*: **Materials for Biomedical Engineering: Inorganic Micro- and Nanostructures**. [s.l.] Elsevier, 2019. p. 211–240.

NASCIMENTO, R. F. DO; FERREIRA, O. P.; PAULA, A. J. DE; OLIVEIRA SOUSA NETO, V. DE. **Nanomaterials applications for environmental matrices: Water, soil and air**. [s.l.] Elsevier, 2019.

NASSAR, N. N. Rapid removal and recovery of Pb(II) from wastewater by magnetic nanoadsorbents. **Journal of Hazardous Materials**, v. 184, n. 1–3, p. 538–546, 15 dez. 2010.

NIE, C.; PEI, H.; JIANG, L.; CHENG, J.; HAN, F. Growth of large-cell and easily-sedimentation microalgae Golenkinia SDEC-16 for biofuel production and campus sewage treatment. **Renewable Energy**, v. 122, p. 517–525, 1 jul. 2018.

OKORO, V.; AZIMOV, U.; MUNOZ, J.; HERNANDEZ, H. H.; PHAN, A. N. Microalgae cultivation and harvesting: Growth performance and use of flocculants - A review. **Renewable and Sustainable Energy Reviews**, v. 115, p. 109364, 2019.

PASCAULT, J.-P.; WILLIAMS, R. J. J. Overview of thermosets: structure, properties and processing for advanced applications. *Em*: **Thermosets**. [s.l.] Elsevier, 2012. p. 3–27.

PASKEVICIUS, M.; WEBB, J.; PITT, M. P.; BLACH, T. P.; HAUBACK, B. C.; GRAY, E. M. A.; BUCKLEY, C. E. Mechanochemical synthesis of aluminium nanoparticles and their deuterium sorption properties to 2 kbar. **Journal of Alloys and Compounds**, v. 481, n. 1–2, p. 595–599, 29 jul. 2009.

PETRY, R.; OLIVEIRA, N. C.; ALVES, A. C.; FILHO, A. G. S.; MARTINEZ, D. S. T.; HWANG, G.; SOUSA, F. A.; PAULA, A. J. Nanomaterials Properties of Environmental Interest and How to Assess Them. *Em*: **Nanomaterials Applications for Environmental Matrices: Water, Soil and Air**. [s.l.] Elsevier, 2019. p. 45–105.

PHUKAN, M. M.; CHUTIA, R. S.; KONWAR, B. K.; KATAKI, R. Microalgae Chlorella as a potential bio-energy feedstock. **Applied Energy**, v. 88, n. 10, p. 3307–3312, 1 out. 2011.

POOYAN, S. S. Sol-gel process and its application in Nanotechnology. **Journal of Polymer Engineering and Technology**, v. 13, p. 38–41, 1 set. 2005.

PROCHAZKOVA, G.; SAFARIK, I.; BRANYIK, T. Harvesting microalgae with microwave synthesized magnetic microparticles. **Bioresource Technology**, v. 130, p. 472–477, 1 fev. 2013.

RANE, A. V.; KANNY, K.; ABITHA, V. K.; THOMAS, S. Methods for Synthesis of Nanoparticles and Fabrication of Nanocomposites. *Em*: **Synthesis of Inorganic Nanomaterials**. [s.l.] Elsevier, 2018. p. 121–139.

RANGANATHAN, P.; AMAL, J. C.; SAVITHRI, S.; HARIDAS, A. Experimental and modelling of Arthrospira platensis cultivation in open raceway ponds. **Bioresource Technology**, v. 242, p. 197–205, 1 out. 2017.

RUÍZ-BALTAZAR, Á. DE J. Green synthesis assisted by sonochemical activation of Fe3O4-Ag nano-alloys: Structural characterization and studies of sorption of cationic dyes. **Inorganic Chemistry Communications**, v. 120, p. 108148, 1 out. 2020.

SABÍN LÓPEZ, A.; PAREDES RAMOS, M.; HERRERO, R.; LÓPEZ VILARINÕ, J. M. Synthesis of magnetic green nanoparticle-Molecular imprinted polymers with emerging contaminants templates. **Journal of Environmental Chemical Engineering**, v. 8, n. 4, p. 103889, 1 ago. 2020.

SADHASIVAM, S.; VINAYAGAM, V.; BALASUBRAMANIYAN, M. Recent advancement in biogenic synthesis of iron nanoparticles. **Journal of Molecular Structure**, v. 1217, p. 128372, 5 out. 2020.

SALIM, S.; SHI, Z.; VERMUË, M. H.; WIJFFELS, R. H. Effect of growth phase on harvesting characteristics, autoflocculation and lipid content of Ettlia texensis for microalgal biodiesel production. **Bioresource Technology**, v. 138, p. 214–221, 1 jun. 2013.

SEO, J. Y.; LEE, K.; LEE, S. Y.; JEON, S. G.; NA, J. G.; OH, Y. K.; PARK, S. BIN. Effect of barium ferrite particle size on detachment efficiency in magnetophoretic harvesting of oleaginous Chlorella sp. **Bioresource Technology**, v. 152, p. 562–566, 1 jan. 2014.

SEO, J. Y.; LEE, K.; PRAVEENKUMAR, R.; KIM, B.; LEE, S. Y.; OH, Y. K.; PARK, S. BIN. Tri-functionality of Fe3O4-embedded carbon microparticles in microalgae harvesting. **Chemical Engineering Journal**, v. 280, p. 206–214, 5 nov. 2015.

SHURAIR, M.; ALMOMANI, F.; BHOSALE, R.; KHRAISHEH, M.; QIBLAWEY, H. Harvesting of intact microalgae in single and sequential conditioning steps by chemical and biological based – flocculants: Effect on harvesting efficiency, water recovery and algal cell morphology. **Bioresource Technology**, v. 281, p. 250–259, 1 jun. 2019.

SINGH, J. P.; GAUTAM, S.; SRIVASTAVA, R. C.; ASOKAN, K.; KANJILAL, D.; CHAE, K. H. Crystallite size induced crossover from paramagnetism to

superparamagnetism in zinc ferrite nanoparticles. **Superlattices and Microstructures**, v. 86, p. 390–394, 1 out. 2015.

ŞIRIN, S.; TROBAJO, R.; IBANEZ, C.; SALVADÓ, J. Harvesting the microalgae Phaeodactylum tricornutum with polyaluminum chloride, aluminium sulphate, chitosan and alkalinity-induced flocculation. **Journal of Applied Phycology**, v. 24, n. 5, p. 1067–1080, 5 out. 2012.

SMOLKOVA, I. S.; KAZANTSEVA, N. E.; PARMAR, H.; BABAYAN, V.; SMOLKA, P.; SAHA, P. Correlation between coprecipitation reaction course and magneto-structural properties of iron oxide nanoparticles. **Materials Chemistry and Physics**, v. 155, p. 178–190, 1 abr. 2015.

SUPARMANIAM, U.; LAM, M. K.; UEMURA, Y.; LIM, J. W.; LEE, K. T.; SHUIT, S. H. Insights into the microalgae cultivation technology and harvesting process for biofuel production: A review. **Renewable and Sustainable Energy Reviews**, v. 115, p. 109361, 1 nov. 2019.

TAKAMI, S.; SATO, T.; MOUSAVAND, T.; OHARA, S.; UMETSU, M.; ADSCHIRI, T. Hydrothermal synthesis of surface-modified iron oxide nanoparticles. **Materials Letters**, v. 61, n. 26, p. 4769–4772, 1 out. 2007.

TJONG, S. C.; CHEN, H. Nanocrystalline materials and coatings. **Materials Science and Engineering R: Reports**, v. 45, n. 1–2, p. 1–88, 30 set. 2004.

TOH, P. Y.; NG, B. W.; AHMAD, A. L.; CHIEH, D. C. J.; LIM, J. K. Magnetophoretic separation of Chlorella sp.: Role of cationic polymer binder. **Process Safety and Environmental Protection**, v. 92, n. 6, p. 515–521, 1 nov. 2014.

TOH, P. Y.; YEAP, S. P.; KONG, L. P.; NG, B. W.; CHAN, D. J. C.; AHMAD, A. L.; LIM, J. K. Magnetophoretic removal of microalgae from fishpond water: Feasibility of high gradient and low gradient magnetic separation. **Chemical Engineering Journal**, v. 211–212, p. 22–30, 15 nov. 2012.

UMMALYMA, S. B.; GNANSOUNOU, E.; SUKUMARAN, R. K.; SINDHU, R.; PANDEY, A.; SAHOO, D. Bioflocculation: An alternative strategy for harvesting of microalgae – An overview. **Bioresource Technology**, v. 242, p. 227–235, 2017.

VANDAMME, D.; FOUBERT, I.; MUYLAERT, K. Flocculation as a low-cost method for harvesting microalgae for bulk biomass production. **Trends in Biotechnology**, v. 31, n. 4, p. 233–239, 1 abr. 2013.

VELSANKAR, K.; R.M., A. K.; R., P.; V., M.; SUDHAHAR, S. Green synthesis of CuO nanoparticles via Allium sativum extract and its characterizations on

antimicrobial, antioxidant, antilarvicidal activities. **Journal of Environmental Chemical Engineering**, v. 8, n. 5, p. 104123, 1 out. 2020.

VIDOTTI, A. D. S.; RIAÑO-PACHÓN, D. M.; MATTIELLO, L.; GIRALDI, L. A.; WINCK, F. V.; FRANCO, T. T. Analysis of autotrophic, mixotrophic and heterotrophic phenotypes in the microalgae Chlorella vulgaris using time-resolved proteomics and transcriptomics approaches. **Algal Research**, v. 51, p. 102060, 1 out. 2020.

WANG, H.; GAO, L.; CHEN, L.; GUO, F.; LIU, T. Integration process of biodiesel production from filamentous oleaginous microalgae Tribonema minus. **Bioresource Technology**, v. 142, p. 39–44, 2013.

WANG, H.; ZHOU, W.; SHAO, H.; LIU, T. A comparative analysis of biomass and lipid content in five Tribonema sp. strains at autotrophic, heterotrophic and mixotrophic cultivation. **Algal Research**, v. 24, p. 284–289, 1 jun. 2017.

WANG, S. K.; STILES, A. R.; GUO, C.; LIU, C. Z. Harvesting microalgae by magnetic separation: A review. **Algal Research**, v. 9, p. 178–185, 1 maio 2015.

WANG, S. K.; WANG, F.; STILES, A. R.; GUO, C.; LIU, C. Z. Botryococcus braunii cells: Ultrasound-intensified outdoor cultivation integrated with in situ magnetic separation. **Bioresource Technology**, v. 167, p. 376–382, 1 set. 2014.

WANG, T.; YANG, W. L.; HONG, Y.; HOU, Y. L. Magnetic nanoparticles grafted with amino-riched dendrimer as magnetic flocculant for efficient harvesting of oleaginous microalgae. **Chemical Engineering Journal**, v. 297, p. 304–314, 1 ago. 2016.

WANG, X.; SHENG, L.; YANG, X. Pyrolysis characteristics and pathways of protein, lipid and carbohydrate isolated from microalgae Nannochloropsis sp. **Bioresource Technology**, v. 229, p. 119–125, 1 abr. 2017.

WANG, X.; ZHAO, Y.; JIANG, X.; LIU, L.; LI, X.; LI, H.; LIANG, W. In-situ self-assembly of plant polyphenol-coated Fe3O4 particles for oleaginous microalgae harvesting. **Journal of Environmental Management**, v. 214, p. 335–345, 15 maio 2018.

XU, L.; GUO, C.; WANG, F.; ZHENG, S.; LIU, C. Z. A simple and rapid harvesting method for microalgae by in situ magnetic separation. **Bioresource Technology**, v. 102, n. 21, p. 10047–10051, 1 nov. 2011.

XU, Y.; MILLEDGE, J. J.; ABUBAKAR, A.; SWAMY, R. A. R.; BAILEY, D.; HARVEY, P. J. Effects of centrifugal stress on cell disruption and glycerol leakage from Dunaliella salina. **Microalgae Biotechnology**, v. 1, n. 1, 27 jul. 2015.

YIN, Z.; ZHU, L.; LI, S.; HU, T.; CHU, R.; MO, F.; HU, D.; LIU, C.; LI, B. A comprehensive review on cultivation and harvesting of microalgae for biodiesel production: Environmental pollution control and future directions. **Bioresource Technology**, v. 301, p. 122804, 1 abr. 2020.

ZHANG, X.; AMENDOLA, P.; HEWSON, J. C.; SOMMERFELD, M.; HU, Q. Influence of growth phase on harvesting of Chlorella zofingiensis by dissolved air flotation. **Bioresource Technology**, v. 116, p. 477–484, 1 jul. 2012.

ZHANG, Z.; WEN, G. Synthesis and characterization of carbon-encapsulated magnetite, martensite and iron nanoparticles by high-energy ball milling method. **Materials Characterization**, v. 167, p. 110502, 1 set. 2020.

ZHAO, Y.; FAN, Q.; WANG, X.; JIANG, X.; JIAO, L.; LIANG, W. Application of Fe3O4 coated with modified plant polyphenol to harvest oleaginous microalgae. **Algal Research**, v. 38, p. 101417, 1 mar. 2019.

Chapter 3

Optimized magnetic flocculation of *Chlorella sp.* using magnetic nanoparticles functionalized with tannins from *Rhizophora mangle*

ABSTRACT

Harvesting is the most difficult and costly step in microalgae cultivation. Tannins are flocculants highly applied in microalgae flocculation, however, moving forward attached to biomass in the downstream steps, which is not interesting in some applications, such as in food, feed, and cosmetics production. Associate the tannins, with magnetic nanoparticles (MNPs) can solve this issue. Thus, in this work, the MNPs were synthesized (chemical precipitation), characterized (X-Ray Diffraction (XDR), Transmission electron microscopy (TEM), Fourier transform infrared (FTIR), Zeta potential), functionalized using tannins from *Rhizophora mangle* and applied in the harvesting of *Chlorella sp.* At the optimum conditions, the adsorbent achieved a harvesting efficiency (HE%) of 92.6% ((MNP-TNs concentration=1,000 mg. L^{-1}; q_{exp}= 1.39 g. mg^{-1}; pH= 4), maintaining this efficiency during 5 reuse cycles. Even at pH 10.4 (pH at end of cultivation), the MNP-TNs were able to maintain a HE%= 63% (q_{exp}= 0.96 g. mg^{-1}). The isotherm model better fitting to the data was of Langmuir, indicating monolayer adsorption. The process was considered exothermic, favorable, and spontaneous. Based on the results are possible to assume that tannins from *Rhizophora mangle*, the first time applied in this finality (as we know), is an interesting option to functionalize magnetite nanoparticles applied to magnetic flocculation of Chlorella sp., achieving high harvesting efficiency in a short time with reusing potential.

Keywords: Microalgae, biomass, nanomaterial, harvesting, magnetism.

1. Introduction

Microalgae are among Earth's oldest organisms. They are responsible for approximately 50% of the world's photosynthetic activity, fixing high levels of CO_2 during their respiration process. They can be cultivated in a simple way, in a synthetic medium, or in other media- rich in phosphorus and nitrogen, such as wastewater (Chiu *et al.*, 2015). They don't require any arable land for their cultivation and give rise to a versatile biomass that is used for the production of different types of biofuels (Estudillo-del Castillo, Ligot and Nudo, 2023), animal feeds, food supplements (Chen, C. *et al.*, 2022), and cosmetics (Vázquez-Romero *et al.*, 2022). Among the known species, Chlorella is one of the most studied. It has a high content of proteins, carbohydrates, lipids, fibers, and pigments (Yuan *et al.*, 2020). However, its low density, similar to water, small size (< 10 μm), and negative charge make harvesting difficult and costly (Kim, J. *et al.*, 2013), representing more than 20% of the total cost of production (Wen *et al.*, 2021; Yuan *et al.*, 2020).

During the flocculation process, a complex physicochemical process occurs that takes place to the formation of the flocs with a density greater than water, accelerating biomass decantation (Abdul Hamid *et al.*, 2014). Two classes of flocculant could be applied, inorganic (aluminum sulfate (Al_2 (SO_4)$_3$), poly aluminum chloride (PAC), and iron chloride ($FeCl_3$)) and organic (*Moringa oleifera* (Abdul Hamid *et al.*, 2014), chitosan (Acosta-Ferreira *et al.*, 2020)). In the first one, high harvesting efficiency is obtained, but the biomass will present high metal levels, limiting their applications. For example, in biodiesel production, high levels of metals on biomass can inactivate the basic catalysts involved in transesterification, affecting the production yield (Chen, Chang and Lee, 2015). Regarding organic ones, they are usually non-toxic substances, however, flocculants still may be present in trace amounts on biomass (Abdul Hamid *et al.*, 2014).

Tannins is a great example of an organic flocculant, highly applied on water and wastewater flocculation (Ibrahim, Yaser and Lamaming, 2021). Considered a secondary metabolite from advanced plants, although naturally presents a negative charge, through some modifications by amines and other cationic groups (e.g., *Mannich* reaction (You, Y. *et al.*, 2022)) can improve their flocculation potential. If positively charged, tannins are able to neutralize and/or destabilize the negative microalgae cell charge, inducing flocculation (Ho *et al.*, 2022).

The application of flocculants in the magnetic nanoparticles (MNPs) functionalization can be considered a good strategy to obtain biomass without traces of the downstream flocculant. The application of magnetic nanoparticles in harvesting microalgae biomass has already been studied for some time (Seo *et al.*, 2015; Wang *et al.*, 2018; Zhao *et al.*, 2019). This method consists in to add magnetic nanoparticles at the end of the cultivation step, that promptly react with microalgae cells building magnetic flocs that quickly decant when exposed to the magnetic field (Abo Markeb *et al.*, 2019). The presence of molecules revesting the NPs can change their surface characteristics and enhance the harvesting process, providing, in addition, fast decantation, reusable flocculant, and pure biomass (Wang *et al.*, 2015). In this way, this work evaluated the production of magnetic nanoparticles functionalized with tannins from *Rhizophora mangle* (applied for the first time to this purpose), as well as their performance in the harvesting of *Chlorella sp.* through factorial experiments in two stages (fractional and complete) considering the influence of the main interfering variables in the system (microalgae concentration, pH, temperature, agitation, contact time, and MNPs concentration).

2. Materials and methods

2.1 Materials

$FeCl_2 \cdot 4H_2O$ (Sigma-Aldrich 44939), $FeCl_3 \cdot 6H_2O$ (Sigma-Aldrich F2877), Ammonium Hydroxide (Prochemios), Sodium Citrate (Dynamica 1146), 3-Aminopropyltriethoxysilane ((APTES) Sigma-Aldrich 440140), ethanol (P.A Sigma-Aldrich 64-17-5) tannins extract from *Rhizophora mangle* leaves (Piraquê Açú-Mirim estuary (autumn; 19º57'S, 40º10'W)). Formaldehyde (37 %; Sigma-Aldrich 252549), Dimethylamine (33 %; Sigma-Aldrich 38950), Ultrapure Water (Sartorius), Neodymium magnet 50× 50× 12 mm (Supermagnet, Brazil). *Chlorella sp.* strain (L06, from Laboratory of Chemical, Physical and microbiology characterization of Federal University of Espirito Santo). BG11 medium ($NaNO_3$ (1.5 g. L^{-1}); $K_2HPO_4.3H_2O$ (40 mg. L^{-1}); $MgSO_4.7H_2O$ (75 mg. L^{-1}); $CaCl.2H_2O$ (36 mg. L^{-1}); $C_6H_8O_7$ (6 mg. L^{-1}); $C_6H_5FeO_7$ (6 mg. L^{-1}); Na_2CO_3 (20 mg. L^{-1}); (Andersen, 2005)). Laboratory glassware such as beakers, volumetric flasks, falcon tubes. All glassware was sanitized using aqua regia (HCl: HNO_3) for 5 times and washed ten times with ultrapure water before the experiments.

2.2 Synthesis of magnetic nanoparticles

The synthesis of MNPs was based on Zhou et. al (Zhou *et al.*, 2012) where 1.622 g of $FeCl_3.6H_2O$ and 0.9941 of $FeCl_2.4H_2O$ was dissolved in 40 ml of deionized water until reagents had completely dissolved. Subsequently, was added 5 ml of ammonium hydroxide (28% w/v%) to the mixture and stirred for 10 min. After this, was added 4.4 g of sodium citrate under continuous stirring, at 90° C, for 30 min. The reaction was finished using an ice bath and the MNPs produced were stored in falcon tubes.

2.3 Functionalization of magnetic nanoparticles

Firstly, the MNPs were stabilized using 3-Aminopropyltriethoxysilane (APTES). In this way, 3 ml of APTES was dissolved in 25 ml of ethanol and stirred for 10 min. at room temperature. Then 0.6946 g of MNPs was added to the mixture and constantly stirred for 48 h. After this, the nanoparticles were washed until the unreacted APTES in

the supernatant were completely removed. Following, MNPs-APTES were functionalized using modified tannins.

The extraction of tannins was based on Abilleira *et al.* (2021) and the *Rhizophora mangle* was used as feedstock for tannins extraction. Healthy leaves of *R. mangle* were collected in the Piraquê Açú-Mirim estuary, washed and dried at (40º C) until they reached constant weight. 500 ml of distilled water and 12.5 g of milled leaves (42 mesh/0,35 mm) were mixed under constant stirring at 80±5° C for 2 h. Then, the tannins extracted was modified according to Wang *et al.* (2013). The modification was realized by the Mannich reaction, where 100 ml of tannins solution was warming at 70º C, under an argon atmosphere and constant stirring. In sequence, 5 ml of formaldehyde (37 %) and 3 mL of dimethylamine (33 %) were added into the flask at the same time drop by drop. Then 0.03 mL of acetic acid was added and the reaction occurred for 3h under constant stirring and the final solution was stored in falcon tubes at 8° C.

The functionalization of MNPs was based on. Zhao *et al.* (2019), where 1 g of MNPs and 40 ml of modified tannins solution was mixed under constant stirring and temperature (25º C) for 2 h. The functionalized nanoparticles (MNP-TNs) were washed until the unreacted tannins in the supernatant was completely removed and stored in falcon tubes at 8° C in the dark.

2.4 Characterization of magnetic nanoparticles

The magnetic nanoparticles were characterized using many techniques aiming to identify synthesis and functionalization effectiveness. The crystalline phase was identified using an X-Ray Diffractometer (XRD- 6000, Shimadzu) in range 2Ɵ from 20 up to 70. The shape, dispersion, size, and composition of nanoparticles were analyzed by transmission electron microscopy (TEM (JEOL, JEM1400)). The functionalization efficacy was identified by Fourier transform infrared (FTIR). The superficial charge of MNPs, MNPs-TNs and *Chlorella sp*. were estimated by Zeta potential, in a pH range of 4, 7, 8, and 10.

2.5 *Chlorella sp.* cultivation

The *Chlorella sp.* was cultivated in BG11 medium, in 5 L tubular photobioreactors (batch assays), under stirring at 70 rpm, and natural lighting (approximately 1500 lux). The microalgae growth was monitored until the achieving stationary phase and the final concentration was determined (680 nm).

2.6 Factorial experiments design

Due to the high number of variables interfering in the harvesting process; a factorial experimental design was utilized. In this way, firstly was realized a fractional factorial design ($2^{(5-1)}$) for identifying the most significant variables. The variables (microalgae concentration, nanoparticles concentration, pH, temperature, agitation, and contact time) and its levels were selected based on a literature review (Table 1), and combined in an experimental matrix (Table 2). Then, a full factorial (2^3) was carried out based on two main variables identified, to promote the optimized harvesting process (Table 3).

Table 1. Levels of fractional factorial.

Variables	**Levels**		**Ref.**
	(-1)	**(+1)**	
Microalgae concentration	0,2 g. L^{-1}	1,5 g. L^{-1}	(Liu *et al.*, 2017) (Wang *et al.*, 2018)
MNPs-TN concentration	20 mg. L^{-1}	300 mg. L^{-1}	(Hu *et al.*, 2014) (Xu *et al.*, 2011)
pH	4	9	(Hu *et al.*, 2014) (Wang *et al.*, 2018)
Temperature	25	35	(Wang *et al.*, 2018) (Hu *et al.*, 2014)
Agitation	120 rpm	800 rpm	(Hu *et al.*, 2014) (Liu, Jin, Zhou, *et al.*, 2019)
Contact time (MNPs-TN/ microalgae)	1 min.	20 min.	(Gerulová *et al.*, 2018) (Liu *et al.*, 2017)

Table 2. Design matrix of fractional factorial (2^{5-1}).

Factors						Treatments
Microalgae concentration	MNP-TNs concentration	pH	Temperature	Agitation	Contact time (NPs/ microalgae)	
-1	-1	-1	-1	-1	-1	28
1	-1	-1	-1	-1	1	29
-1	1	-1	-1	-1	1	9
1	1	-1	-1	-1	-1	21
-1	-1	1	-1	-1	1	22
1	-1	1	-1	-1	-1	11
-1	1	1	-1	-1	-1	30
1	1	1	-1	-1	1	16
-1	-1	-1	1	-1	1	23
1	-1	-1	1	-1	-1	3
-1	1	-1	1	-1	-1	31
1	1	-1	1	-1	1	13
-1	-1	1	1	-1	-1	7
1	-1	1	1	-1	1	27
-1	1	1	1	-1	1	6
1	1	1	1	-1	-1	12
-1	-1	-1	-1	1	1	26
1	-1	-1	-1	1	-1	15
-1	1	-1	-1	1	-1	17
1	1	-1	-1	1	1	5
-1	-1	1	-1	1	-1	18
1	-1	1	-1	1	1	4
-1	1	1	-1	1	1	2
1	1	1	-1	1	-1	25
-1	-1	-1	1	1	-1	19
1	-1	-1	1	1	1	1
-1	1	-1	1	1	1	14
1	1	-1	1	1	-1	32
-1	-1	1	1	1	1	20
1	-1	1	1	1	-1	8
-1	1	1	1	1	-1	24
1	1	1	1	1	1	10

Table 3. Design matrix of full factorial (2^3).

Test	Variable 1	Variable 2	Treatments
1	-1	-1	6
2	-1	1	4
3	1	-1	9
4	1	1	5
5	-1	0	10
6	1	0	11
7	0	-1	8
8	0	1	1
9	0	0	7
10	0	0	12
11	0	0	2
12	0	0	3
13	0	0	13

In both, the harvesting efficiency (HE% (Equation 1)) was adopted as the response variable (680 nm). The adsorption capacity at equilibrium (q_{exp} (Equation 2)) was estimated in optimum conditions. All experiments were carried out in batch, in 1 ml of microalgae solution. After the reaction time (1 min.), the solutions were exposed to a magnetic field for 3 min. and the HE% was estimated based on microalgae concentration in the supernatant (680 nm). The Statistica software, version 13.3.721.1, was used to analyze the design matrix of all factorial experiments.

$$\text{HE\%} = (C_0 - C_e).\left({}^{1}/_{C_0}\right).100 \quad (1)$$

$$q_{exp} = \left(\frac{C_0 - C_e}{m}\right) . \text{ V} \quad (2)$$

Where C_0 and C_e are the initial and final concentrations of microalgae (mg. L^{-1}), V is the volume of solution (L) and m is the mass of adsorbent (g).

2.7 Isotherms and thermodynamic parameters

The adsorption isotherms were performed at batch regime, at temperatures of 25,35, and 45° C. All experiments were realized using an MNPs-TN concentration of 1,000 mg. L^{-1}, pH of 4, and 1 mL of microalgae solution varying in range from 200 mg. L^{-1} up to 3,000 mg. L^{-1} under stirring of 120 rpm, for 1 min. After this, the solutions were exposed to a magnetic field for 3 min. and the HE% was estimated based on microalgae concentration in the supernatant (680 nm). The Langmuir (Equation 3) and Freundlich (Equation 4) models were applied to the data aiming to establish the most appropriate correlation.

$$q = q_{max} K_L C_e / 1 + K_L C_e \quad (3)$$

$$q = K_F {C_e}^{1/n} \quad (4)$$

Where q is the solute adsorbed per gram of adsorbent at equilibrium (mg. g^{-1}), q_{max} is the maximum adsorption capacity (mg. g^{-1}), K_L is the interaction constants between adsorbate and adsorbent (mg. L^{-1}) and K_F Freundlich adsorption capacity constant (mg. L^{-1}), C_e is the concentration of adsorbate at equilibrium (mg. L^{-1}) and 1/n the surface heterogeneity constant (Nascimento *et al.*, 2014).

As for thermodynamic parameters, the Gibbs free energy variation ΔG°, the enthalpy changes ΔH°, and the entropy change ΔS° were determined by applying Equations 5, 6 and 7 to temperatures 25, 35 and 45 °C:

$$\Delta G^\circ = -RT ln K \quad (5)$$

$$\Delta G^\circ = \Delta H^\circ - T\,\Delta S^\circ \quad (6)$$

$$ln K = {\Delta S^\circ}/{R} - {\Delta H^\circ}/{R^x}\,{1}/{T} \quad (7)$$

Where R is the ideal gas constant (8.3144 J. K^{-1}. mol^{-1}), T is the temperature in Kelvin and K is the equilibrium constant (SILVEIRA *et al.*, 2017).

2.8 Reuse of nanoparticles

The reuse of MNPs was done according to Lee *et al.* (Lee *et al.*, 2014b). The experiments were performed at batch regime, in 1 mL of microalgae solution (1,000 mg. L^{-1}) at 25° C, and pH 4. After the reaction time (1 min.), the solutions were exposed to an external magnetic field for 3 min., and the HE% was estimated based on microalgae concentration in the supernatant (680 nm). The biomass with MNP-TNs obtained in the end harvesting cycle was resuspended in 300 µL of distilled water at pH 12. In sequence, was let in the vortex for 30 s and in ultrasonic for 1 min. The recovered MNP-TNs were separated under the influence of an external magnetic field, washed, and recycled during ten cycles.

3 Results and discussion

3.1 Characterization of magnetic nanoparticles

The MNP-TNs shape was analyzed on TEM images (Figure 1A). Their estimated size, based on the measurement of 1,000 MNPs, was around 11.5±2.6 nm, (Figure 1B), with an aspect ratio (AR= 1.1±0.4) very close to 1 (Figure 1C), indicating quasi-spherical MNPs. The normal distribution of size; and aspect ratio near one indicated a uniform distribution of size and shape of nanoparticles which favors a uniform behavior, increasing the reproducibility of harvesting essays (Singh *et al.*, 2022). The size of MNPs has a direct relation with their superficial area and magnetism. The smaller size the higher the superficial area, which usually elevates the HE% (Sajid and Płotka-Wasylka, 2020). Superparamagnetism occurs generally in particles <30 nm (Kristiansen, Church e Ucar, 2023), however, the magnetism type is also material dependent, occurring only in magnetite e maghemite (Clemons, Kerr and Joos, 2019).

Through XDR diffractogram interpretation (Figure 1D) was possible to confirm that the crystalline structure MNPs were really magnetite, with characteristic peaks found in 30.10°, 35.46°, 45.54°, 56.6°, 62.60°, corresponding to (220), (311), (400), (422) and (440) (Clemons, Kerr and Joos, 2019).

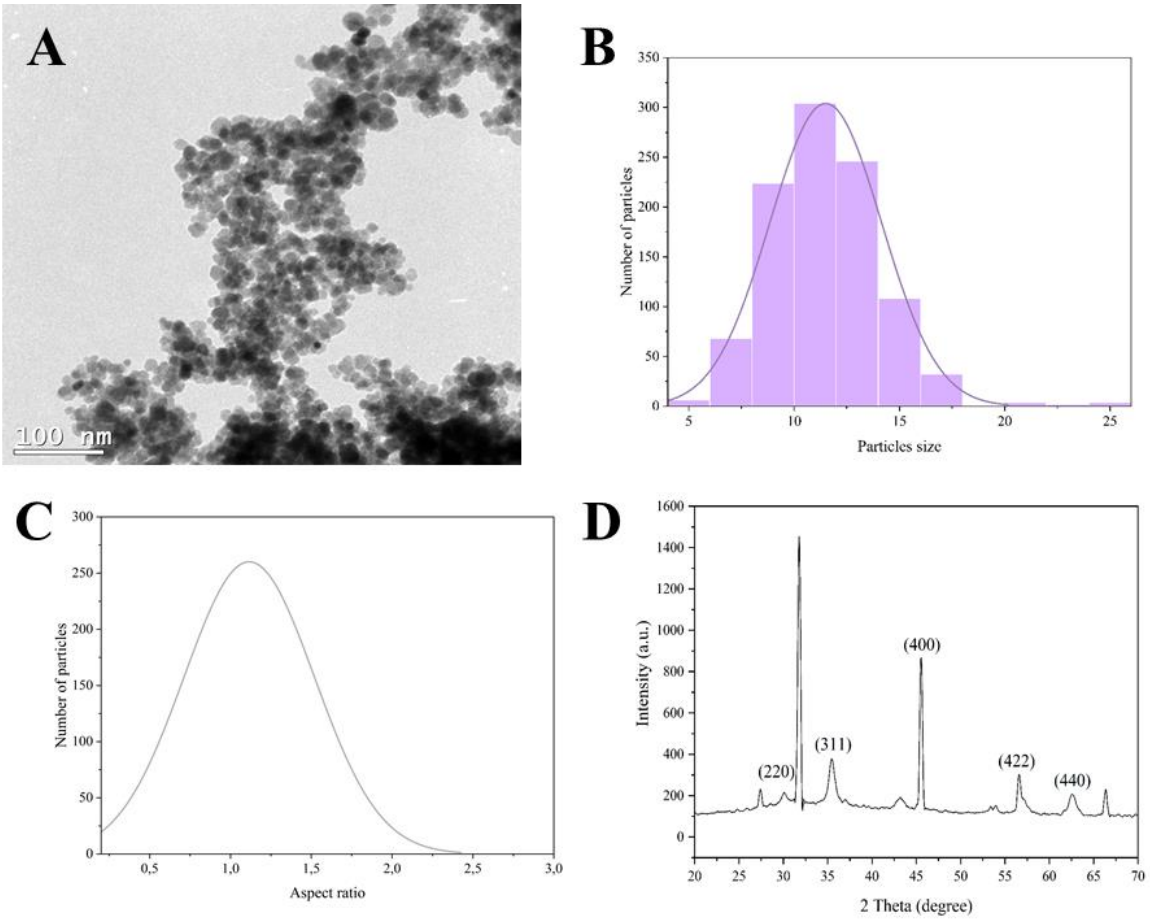

Figure 1. A) TEM of MNPs; B) Histogram of MNP size distribution, based on Figure 1A; C) Aspect ratio of MNP-TNs based on Figure 1A; D) XDR diffractogram of MNPs.

The steps of MNPs functionalization were traced by FTIR. The peaks in 1,021 cm^{-1} can be related to symmetric Si-O-Si, and 995 cm^{-1}, and 908 cm^{-1} can be related to asymmetric Si-OH, (Figure 2A). The Silicon in the structure indicates the success of the stabilization process by APTES. About the peak 1,990 cm^{-1}, it can be related to the overtones that reflect the replacement pattern of the benzene ring; the 1,603 cm^{-1} can indicate a C=N bond or a C=C vibration from the aromatic ring, and the 1,396 cm^{-1} demonstrates the C-H stretching (Figure 2B) (Stuart, 2004). The presence of amine groups is a great indication that the functionalization of MNPs by tannins occurred adequately since the Mannich reaction inserts some amine groups in tannins structure resulting in a positively charged high molecular weight polymer (Machado *et al.*, 2020).

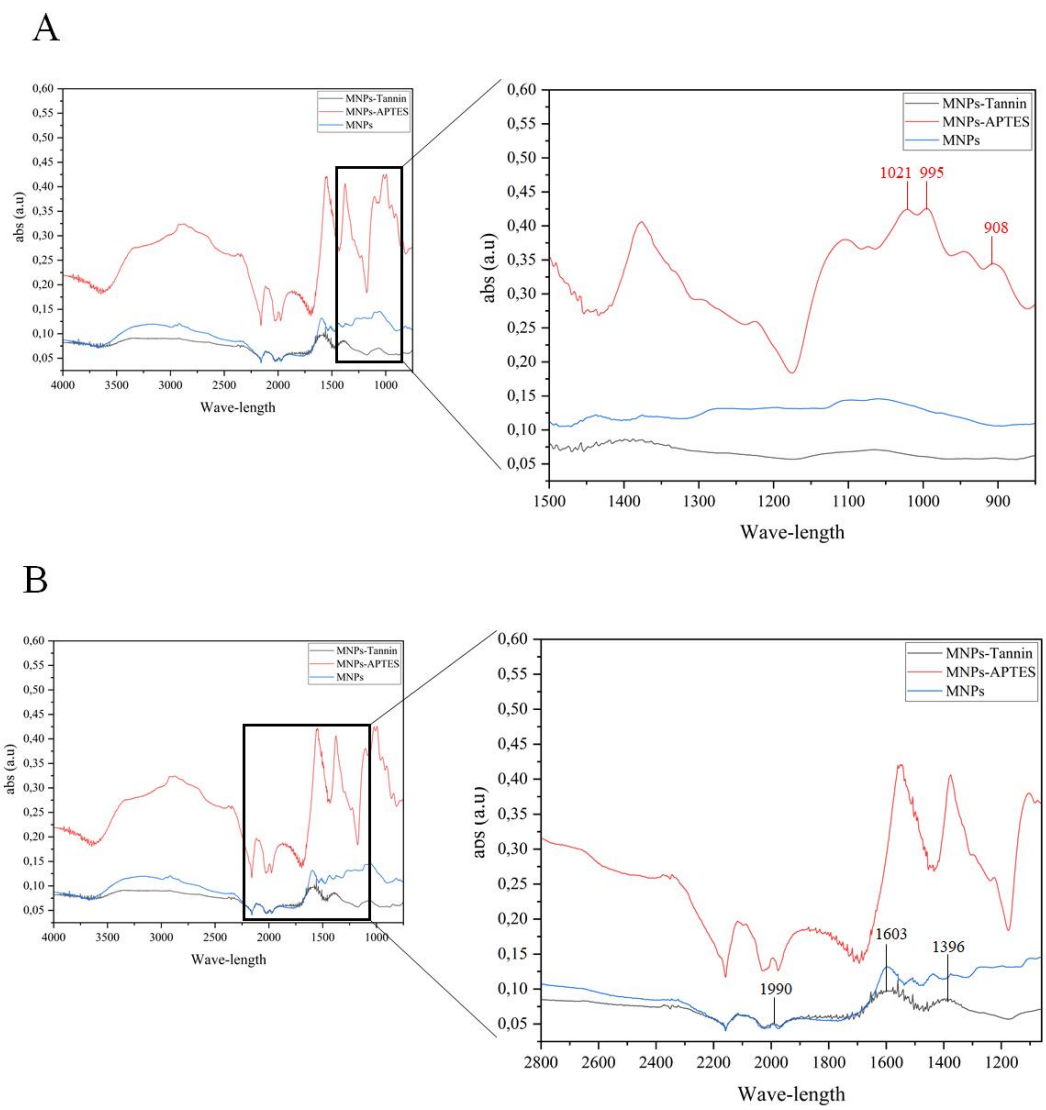

Figure 2. A) FTIR of MNPs, emphasizing characteristic peaks of APTES; B) FTIR of MNPs, emphasizing characteristic peaks of tannins.

3.2 *Chlorella sp.* cultivation

The growth of *Chlorella* sp. was monitored for 13 days and the growth curve was obtained (Figure 3). The end of the exponential phase was observed in 8 days, where the maximum amount of microalgae biomass was achieved (1.5 g. L^{-1}, pH=10.4). In this way, this concentration was adopted as the maximum biomass concentration in factorial experiments.

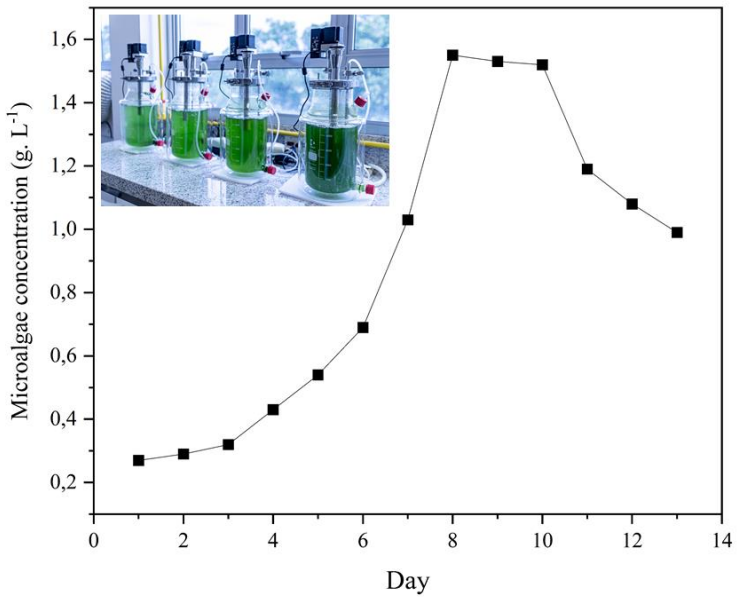

Figure 3. Growth curve of *Chlorella sp.* with photobioreactors in different cultivation phases (From left to right; Photobioreactor 1: lag-phase; Photobioreactors 2 and 3: exponential phase; and Photobioreactor 4: stationary phase).

3.3 Factorial experiments

Fractional factorials design is used to reduce the size of the experiments and/ also to guide the choice of variables tested. This design allows the researchers to understand the main effects and interaction effects of the system in a reduced trial (Antony, 2014). Here, this design was adopted to identify the key variables, resulting in the Pareto chart (Figure 4; ANOVA Table 1 (Appendix I)), in which the pH and MNP-TNs concentration were the main variables involved in the harvesting efficiency of *Chlorella sp.* The MNPs concentration presented a positive influence, then the higher the concentration the higher the microalgae harvesting. By contrast, the minor pH presented higher harvesting. Thus. the full factorial experiments were planned based on fractional factorial. Their levels were selected, increasing the MNP-TNs concentration and reducing the pH (Table 5).

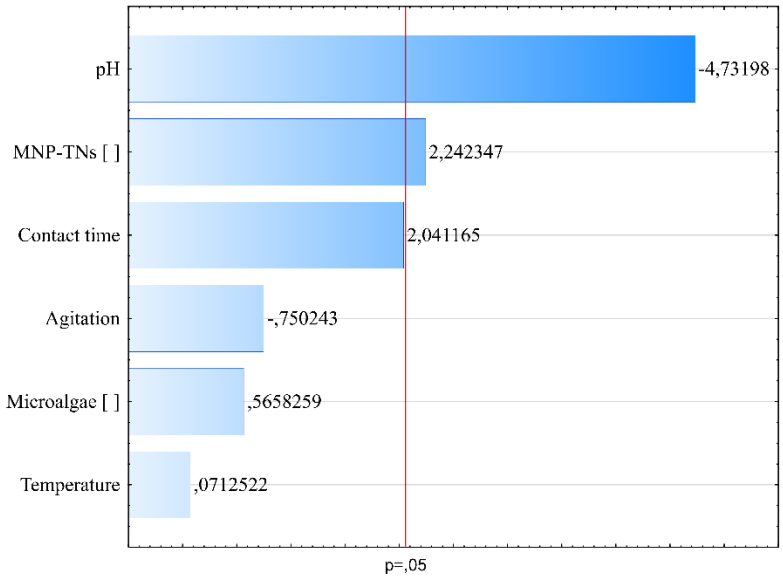

Figure 4. Pareto chart from fractional factorial experiments.

Table 5. Levels of full factorial experiments.

VARIABLES	Levels		
	(-1)	0	(+1)
pH	4	5	6
MNPs concentration (mg. L^{-1})	800	1,000	1,200

Both variables were significant in the harvesting process (Figure 5A and ANOVA Table 2 (Appendix I)). The model presented a great adjustment to the data, with R^2= 0.96, which is considered an acceptable value, indicating similar results from the model and experiments (Bayat Tork, Khalilzadeh and Kouchakzadeh, 2017). The pH followed the same trend as observed in the previous experiments, presenting high significance and achieving the optimal point at pH 4 (Figure 5A and B).

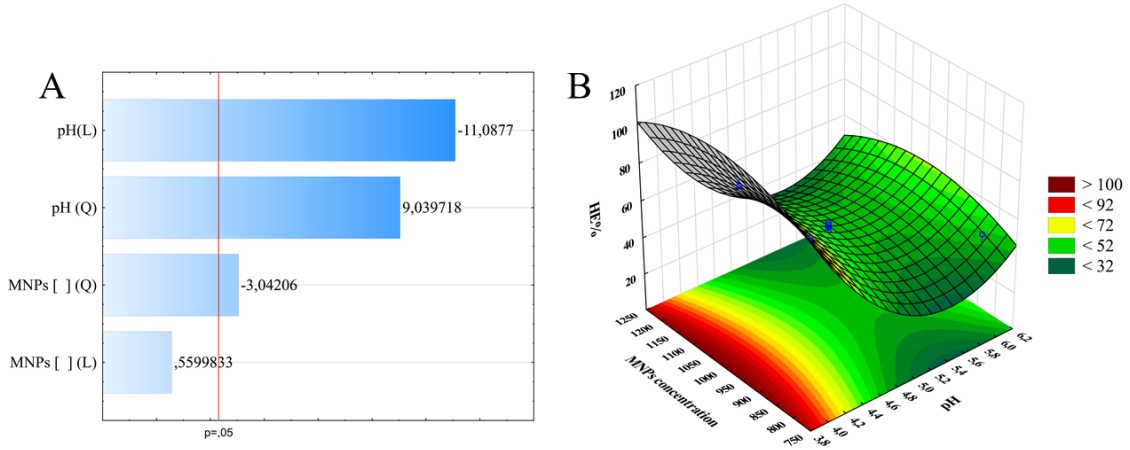

Figure 5. A) Pareto chart from full factorial experiments; B) Response surface chart from full factorial.

The Zeta potential results were compatible which was observed in the factorial experiments (Figure 6). As expected, microalgae presented a negative charge in all pH ranges, including pH 10, the final pH of cultivation. This is a common characteristic identified in different microalgae species, such as *Chlorella vulgaris* and *Microcystis aeruginosa* (Hadjoudja, Deluchat and Baudu, 2009). This happens due to the extracellular polymeric substances (EPS) that involve microalgae cells, and present negative groups, such as carboxylic, hydroxyl, and amine, resulting in microalgae being ordinarily negatively charged (Li, N. *et al.*, 2022). Looking at, in the MNPs, the superficial charge was also negative in all pH, probably due to hydroxyl groups present in the nanoparticles. Almost the same was observed with MNP-TNs, except in pH 4, in what the superficial charge was positive and bigger than +10 mV, favoring the charge attraction with microalgae.

Regarding to the MNP-TNs concentration, the HE% increased according to the increasing concentration of nanoparticles until 1,000 mg. L^{-1}, where achieved the optimum point, resulting in HE%= 92.6 (Figure 5A and B). From then, the increase of MNPs concentration has become a negative influence on HE%. This phenome usually happens when the equilibrium concentration of adsorbent is exceeded, with the dispersion restabilization, probably due to the steric hindrance and/or electrostatic repulsion (Liu *et al.*, 2013; Vandamme *et al.*, 2010). At the optimum point the q_{exp}= 1.39 g. mg^{-1} (each

milligram of adsorbent was able to harvest 1.39 g of microalgae) which can be considered a promissory due to the favorable proportion of adsorbent/ adsorbate.

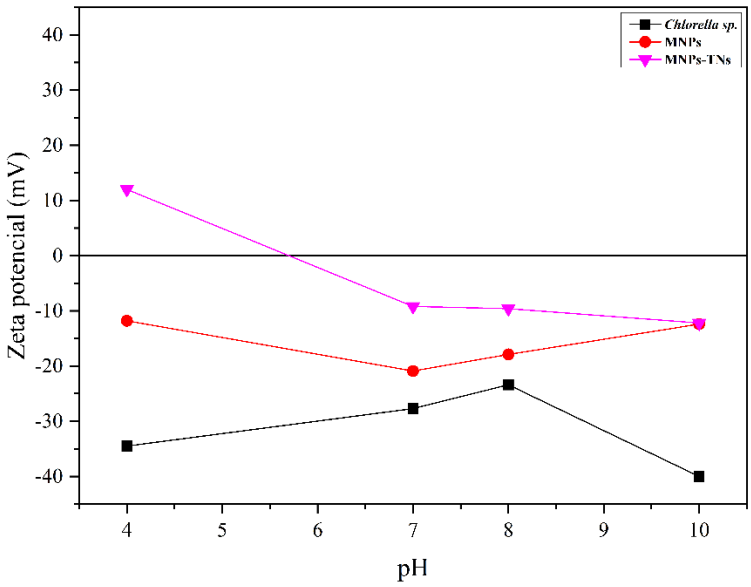

Figure 6. Zeta potential of *Chlorella* sp., MNPs and MNP-TNs.

Despite satisfactory HE% obtained at pH 4, it is relevant to note that the final pH of microalgae cultivation was 10.4, then an analysis of the HE% at this pH was also considered (Figure 7A). Although in pH 10, both microalgae and MNP-TNs presented a negative charge, a HE%= 63% was achieved (q_{exp}= 0,96), indicating that the charge attraction is not the only mechanism involved in the harvesting process; probably hydrogen bridges and dipole-dipole can act in this case (Vandamme, Foubert and Muylaert, 2013).

As in pH 4, increasing the MNP-TNs concentration beyond 1,000 mg. L^{-1} doesn't elevate the HE% (Figure 7B), probably due to the previously commented phenomenon of dispersion restabilization. Just when the MNP-TNs concentration achieved 2,500 mg. L^{-1} the HE% softly rise again, however, q_{exp} remained decreasing, due to the high amount of MNP-TNs (500 mg. L^{-1}) necessary to elevate the HE% in 7%. Besides the optimal point, considering the natural conditions of the system is also important and can enhance the viability of the technique. Working with smaller concentrations of microalgae will likely increase the HE%; in addition, working at a pH similar to that of microalgae may make the process cheaper and feasible on a large scale.

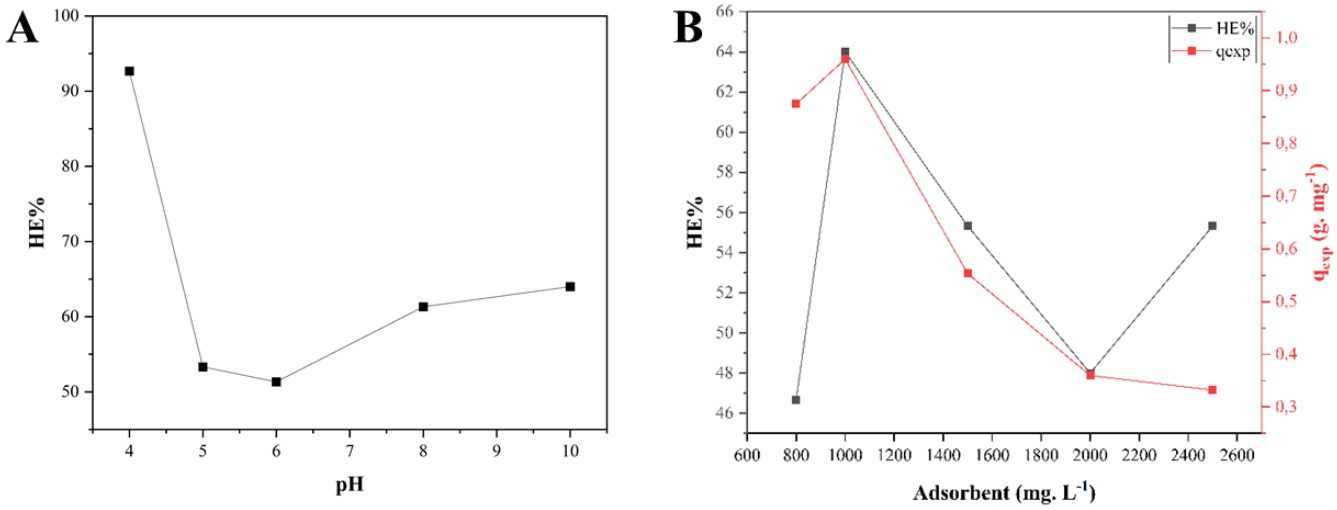

Figure 7. A) HE% at pH ranges from 4 to 10 (MNP-TNs concentration= 1,000 mg. L^{-1}); B) Different MNPs concentration at pH 10.

3.4 Isotherms and thermodynamic parameters

Adsorption isotherms are essential tools to understand the interaction between adsorbent and adsorbate and optimize the process at a constant temperature (Saleh, 2022). The HE% was reduced as the temperature was elevated, indicating an exothermic process (Figure 8A). Due to not requiring external heat sources, exothermic processes can lead to higher energy efficiency and simplify the necessary harvesting system, which can directly result in cost reduction during the implementation of the technique (Dabizha and Kersten, 2020).

The data were fitting with the two main used models to comprehend adsorption behavior. In this case, the best-fitty model with data was the Langmuir (Figure 8B). Thus, a few assumptions are made about the process: i) There are a specific number of active sites with equivalent energy; ii) The adsorption occurs in a monolayer, where each site accommodates only one molecule and there isn't an interaction between adsorbed molecules (Nascimento *et al.*, 2014). The model presented a great fitting to data, with an R^2=0.94 and a $q_{máx}$= 1.34 g. mg^{-1} closely to q_{exp}= 1.39 g. mg^{-1}, obtained in the

experiments. The isotherm type (extremally favorable) indicated that the adsorbate (microalgae) mass retained per unit of adsorbent (MNP-TNs) mass is high for a low equilibrium concentration of the adsorbate in the liquid phase. In other words, when the concentration of the adsorbate in the liquid phase is low, there are fewer molecules competing for adsorption sites, allowing a higher proportion of adsorbate molecules to be retained by the adsorbent. This leads to a high adsorption capacity per unit mass of the adsorbent (Cardoso *et al.*, 2012).

This behavior is advantageous in adsorption processes as it means that a significant amount of adsorbate can be removed from the liquid phase using a relatively small amount of adsorbent. This results in higher process efficiency and a reduction in the costs associated with the large-scale use of the MNP-TNs. However, it is important to note that isotherm models assume ideal conditions and simplifications, and the actual performance of the adsorption process may vary depending on various factors such as the presence of other species in the liquid phase, competition for adsorption sites, and the specific characteristics of the adsorbent and adsorbate in question (Nascimento *et al.*, 2014).

About Gibbs free energy, in all temperatures the $\Delta G°$ was negative, being -27.47 kJ. mol^{-1} (25° C), -7.66 kJ. mol^{-1} (35° C), and -24.79 kJ. mol^{-1} (45° C), which indicates that the adsorption was a spontaneous and favorable process, naturally occurring, without external interferences in all of them. The negative $\Delta H°$= -73.66 J. mol^{-1} and positive $\Delta S°$= 174.25 kJ. mol^{-1}, indicated an increase in the disorder of the system (Nascimento *et al.*, 2014).

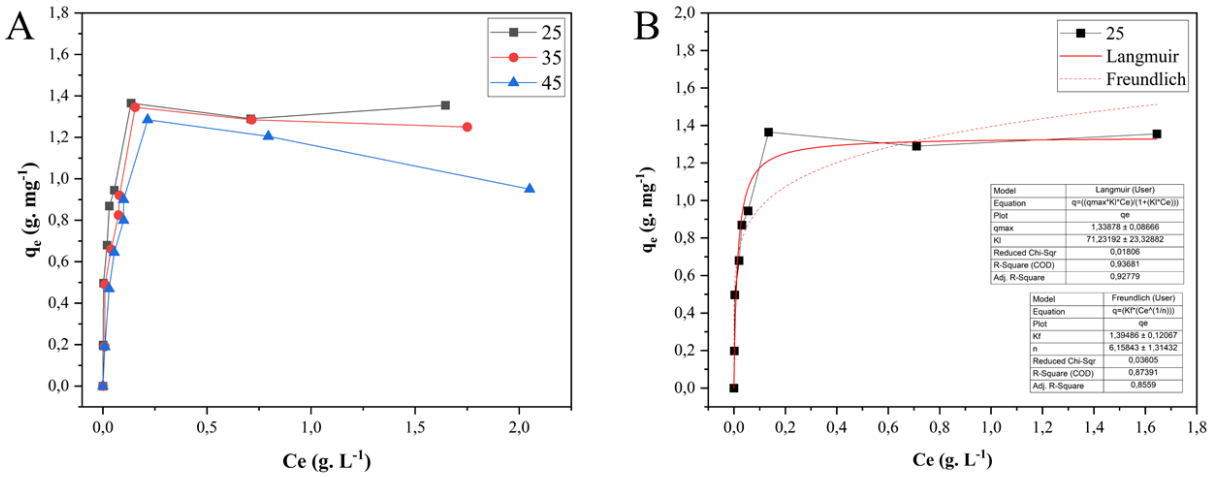

Figure 8. A) Adsorption isotherms at 25° C, 35° C, and 45° C; B) Adsorption isotherm at 25° C and isotherm models of Langmuir and Freundlich.

3.5 Reuse of nanoparticles

The HE% of MNP-TNs was analyzed in 10 reuse cycles (Figure 6). The HE≅ 93% was maintained for 6 cycles. From the 7th cycle onwards, there was a decrease until HE%= 74.2% was reached in the 10th cycle. The results obtained were satisfactory and proved the efficiency of the selected method in this context. Basically, two different methods are found in the literature to detach MNPs (acidy and basic), acidy dissolution, at pH< 4, where the particles are dissolved and separated from biomass by filtration (Wang *et al.*, 2015). However, as this work used MNPs functionalized, dissolving the nanoparticles seems not the best option, since after all reuse cycles the MNPs would need to be rebuilt. In the basic detachment, the microalgae and MNP-TNs presented a weak interaction, due to the negative superficial charges on both, facilitating the harvesting.

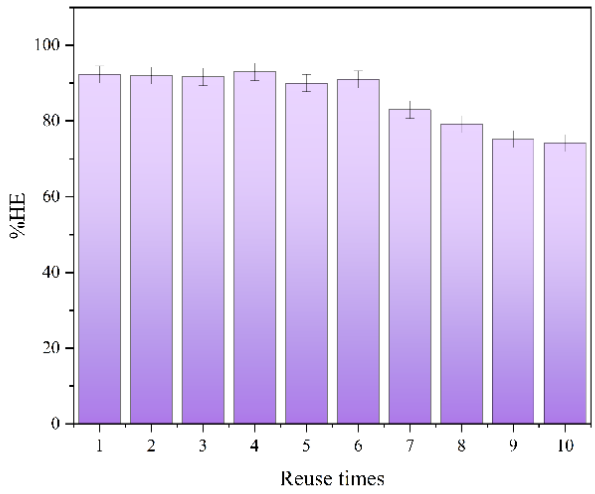

Figure 6. Reuse cycles of MNP-TNs applied in *Chlorella sp.* biomass harvesting.

4 Conclusions

It is possible to conclude that MNP-TNs presented a satisfactory result when applied in microalgae biomass harvesting. At the optimal conditions (MNP-TNs concentration=1,000 mg. L^{-1}; pH= 4) an HE% 92.6 with q_{exp}= 1.39 g. mg^{-1} was achieved. Even out of optimal conditions, but near to real cultivation conditions, the HE% was maintained at 63% (MNP-TNs concentration=1,000 mg. L^{-1}; pH= 10); which may reduce the costs on industrial-scale application. In addition, was possible to maintain the HE≅ 93%, during 5 reuse cycles, don't requiring the addition of new MNP-TNs, which also can contribute to cost reduction. In general, the results are promising, however, the application of this material on the pilot scale can validate the applicability of the technique on a wide scale. The utilization of less noble magnetic nanomaterials could be a great strategy to enable the process.

5. References

ABDUL HAMID, S. H.; LANANAN, F.; DIN, W. N. S.; LAM, S. S.; KHATOON, H.; ENDUT, A.; JUSOH, A. Harvesting microalgae, Chlorella sp. by bio-flocculation of Moringa oleifera seed derivatives from aquaculture wastewater phytoremediation. **International Biodeterioration & Biodegradation**, v. 95, n. PA, p. 270–275, 1 nov. 2014.

ABILLEIRA, F.; VARELA, P.; CANCELA, Á.; ÁLVAREZ, X.; SÁNCHEZ, Á.; VALERO, E. Tannins extraction from Pinus pinaster and Acacia dealbata bark with

applications in the industry. **Industrial Crops and Products**, v. 164, p. 113394, 1 jun. 2021.

ABO MARKEB, A.; LLIMÓS-TURET, J.; FERRER, I.; BLÁNQUEZ, P.; ALONSO, A.; SÁNCHEZ, A.; MORAL-VICO, J.; FONT, X. The use of magnetic iron oxide-based nanoparticles to improve microalgae harvesting in real wastewater. **Water Research**, v. 159, p. 490–500, 1 ago. 2019.

ACOSTA-FERREIRA, S.; CASTILLO, O. S.; MADERA-SANTANA, J. T.; MENDOZA-GARCÍA, D. A.; NÚÑEZ-COLÍN, C. A.; GRIJALVA-VERDUGO, C.; VILLA-LERMA, A. G.; MORALES-VARGAS, A. T.; RODRÍGUEZ-NÚÑEZ, J. R. Production and physicochemical characterization of chitosan for the harvesting of wild microalgae consortia. **Biotechnology Reports**, v. 28, p. e00554, 1 dez. 2020.

ANDERSEN, R. A. **Algal Culturing Techniques**. [2017].

ANTONY, J. Fractional Factorial Designs. *Em*: **Design of Experiments for Engineers and Scientists**. [2022] Elsevier, 2014. p. 87–112.

BAYAT TORK, M.; KHALILZADEH, R.; KOUCHAKZADEH, H. Efficient harvesting of marine Chlorella vulgaris microalgae utilizing cationic starch nanoparticles by response surface methodology. **Bioresource Technology**, v. 243, p. 583–588, 1 nov. 2017.

CARDOSO, N. F.; LIMA, E. C.; ROYER, B.; BACH, M. V; DOTTO, G. L.; PINTO, L. A.; CALVETE, T. Comparison of Spirulina platensis microalgae and commercial activated carbon as adsorbents for the removal of Reactive Red 120 dye from aqueous effluents. **Journal of Hazardous Materials**, p. 146–153, 2012.

CHEN, C. L.; CHANG, J. S.; LEE, D. J. Dewatering and Drying Methods for Microalgae. **https://doi.org/10.1080/07373937.2014.997881**, v. 33, n. 4, p. 443–454, 12 mar. 2015.

CHEN, C.; TANG, T.; SHI, Q.; ZHOU, Z.; FAN, J. The potential and challenge of microalgae as promising future food sources. **Trends in Food Science & Technology**, v. 126, p. 99–112, 1 ago. 2022.

CHIU, S. Y.; KAO, C. Y.; CHEN, T. Y.; CHANG, Y. BIN; KUO, C. M.; LIN, C. S. Cultivation of microalgal Chlorella for biomass and lipid production using wastewater as nutrient resource. **Bioresource Technology**, v. 184, p. 179–189, 1 maio 2015.

CLEMONS, T. D.; KERR, R. H.; JOOS, A. Multifunctional Magnetic Nanoparticles: Design, Synthesis, and Biomedical Applications. **Comprehensive Nanoscience and Nanotechnology**, v. 1–5, p. 193–210, 1 jan. 2019.

DABIZHA, A.; KERSTEN, M. Exothermic adsorption of chromate by goethite. **Applied Geochemistry**, v. 123, p. 104785, 1 dez. 2020.

ESTUDILLO-DEL CASTILLO, C.; LIGOT, E. M.; NUDO, L. P. Growth performance and lipid profiles of some tropical microalgae: An assessment of their potential as biofuel source. **Biocatalysis and Agricultural Biotechnology**, v. 50, p. 102699, 1 jul. 2023.

GERULOVÁ, K.; BARTOŠOVÁ, A.; BLINOVÁ, L.; BÁRTOVÁ, K.; DOMÁNKOVÁ, M.; GARAIOVÁ, Z.; PALCUT, M. Magnetic Fe3O4-polyethyleneimine nanocomposites for efficient harvesting of Chlorella zofingiensis, Chlorella vulgaris, Chlorella sorokiniana, Chlorella ellipsoidea and Botryococcus braunii. **Algal Research**, v. 33, p. 165–172, 1 jul. 2018.

HADJOUDJA, S.; DELUCHAT, V.; BAUDU, M. Cell surface characterisation of Microcystis aeruginosa and Chlorella vulgaris. **Journal of Colloid And Interface Science**, v. 342, p. 293–299, 2009.

HO, Q. N.; FETTWEIS, M.; HUR, J.; DESMIT, X.; KIM, J. I.; JUNG, D. W.; LEE, S. D.; LEE, S.; CHOI, Y. Y.; LEE, B. J. Flocculation kinetics and mechanisms of

microalgae- and clay-containing suspensions in different microalgal growth phases. **Water Research**, v. 226, p. 119300, 1 nov. 2022.

HU, Y. R.; GUO, C.; WANG, F.; WANG, S. K.; PAN, F.; LIU, C. Z. Improvement of microalgae harvesting by magnetic nanocomposites coated with polyethylenimine. **Chemical Engineering Journal**, v. 242, p. 341–347, 15 abr. 2014.

IBRAHIM, A.; YASER, A. Z.; LAMAMING, J. Synthesising tannin-based coagulants for water and wastewater application: A review. **Journal of Environmental Chemical Engineering**, v. 9, n. 1, 1 fev. 2021.

KIM, J.; YOO, G.; LEE, H.; LIM, J.; KIM, K.; KIM, C. W.; PARK, M. S.; YANG, J. W. Methods of downstream processing for the production of biodiesel from microalgae. **Biotechnology Advances**, v. 31, n. 6, p. 862–876, 1 nov. 2013.

KRISTIANSEN, A. B.; CHURCH, N.; UCAR, S. Investigation of magnetite particle characteristics in relation to crystallization pathways. **Powder Technology**, v. 415, p. 118145, 1 fev. 2023.

LEE, K.; LEE, S. Y.; PRAVEENKUMAR, R.; KIM, B.; SEO, J. Y.; JEON, S. G.; NA, J. G.; PARK, J. Y.; KIM, D. M.; OH, Y. K. Repeated use of stable magnetic flocculant for efficient harvest of oleaginous Chlorella sp. **Bioresource Technology**, v. 167, p. 284–290, 1 set. 2014.

LI, N.; WANG, P.; WANG, S.; WANG, C.; ZHOU, H.; KAPUR, S.; ZHANG, J.; SONG, Y. Electrostatic charges on microalgae surface: Mechanism and applications. **Journal of Environmental Chemical Engineering**, v. 10, n. 3, p. 107516, 1 jun. 2022.

LIU, D.; WANG, P.; WEI, G.; DONG, W.; HUI, F. Removal of algal blooms from freshwater by the coagulation-magnetic separation method. **Environmental Science and Pollution Research**, v. 20, n. 1, p. 60–65, 1 jan. 2013.

LIU, P. R.; WANG, T.; YANG, Z. Y.; HONG, Y.; HOU, Y. L. Long-chain poly-arginine functionalized porous Fe3O4 microspheres as magnetic flocculant for efficient harvesting of oleaginous microalgae. **Algal Research**, v. 27, p. 99–108, 1 nov. 2017.

LIU, Y.; JIN, W.; ZHOU, X.; HAN, S. F.; TU, R.; FENG, X.; JENSEN, P. D.; WANG, Q. Efficient harvesting of Chlorella pyrenoidosa and Scenedesmus obliquus cultivated in urban sewage by magnetic flocculation using nano-Fe3O4 coated with polyethyleneimine. **Bioresource Technology**, v. 290, p. 121771, 1 out. 2019.

MACHADO, G.; SANTOS, C. A. B. DOS; GOMES, J.; FARIA, D.; SANTOS, F.; LOUREGA, R. Chemical modification of tannins from Acacia mearnsii to produce formaldehyde free flocculant. **Science of The Total Environment**, v. 745, p. 140875, 25 nov. 2020.

NASCIMENTO, R. F.; LIMA, A. C. A.; VIDAL, C. B.; MELO, D. Q.;; RAULINO, G. S. C. **Adsorption: Theoric aspects and environmental applications**. [s.l: s.n.].

SAJID, M.; PŁOTKA-WASYLKA, J. Nanoparticles: Synthesis, characteristics, and applications in analytical and other sciences. **Microchemical Journal**, v. 154, p. 104623, 1 maio 2020.

SALEH, T. A. Isotherm models of adsorption processes on adsorbents and nanoadsorbents. **Interface Science and Technology**, v. 34, p. 99–126, 1 jan. 2022.

SEO, J. Y.; LEE, K.; PRAVEENKUMAR, R.; KIM, B.; LEE, S. Y.; OH, Y. K.; PARK, S. BIN. Tri-functionality of Fe3O4-embedded carbon microparticles in microalgae harvesting. **Chemical Engineering Journal**, v. 280, p. 206–214, 5 nov. 2015.

SILVEIRA, C.; SHIMABUKU, L. Q.; FERNANDES, M. S.; BERGAMASCO, R. Iron-oxide Nanoparticles by Green Synthesis Method Using Moringa oleifera Leaf Extract for Fluoride Removal. **Environmental Technology**, v. 3330, n. August, p. 1–40, 2017.

SINGH, G.; AGRAWAL, T.; LESANI, P.; BISHT, P. B.; ZREIQAT, H. Tuning the size, concaveness, and aspect ratio of concave cubic gold nanoparticles produced with high reproducibility. **Materials Today Chemistry**, v. 23, p. 100657, 1 mar. 2022.

STUART, B. **Infrared Spectroscopy_ Fundamentals and Applications**. [s.l: s.n.]. v. 1

VANDAMME, D.; FOUBERT, I.; MEESSCHAERT, B.; MUYLAERT, K. Flocculation of microalgae using cationic starch. **Journal of Applied Phycology**, v. 22, n. 4, p. 525–530, 27 nov. 2010.

VANDAMME, D.; FOUBERT, I.; MUYLAERT, K. Flocculation as a low-cost method for harvesting microalgae for bulk biomass production. **Trends in Biotechnology**, v. 31, n. 4, p. 233–239, 1 abr. 2013.

VÁZQUEZ-ROMERO, B.; PERALES, J. A.; PEREIRA, H.; BARBOSA, M.; RUIZ, J. Techno-economic assessment of microalgae production, harvesting and drying for food, feed, cosmetics, and agriculture. **Science of The Total Environment**, v. 837, p. 155742, 1 set. 2022.

WANG, L.; LIANG, W.; YU, J.; LIANG, Z.; RUAN, L.; ZHANG, Y. Flocculation of Microcystis aeruginosa using modified larch tannin. **Environmental Science and Technology**, v. 47, n. 11, p. 5771–5777, 4 jun. 2013.

WANG, S. K.; STILES, A. R.; GUO, C.; LIU, C. Z. Harvesting microalgae by magnetic separation: A review. **Algal Research**, v. 9, p. 178–185, 1 maio 2015.

WANG, X.; ZHAO, Y.; JIANG, X.; LIU, L.; LI, X.; LI, H.; LIANG, W. In-situ self-assembly of plant polyphenol-coated Fe3O4 particles for oleaginous microalgae harvesting. **Journal of Environmental Management**, v. 214, p. 335–345, 15 maio 2018.

WEN, H.; ZHANG, H.; HE, M.; ZHANG, X. A novel approach for harvesting of the microalgae Chlorella vulgaris with Moringa oleifera extracts microspheres by Buoy-bead flotation method. **Algal Research**, v. 60, p. 102479, 1 dez. 2021.

XU, L.; GUO, C.; WANG, F.; ZHENG, S.; LIU, C. Z. A simple and rapid harvesting method for microalgae by in situ magnetic separation. **Bioresource Technology**, v. 102, n. 21, p. 10047–10051, 1 nov. 2011.

YOU, Y.; YANG, L.; SUN, X.; CHEN, H.; WANG, H.; WANG, N.; LI, S. Synthesized cationic starch grafted tannin as a novel flocculant for efficient microalgae harvesting. **Journal of Cleaner Production**, v. 344, p. 131042, 10 abr. 2022.

YUAN, Q.; LI, H.; WEI, Z.; LV, K.; GAO, C.; LIU, Y.; ZHAO, L. Isolation, structures and biological activities of polysaccharides from Chlorella: A review. **International Journal of Biological Macromolecules**, v. 163, p. 2199–2209, 15 nov. 2020.

ZHAO, Y.; FAN, Q.; WANG, X.; JIANG, X.; JIAO, L.; LIANG, W. Application of Fe3O4 coated with modified plant polyphenol to harvest oleaginous microalgae. **Algal Research**, v. 38, 1 mar. 2019.

ZHOU, H.; LEE, JAEWOOK; PARK, T. J.; LEE, S. J.; PARK, J. Y.; LEE, JAEBEOM. Ultrasensitive DNA monitoring by Au–Fe3O4 nanocomplex. **Sensors and Actuators B: Chemical**, v. 163, n. 1, p. 224–232, 1 mar. 2012.

Chapter 4

Harvesting microalgae biomass by magnetic nanoparticles derived from alternative source

ABSTRACT

The utilization of magnetic nanoparticles for the efficient harvesting of microalgae has shown promising results in terms of enhanced harvesting efficiency within a reduced time frame. However, the cost associated with nanoparticle synthesis presents a potential constraint for the widespread implementation of this technique. In this way, this work investigated, for the first time, the efficacy of magnetic nanoparticles (MNPs) derived from particulate matter applied to microalgae (*Chlorella sp.*) harvesting in both form naked and functionalized with commercial tannin. The nanoparticles were characterized by (X-Ray Diffraction (XDR), Transmission electron microscopy (TEM), Scanning electron microscopy (SEM), Energy Dispersive X-Ray (EDS), Fourier transform infrared (FTIR), and Zeta potential. The MNPs present in particulate material were magnetite with an estimated size (based on 1,000 particles) around 30.5± 9.56 nm. The harvesting efficiency (HE%) was optimized by full factorial experiments, which the most influent variables (pH and MNPs concentration) were combinate in different levels achieving found the optimal harvesting efficiency. The MNPs (naked) obtained higher harvesting efficiency (HE%= 86%; MNPs concentration= 1,250mg. L^{-1}; pH= 3) than functionalized nanoparticles (HE%= 77%; MNP-TANs concentration= 1,100 mg/L; pH= 3.5), however was necessary a higher MNPs concentration in a lower pH. The functionalization contributed to particle stabilization increasing its reuse cycles from 3 (MNSs) to 7 cycles (MNP-TANs). At pH 10 (the final pH of the microalgae cultivation) both exhibited a similar HE% of 60%.

Keywords: *Chlorella sp.*, nanomaterial, optimization, iron oxide, isotherms.

1. Introduction

The increasing frequency and intensity of worldwide extreme climate events implied the urgent need for the transition from fossil fuel to renewable energy sources as a key strategy to mitigate the ongoing climate change scenarios (Mata, Martins e Caetano, 2010). Through this, microalgae biomass production emerges as a promising alternative renewable sustainable energy source for biofuels production through its potential for producing large amounts of biomass as well as high CO_2 fixation rates during the photosynthesis process (potential generation of carbon credits to reach regional to international climate agreements (Barizão *et al.*, 2023)). without using arable lands for cultivation, and in addition high potential in the removal of nutrients and contaminants from wastewater (Xu *et al.*, 2023).

However, one of the major challenges to large-scale production of microalgae is to perform the harvesting step efficiently, quickly and at low cost. The morphological characteristics of microalgae, such as high negative surface charge and low density, make the biomass concentration stage difficult (Yin *et al.*, 2022). To overcome this limitation, methods such as filtration (Zhao, Muylaert and Vankelecom, 2021), flocculation (Okoro *et al.*, 2019), and centrifugation (Najjar and Abu-Shamleh, 2020) have been studied over the years. In this scenario, the use of reusable magnetic nanoparticles (MNPs; e.g., magnetite (Fe_3O_4)) has been highlighted to provide fast and efficient harvesting, resulting in high quality biomass with no residual contamination from the harvesting stage (Fu *et al.*, 2021).

Brazil presents one of the most mineral reserves in the world, being the second country with the most significant iron reserves in the world (19.6% of worldwide reserves or 33.000 tons), behind just Australia. The mining of metallics substances corresponds to 89% of the total value of commercialized production since iron ore is responsible for 80,1% of it (AGÊNCIA NACIONAL DE MINERAÇÃO – ANM, 2021). Pará and Minas Gerais (gross production) are the main producers of iron from Brazil, followed by Espírito Santo (beneficiation), in the third position. Despite the state doesn't count iron mines, is responsible for the beneficiation and exportation of a considerable part of iron ore produced in the country (AGÊNCIA NACIONAL DE MINERAÇÃO – ANM, 2021).

During the transport, processing, and storage of iron, the small particles can be dissipated in the air and become part of the particle material composition (Galvão *et al.*, 2022). The appropriate application of this nanomaterial can include it in a circular economy perspective, giving it an economically efficient destination while reducing the costs associated with harvesting microalgae. In addition, some techniques (functionalization) can be used to modify the nanoparticle's surface and improve its properties favoring the MNPs/ microalgae interaction (Keçili *et al.*, 2021; Upadhyay *et al.*, 2023). The utilization of tannins derived from different plants, such as Rhizophora mangle (Chapter 3), has been shown to be efficient in the functionalization of magnetite nanoparticles produced via chemical precipitation, achieving harvest efficiencies exceeding 90%, making it a good candidate for functionalizing nanoparticles from alternative sources. In this way, this work investigated, for the first time, the efficacy of magnetic nanoparticles (MNPs) derived from particulate matter applied to microalgae (*Chlorella sp.*) harvesting in both form naked and functionalized with commercial tannin.

2. Materials and methods

2.1 Materials

Particulate material collected at Guarapari, ES, Brazil (20º39'14.48"S; 40º29'14.85"O), commercial tannins (TANFLOC, from TANAC), Ultrapure Water (Sartorius), Neodymium magnet 50× 50× 12 mm (Supermagnet, Brazil). *Chlorella sp.* strain (L06, from Laboratory of Chemical, Physical and microbiology characterization of Federal University of Espirito Santo). BG11 medium ($NaNO_3$ (1.5 g. L^{-1}); $K_2HPO_4.3H_2O$ (40 mg. L^{-1}); $MgSO_4.7H_2O$ (75 mg. L^{-1}); $CaCl.2H_2O$ (36 mg. L^{-1}); $C_6H_8O_7$ (6 mg. L^{-1}); $C_6H_5FeO_7$ (6 mg. L^{-1}); Na_2CO_3 (20 mg. L^{-1}); (Andersen, 2005)). Laboratory glassware such as beakers, volumetric flasks, falcon tubes. All glassware was sanitized using aqua regia (HCl: HNO_3) for 5 times and washed ten times with ultrapure water before the experiments.

2.2 Selection of magnetic nanoparticles source and functionalization

The source of nanoparticles was selected based on the literature, considering the local availability, costs, and magnetic iron oxide content. The particulate matter (selected source) was collected on a clean surface (open area (15 m^2)) at Guarapari, Espírito Santo, Brazil, for 15 days. Firstly, the raw material was screened to remove coarse materials, such as leaves and dust. The remaining particles were resuspended in 200 ml of ultrapure water and left under stirring for 1 min. The resulting solution was submitted to magnetic field influence at 1 min. separating the magnetic nanoparticles. This procedure was repeated 7 times. The washed nanoparticles were processed at muffle (500º C) during 30 min. to eliminate the remaining organic matter in the sample.

The functionalization process was performed initially using 3-Aminopropyltriethoxysilane (APTES), adding up 0.6947 g of MNPs in 3 ml of APTES previously dissolved in 25 ml of ethanol and stirred for 10 min. at room temperature. 0.6947 g of MNPs was added to the mixture and stirred for 48 h. In sequence, the MNPs were washed until completely remove unreacted APTES in the supernatant. After this, the MNPs were functionalized using commercial tannin. The functionalization was done according to Zhao *et al.* (Zhao *et al.,* 2019c), using 1 g of MNPs and 40 ml of tannins solution at 25 g. L^{-1}, the mixture was stirred (25º C) during 2 h. The MNPs functionalized

(MNP-TANs) were washed until completely remove the excess of tannins in supernatant and, stored in falcon tubes at 8° C in the dark.

2.3 Characterization of magnetic nanoparticles

The magnetic nanoparticles were characterized different techniques. The crystalline phase was identified using an X-Ray Diffractometer (XRD- 6000, Shimadzu) in range 2Θ from 20 up to 70. The shape, dispersion, size, and composition of nanoparticles were analyzed by transmission electron microscopy (TEM (JEOL, JEM1400)), scanning electron microscopy (SEM (JEOL, JSM6610LV)) coupling with Energy Dispersive X-Ray Detector (EDS). The functionalization was monitored by Fourier transform infrared (FTIR) and elementary analyses of CHNS. The superficial charge of nanoparticles and *Chlorella sp.* were determinates by Zeta potential, in a pH range of 4, 7 and 10.

2.4 Molecular docking

The docking analysis was performed to evaluate the interaction mechanisms between nanoparticles and their stabilizer (APTES) and functionalizer (TANFLOC™). Firstly the magnetite supercell (2x2x2) and the TANFLOC™ molecule were both modeled in Avogadro (1), with the latter based on the two-dimensional polymeric structure depicted in Mangrich (2014) (2). The magnetite supercell was subjected to the UFF force field, while TANFLOC™ was separately treated with four different force fields (GAFF, Ghemical, MMFF94, and UFF). Overall, five distinct PDB files were obtained, although this work focuses exclusively on the docking experiments of MNPs with TANFLOC™ under the Ghemical force field, as it has shown the best results in another work being developed by the team.

The magnetite supercell was prepared in AutoDock Tools 1.5.7 as a receptor for docking experiments. The preparation steps included removing water (3), adding polar hydrogen atoms (3–5), calculating Gasteiger charges (6), and assigning AD4 atom type to the macromolecule's atoms. Meanwhile, Tanfloc™ was prepared as the ligand. Since it presented over 100 torsions, surpassing the allowed maximum of 32, the number of torsions set was 32. Both molecules were saved as PDBQT files.

Since AutoDock Vina 1.2.3 doesn't support PDBQT files that contain HETATM and CONECT records, docking was performed by AutoDock 4.2, with 7.964, 9.091, and 10.017 as the x, y, and z centers, respectively; 90 as box size for all three coordinates; grid spacing of 0.375 Å; and 100 runs, following the protocol of Rizvi *et al.*, 2013. The binding energies and RMSD values were extracted from the result tables in the DLG file, and an in-house R script extracted the intermolecular energy values from the runs. The energy and RMSD plots were generated using the ggplot2 package (7) in R 4.2.2, within the RStudio/Posit 2023.03.1+446 environment. Three-dimensional images illustrating the interactions between the magnetite supercell (representing the iron (III) oxide nanoparticle capped with APTES) and Tanfloc™ were rendered using AutoDock Tools, ChimeraX, and PyMOL.

2.5 Factorial experiments design

The *Chlorella sp.* was cultivated in batch assays using 5 L tubular photobioreactors, and BG11 culture medium; under stirring at 70 rpm, and natural lighting (approximately 1500 lux). The microalgae growth was monitored until the achieving stationary phase (680 nm). Then the produced biomass was used in factorial experiments.

A full factorial (2^3) was realized to optimize microalgae harvesting. The independent variables pH and nanoparticles concentration and levels (Table 1) were selected based on our last work (Chapter 3), resulting in the design matrix available in Table 2. The nanoparticles were tested in their naked version (MNPs) and functionalized (MNP-TANs).

Table 1. Levels of full factorial experiments.

VARIABLES	Levels		
	(-1)	0	(+1)
pH	4	7	10
MNPs concentration (mg. L^{-1})	800	1,000	1,200

Table 2. Design matrix of full factorial (2^3).

pH	Naked MNPs/MNP-TAN concentration	Treatments
-1	-1	2
-1	1	7
1	-1	11
1	1	3
-1	0	8
1	0	9
0	-1	4
0	1	10
0	0	5
0	0	6
0	0	13
0	0	12
0	0	1

All experiments were carried out in batch at volume of 1 ml of microalgae solution. The harvesting efficiency (HE% (Equation 1)) was adopted as the dependent variable, and was based on microalgae concentration in supernatant after 1 min. of reaction time (MNPs/ microalgae) and 3 min. of exposition to magnetic field (680 nm). The adsorption capacity was already estimated in optimum conditions ((q_{exp} (Equation 2)).

$$\text{HE\%} = (C_0 - C_e).\left({}^{1}/_{C_0}\right) . 100 \qquad (1)$$

$$q_{exp} = \left(\frac{C_0 - C_e}{m}\right) . \text{ V} \quad (2)$$

Where C_0 and C_e are the initial and final concentrations of dye (mg. L^{-1}), V is the volume of solution (L) and m is the mass of adsorbent (g).

2.6 Isotherms and thermodynamic parameters

The adsorption isotherms were performed at optimal conditions ((MNPs concentration= 1,250 mg. L^{-1}; pH= 3/ MNP-TANs concentration= 1,100 mg/L; pH= 3.5) varying only the microalgae concentration in range from 200 mg. L^{-1} up to 3,000 mg. L^{-1}, and temperature at 25, 35 and 45° C. After reaction time the solutions were exposed to magnetic field 3 min. and the HE% was estimated based on microalgae concentration in the supernatant (680 nm). The Langmuir (Equation 3) and Freundlich (Equation 4) models were applied to the data to establish the most appropriate correlation.

$$q = q_{max} K_L C_e / 1 + K_L C_e \quad (3)$$

$$q = K_F {C_e}^{1/n} \quad (4)$$

Where q is the solute adsorbed per gram of adsorbent at equilibrium (mg. g^{-1}), q_{max} is the maximum adsorption capacity (mg. g^{-1}), K_L is the interaction constants between adsorbate and adsorbent (mg. L^{-1}) and K_F Freundlich adsorption capacity constant (mg. L^{-1}), C_e is the concentration of adsorbate at equilibrium (mg. L^{-1}) and 1/n the surface heterogeneity constant (Nascimento *et al.*, 2014).

The thermodynamic parameters were also determined based at temperatures 25, 35 and 45 °C. The Gibbs free energy variation (ΔG°), the enthalpy (ΔH°) and the entropy (ΔS°) were determined by Equations 5, 6 and 7.

$$\Delta G^\circ = -RT ln K \quad (5)$$

$$\Delta G^\circ = \Delta H^\circ - T\,\Delta S^\circ \quad (6)$$

$$ln K = {\Delta S^\circ}/{R} - {\Delta H^\circ}/{R^x}\,{1}/{T} \quad (7)$$

Where R is the ideal gas constant (8.3144 $J\,K^{-1}\,mol^{-1}$), T is the temperature in Kelvin and K is the equilibrium constant (SILVEIRA *et al.*, 2017).

2.7 Reuse of nanoparticles

The reuse of MNPs and MNP-TAN was based in Lee *et al.* (Lee *et al.*, 2014b). The reuse cycles were realized in the optimal conditions (MNPs concentration= 1,250 mg. L^{-1}; pH= 3/ MNP-TANs concentration= 1,100 mg/L; pH= 3.5). After the reaction time (1 min.), the solutions were exposed to an external magnetic field for 3 min., and the HE% was estimated based on microalgae concentration in the supernatant (680 nm). The flocks (nanoparticles/ microalgae) obtained in any harvesting cycle were suspended in 300 µL of distilled water at pH 12 and let in vortex during 30 s, following 1 min in ultrasound. The recovered nanoparticles were separated by a magnetic field, washed and recycled during ten cycles.

3. Results and discussion

3.1 Selection of MNPs source and functionalization

Firstly, was realized a literature revision to identify possible nanomagnetic iron sources, considering the iron content, positive and negatives points, and when possible, the costs of material requirement (Table 1). Based on these analyses, the particulate material was selected due to its easy acquisition, simple pretreatments, local availability, and, different from others, that don't have negative points capable to limit their potential application in microalgae harvesting, for example heavy metals that can contaminate the biomass.

Table 1. The main potential sources of magnetic iron selected in the literature.

Material	Iron content	Positive	Negative	Costs	Ref.
Blast Furnace Slag	0.45 % (FeO)	-Great availability; -High information; -It`s a residue.	-Low magnetic iron content; -Hard processing due high carbonate content; -High water consume to processing samples;	R$5,00/ tons	(ArcelorMittal, 2023)
Blast furnace Mud	41.76 % (Fe_2O_3)	-Small size (59,5% <0,038 mm); -Highly disponible; -High magnetic iron content;	-Presence of heavy metals; -Contamination of microalgae biomass;	-Sale value not found	(ArcelorMittal, 2023)
Sínter	57.5 (Fe)	-Highly disponible; -High magnetic iron content;	-It`s not a residue; -Very required in steel production;	U$61,23/tons	(Guerriero *et al.*, 2009)
Electrostatic precipitator dust	6~10 (Fe_2O_3)	-Highly disponible;	-Can be collected and reinserted in	-Sale value not found	(Qi, Han e Zhang, 2019)

		-High magnetic iron content; -It`s a residue.	the company itself;		
Particulate material	4% (Fe_3O_4)	-Highly disponible; - Don´t have costs.	-Little information available;	-Don´t have costs.	(Galvão *et al.*, 2022)

The collection place (the roof of a building) is located in the metropolitan area on the southeast coast of Brazil, in the state of Espirito Santo. The region is highly industrialized, including steel and iron pelletizing companies, that are responsible for approximately 70% of all particulate materials emissions in the region (Galvão *et al.*, 2022). Galvão *et al.* (2022) reported the presence of iron oxide in the particulate matter from this region, with magnetite accounting for up to 4% of the settable particulate matter, reaffirming the potential of this source for magnetic nanoparticle acquirement. Furthermore, we are not aware of any other studies that have recognized particulate matter as a potential source of magnetic nanoparticles directed to harvesting microalgae.

3.2 Characterization of magnetic nanoparticles

Firstly, the particulate material (MNPs) was several washed aiming the separation of the magnetic fraction, and muffled to reduce the organic impurities. Trought elementary analysis (3 mg of sample) was observed that the muffle process was able to reduce the samples C content in more the two thirty, passing from 6.135316342% to 1.9559834%. The N (0.472024729%) and H (0.8162449%) were also reduced to 0.277542085% and 0.36298874%, respectively. Despite efficiency, the process didn't completely remove impurities, which can imply the reproducibility of the results, as it makes the surface of the nanoparticles more heterogeneous (Li *et al.*, 2021).

The magnetic fraction of particulate material (MNPs) was analyzed by TEM (Figure 1A). The particles presented an estimated size (based on 1,000 particles) around 30.5± 9.56 nm (Figure 1B), with an aspect ratio (AR= 1.12±0.5) indicating quasi-

spherical (Figure 1C). However, the hydrodynamic size (Figure 1D) observed was 295±40 nm, which could be related to agglomerate tendency of the material in aqueous solution or the polydispersity (Pdl= 1.0). The polydispersity of MNPs was expected, since nanoparticles was obtained from natural source and don't pass for any size selection process (Carnino and Lee, 2022).

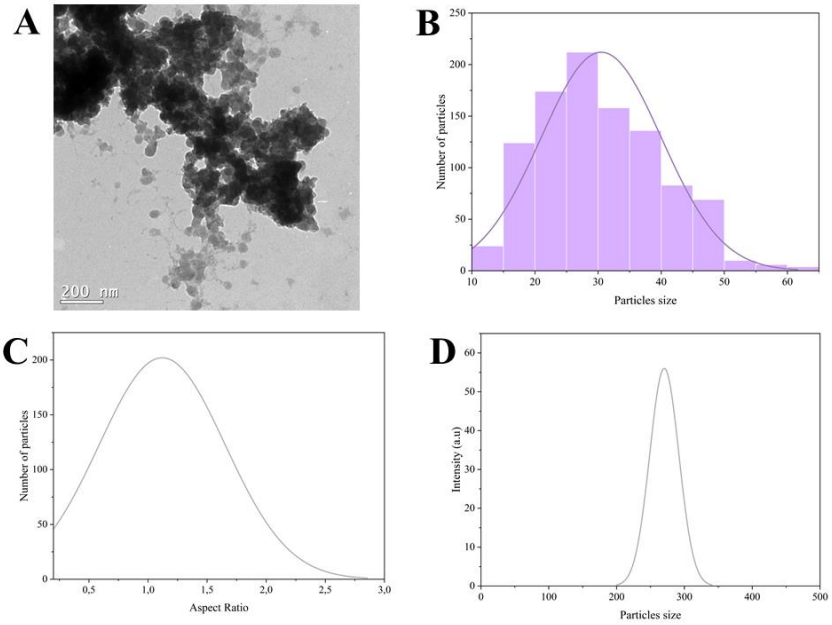

Figure 1. A) TEM of magnetic fraction of particulate material; B) Histogram of MNPs size distribution, based on Figure 1A; C) Aspect ratio of MNPs, based on Figure 1A; D) Hydrodynamic size of MNPs.

Comparing the XDR diffractogram of MNPs from particulate material with magnetite (Fe_3O_4, from Chapter 3) diffractogram, it's possible to observe similarities, with peaks in 35.46°, 56.6°, and 62.60°, corresponding to (311), (422) and (440) (Clemons, Kerr and Joos, 2019) (Figure 2A). The presence of other peaks can be related to residual impurities remaining even after the wash and muffle process. The elementary identification of MNPs in SEM coupled with EDS, supported this hypothesis (Figure 2B and C) where besides high Fe and O content, was observed the presence of Silicon, Sodium, Gold, Calcium, Magnesium and Aluminium. The Gold present was coming sample preparation.

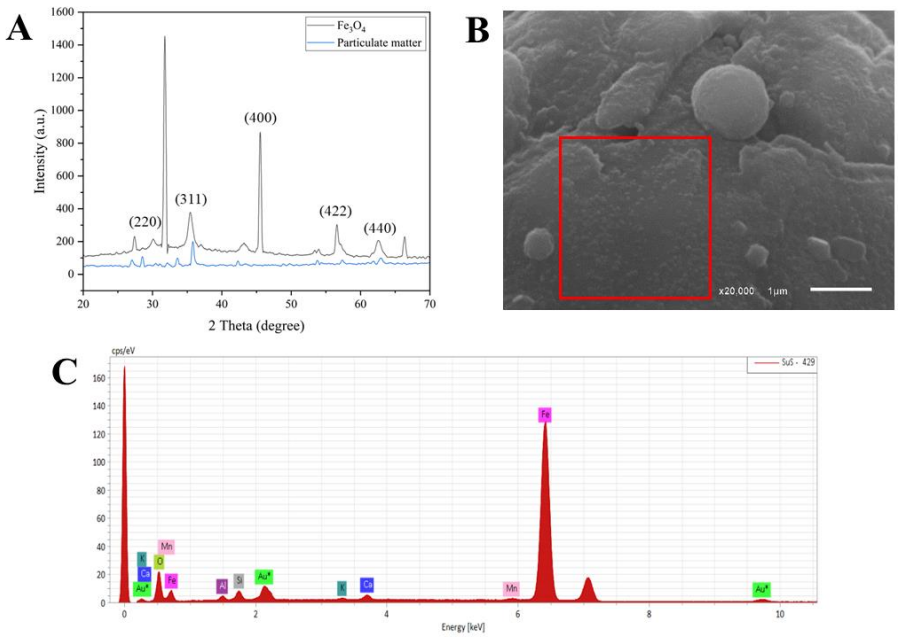

Figure 2. A) XDR diffractogram of MNPs; B) SEM of MNPs; C) EDS of MNPs.

The MNPs obtained were stabilized by APTES and functionalized using commercial tannins (MNP-TANs). By elementary analysis (Table 1) was observed an increase in the N content of functionalized samples. This occurred due the presence of N in the APTES and also due the amines in the tannins structure, that confers them a positive charge.

Table1. Elementary analyses of MNPs and MNP-TANs.

Samples	Nitrogen	Carbon	Hydrogen
MNPs	0.277542085	1.9559834	0.36298874
MNP-TANs	0.312462062	2.071474791	0.463305414
Commercial tannin	5.855441252	35.82078934	6.420233726

In addition, the peaks 1,306 and 1,289 cm^{-1} observed in the FTIR (Figure 3), can be related to aromatic C-N stretching or also NO_2 symmetric stretching, indicating the presence of tannins. At the same time, the peaks 1,800 and 1,770 can be due the C=O stretching supporting above supposition.

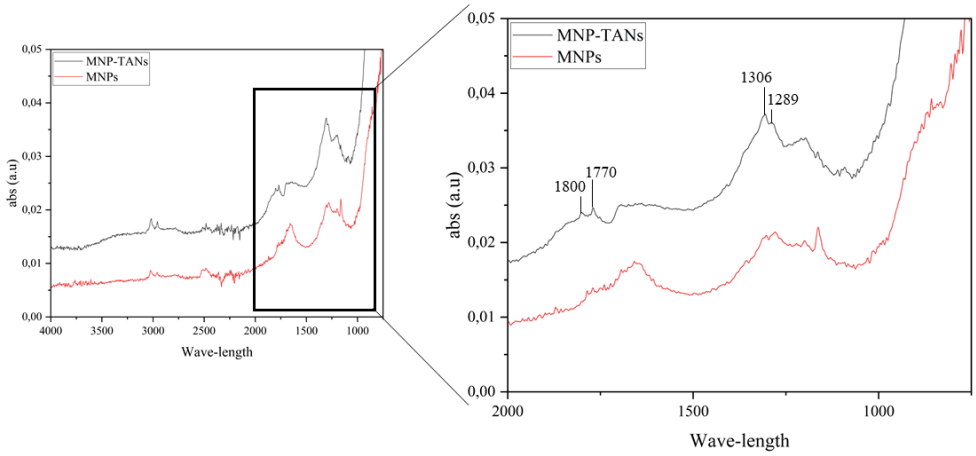

Figure 3. FTIR of MNPs and MNP-TANs.

3.3 Molecular docking

Molecular docking is a type of molecular modeling technique that demonstrates how molecular structures fit together; a useful tool in the comprehension of the protein's behavior (Kufareva and Abagyan, 2012). However, in this work, this effective tool was applied to understand the interaction between the magnetic nucleus of nanoparticles (Fe_3O_4) and the stabilizer/ functionalizer molecules (MNP-APTES-tannins). The binding and intermolecular energy values of the hundred runs are shown in Figure 4, below.

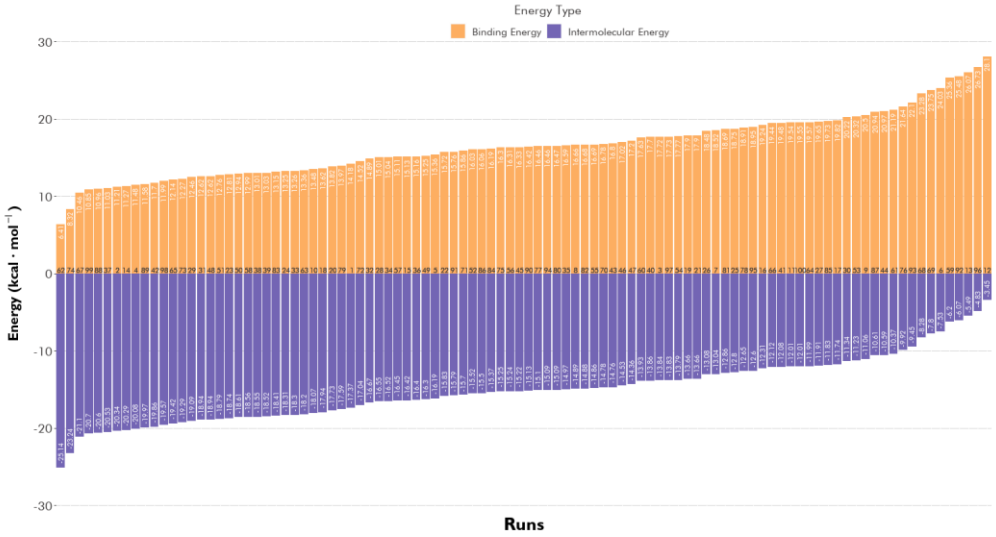

Figure 4. Main energies involved in the interaction between commercial and magnetite (stabilized with APTES). The orange bars refer to the binding energy and the purple bars to the energy of intermolecular interactions, whose final value is a sum of the energies of hydrogen bonds, Van Der Waals, solvation, and electrostatics in AutoDock 4.2. Each bar corresponds to one of hundred runs realized. Energy types involved in MNP-APTES-TAN bonds.

Commercial tannin presented a high root mean square deviation (RMSD; it measures how much the position of the ligand atoms deviated from the position of the first mode) (Yusuf *et al.*, 2008). Varying between 35 and 55 angstroms, in hundred runs (Figure 5). This could be related mainly to the use of a modeled molecule (and not crystallographic), making the result varies according to the defined configurations. The green points represent the worst (point 12) and best (point 62) results of the energy of intermolecular interactions.

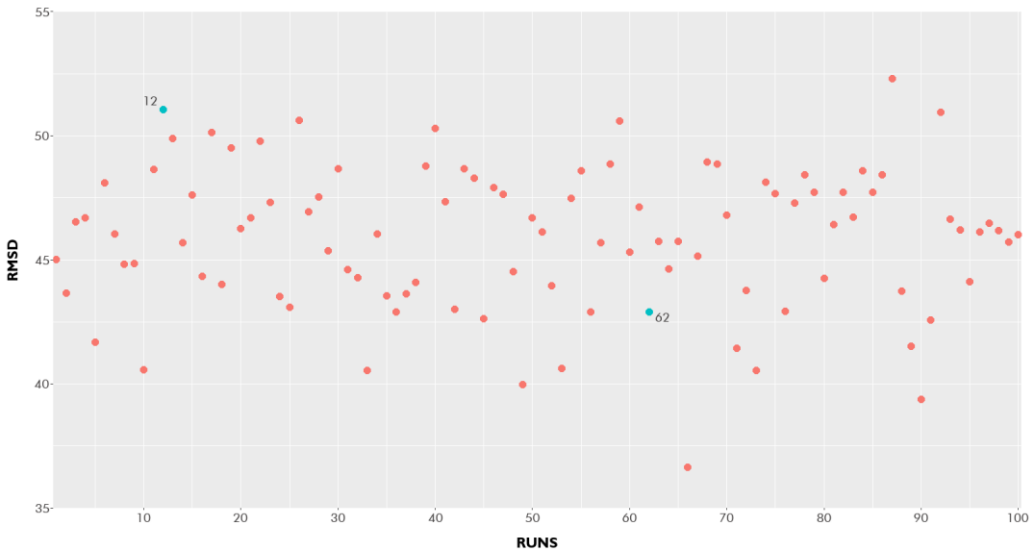

Figure 5. Root mean square deviation (Å) of each one of the hundred conformations of commercial tannin (ligand).

Different from what was expected, the intermolecular energies were predominant (more negative, indicating a spontaneous process). In Figures 6A and B, was observed that hydrogen bonds may be occurring between the O from magnetic iron oxide and the hydroxyl from tannin. The dipole-dipole can be also considered in this case, since Fe_3O_4 is a polar nanoparticle (due to differences in charges caused by the distribution of Fe^{2+} and Fe^{3+}), as well as, tannin which is composed of the bond of flavan-3-ol (Ibrahim, Yaser and Lamaming, 2021; Munoz *et al.*, 2015). Thus, both can present negative and positive regions, leading to interactions between them. It is also important to stress that the presence of impurities in the MNPs, even after pre-treatment, may have interfered with this interaction in ways, that we couldn't predict. The prevalence of weaker bonds doesn't necessarily indicate the inefficiency of the functionalizing layer, or that it will easily detach after the use of nanoparticles, as we were able to confirm in section 3.8.

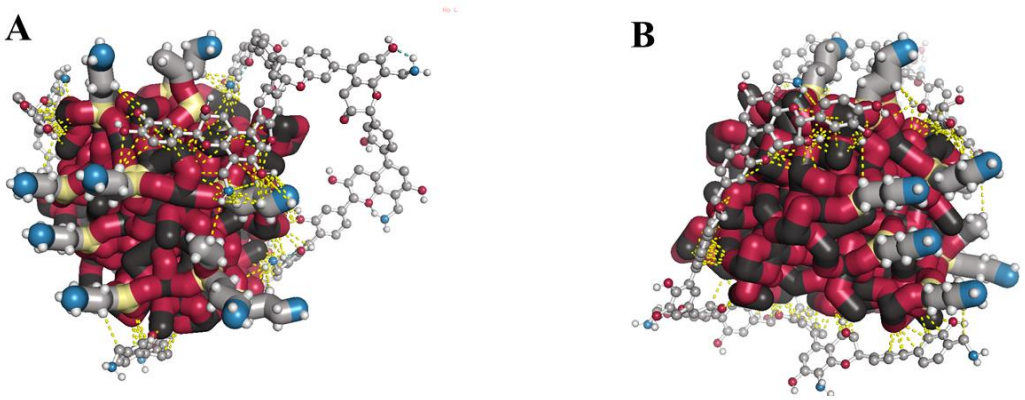

Figure 6. MNP-TAN molecular docking (MNP-APTES-TAN bonds); being atoms in red (O), black (Fe), gray (C), blue (N), white (H), yellow (Si) and dashed yellow line (intermolecular interactions. A) Original molecule position; B) Rotated molecule (45° in Y axis).

3.4 Factorial experiments design

The Full factorial experiments were carried out to optimize the harvesting of *Chlorella sp.* The biomass harvested was cultivated for 8 days (the end of the exponential phase), where achieve biomass concentration of 1.5 g. L^{-1} (pH=10.7). According to Pareto chart, for both nanoparticles (MNPs and MNP-TANs) the two variables were significant (Figure 7A, B, C and C; ANOVA Table 1 and 2 (Appendix II)), however the pH was the most influent in all cases.

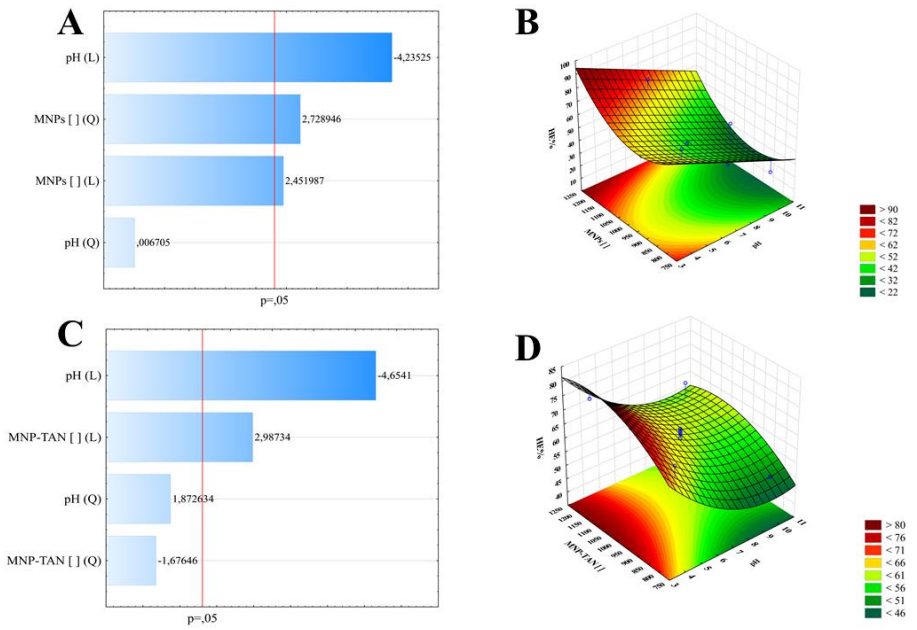

Figure 7. A) Pareto chart from MNPs; B) Response surface chart from MNPs; C) Pareto chart from MNP-TANs; D) Response surface chart from MNP-TANs.

The model demonstrated an acceptable adjustment to the data, with R^2= 0.80 (MNPs) and R^2= 0.81 (MNP-TANs) (Figure 7A and B). The MNPs presented higher HE% (93.5%) than MNP-TANs (82%), however, the nanoparticles concentration necessary was higher (1,250 mg. L^{-1}) and the pH (3) was smaller compared to MNP-TANs (1,100 mg. L^{-1} at pH= 3.5), achieving a near adsorption capacity being q_{exp}= 1.12 g. mg^{-1} for MNPs and q_{exp}= 1.025 g. mg^{-1} for MNP-TANs. The experimental HE% obtained in optimal conditions presented slightly lower than from the model, being HE%= 86% for MNPs and HE%= 77%. This can be justified by the value of R^2, below 90 in both cases.

The higher HE% of MNP-TANs can be justified by their less negative charge (-4 mV) compared to MNPs (-10 mV) (Figure 8). The presence of amine groups on MNP-TANs surface may have favored attraction with microalgae, requiring a lower concentration of nanoparticles. It is also important to consider that naked nanoparticles may be returning to ionic form due to oxidation by low pH, which does not occur with MNP-TANs due to their double protective layer (APTES-TANFLOC). The HE% of both tended to decrease when the pH was increased to 10. which makes sense as both become more negative, increasing the repulsion with microalgae. However, even though they become slightly negative at pH 10, they were capable of maintaining their HE%≈ 60%, a great result, considering that the final pH of microalgae cultivation is around 10.

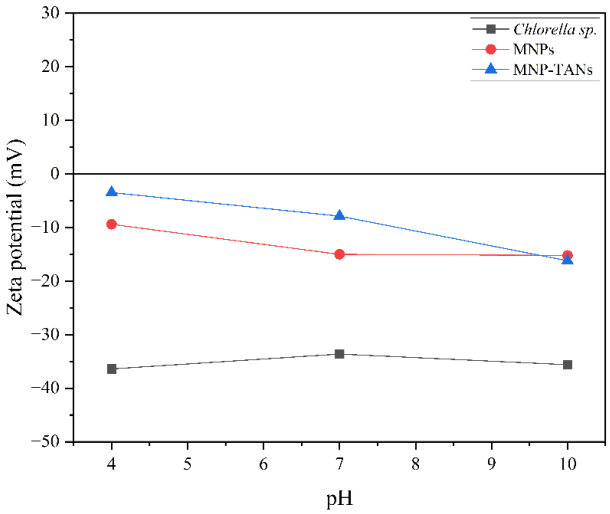

Figure 8. Zeta potential from MNPs and MNP-TANs.

3.5 Isotherms and thermodynamic parameters

The adsorption isotherm models are essential to describe the interaction between adsorbent and adsorbate at equilibrium and constant temperature (Saleh, 2022). For MNPs, increasing of temperature negatively interfere in the HE%, being the 25° C the best temperature, which indicate an exothermic process (Figure 9A). The best-fitty model with data was the Freundlich (Figure 9B), presenting a great adjustment to data, with R^2=0.98. Freundlich model considers a heterogeneous solid, which in some adsorption sites are highly energetic and the adsorbent/ adsorbate interaction is strong; while others present low energy, and the bond is consequently weaker.

These results are consistent with the fact that MNPs are bare nanoparticles sourced from natural materials and contain impurities (molecules other than Fe and O) in their structure, as observed in the characterization, which can interfere with the adsorption process. Nevertheless, this was not enough to disable the adsorption, as n>1 (3.63±0.25) indicates a favorable process. This suggests that adsorption is favorable, as it indicates a higher concentration of active adsorption sites compared to the concentration in the liquid phase. In this case, the amount adsorbed increases more rapidly than the concentration in the liquid phase (Nascimento *et al.*, 2014). The maximum adsorption capacity of adsorbent (q_{max}= 1.5 g. mg^{-1}) was compatible with obtained in factorial experiments (q_{exp}= 1.12 g. mg^{-1}).

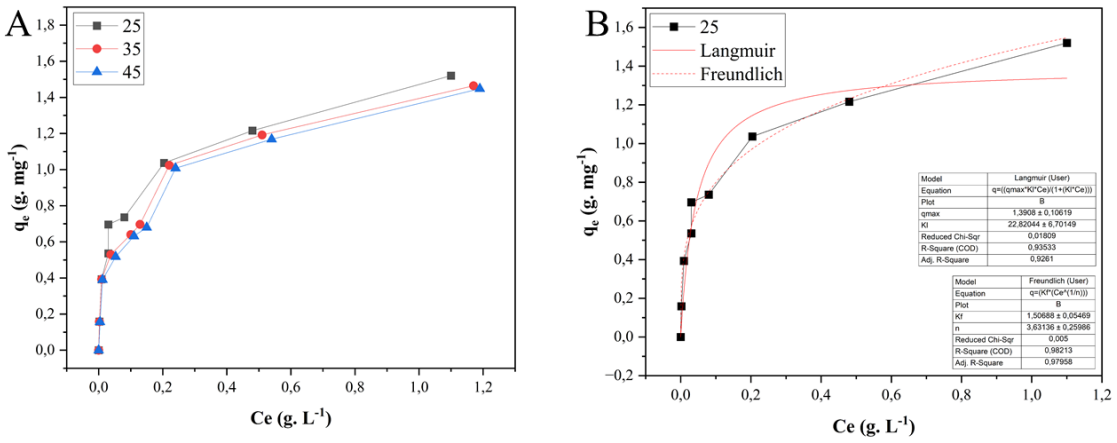

Figure 9. A) Adsorption isotherms (MNPs) at 25° C, 35° C, and 45° C; B) Adsorption isotherm (MNPs) at 25° C and isotherm models of Langmuir and Freundlich.

Similar to MNPs, the adsorption process with MNP-TANs was also an exothermic process (Figure 10A). Exothermic adsorption can lead to cost savings in industrial applications by minimizing the requirement for additional energy sources (Nascimento *et al.*, 2014). The MNP-TANs, the best-fitty model with data was the Langmuir (Figure 10B), with R^2=0.94. Different from Freundlich's model, Langmuir's model assumes adsorption in monolayer, where the bonded sites have equivalent energy (behaving only one molecule at each site). In this case, the functionalization process may have contributed to a more uniform particle surface, resulting in active sites with closer binding energies, different than the naked particle. The maximum adsorption capacity of adsorbent was q_{max}= 1.33 g. mg^{-1}), also compatible with obtained in factorial experiments (q_{exp}= 1.02 g. mg^{-1}).

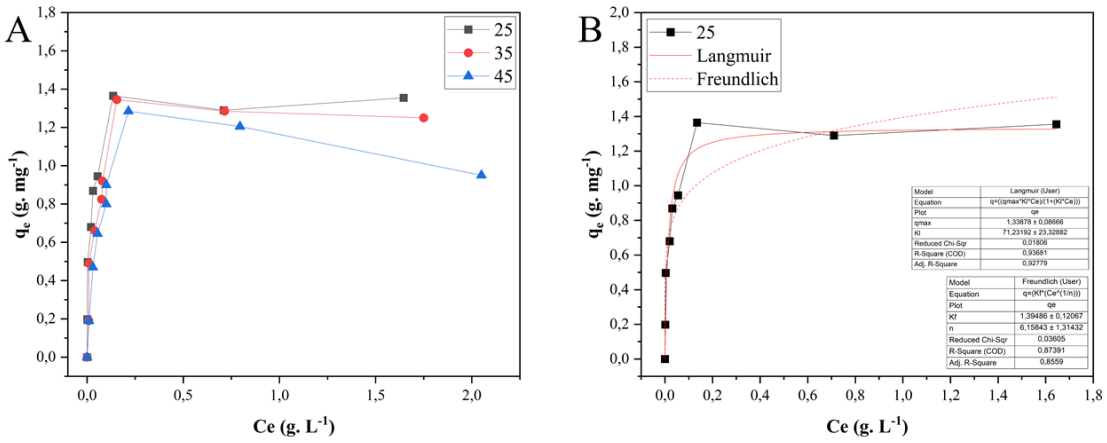

Figure 10. A) Adsorption isotherms (MNP-TANs) at 25° C, 35° C, and 45° C; B) Adsorption isotherm (MNP-TANs) at 25° C and isotherm models of Langmuir and Freundlich.

As for the thermodynamic parameters (Table 4), Gibbs Free Energy was negative for both adsorbents at all temperatures. Associated with positive enthalpy and negative entropy is possible to confirm spontaneous and favorable processes. The negative entropy indicates a reduction in the disorder of the system.

Table 4. Thermodynamic parameters of *Chlorella sp.* harvesting process by MNPs and MNP-TANs.

Nanoparticles	**ΔG°** **(kJ. mol^{-1})**	**ΔH°** **(kJ. mol^{-1})**	**ΔS°** **(kJ. mol^{-1})**
MNPs	25° C = -2.13 35° C = -2.24 45° C = -2.00	4.05	-0.00626
MNP-TANs	25° C = -0.93 35° C = -0.83 45° C = -0.33	9.73	-0.0291

3.6 Reuse of nanoparticles

The reuse of both nanoparticles was analyzed in optimal conditions. Despite the MNPs having shown a higher HE%= 86%, this was only maintained during 3 reuse cycles (Figure 11A), dropping to less than 60% after the seventh cycle. The sharp decrease in HE% of MNPs in the third reuse cycle may be related to the dissolution of naked particles by the action of acidic pH. Iron oxide nanoparticles are easily destabilized at low pH returning to ionic form, as mentioned before. The MNP-TANs sustained an HE%= 77% during 7 cycles, ending the last cycle with HE%≅ 61% (Figure 11B). Proper functionalization of nanoparticles can enhance the overall efficiency of the reuse process by increasing the adsorption capacity, reducing material loss, and minimizing the need for frequent particle regeneration (Tumbelaka *et al.*, 2022).

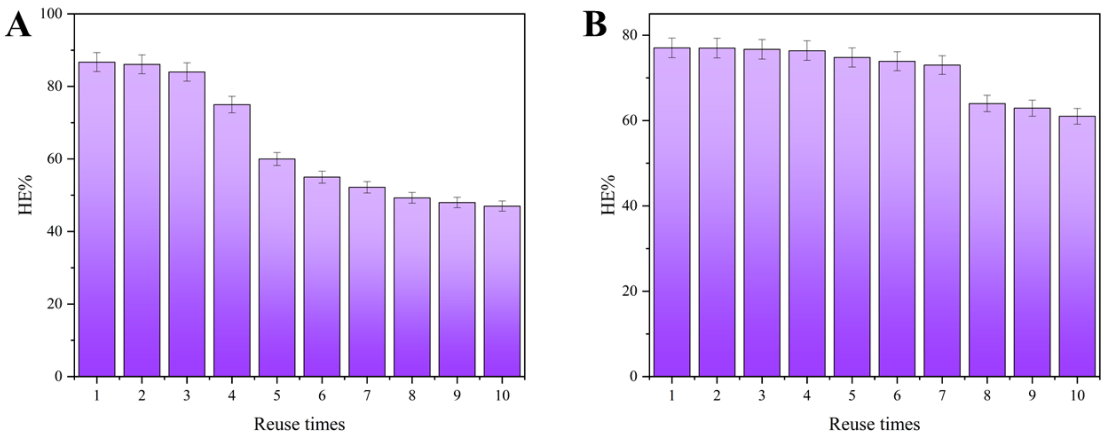

Figure 11.A) Reuse cycles of MNPs applied in *Chlorella sp.* biomass harvesting; B) Reuse cycles of MNP-TAN applied in *Chlorella sp.* biomass harvesting.

4. Conclusions

According to obtained results, it is possible to conclude that the nanoparticles derived from particulate matter are magnetite (Fe_3O_4) nanoparticles. Even after multiple washes and muffling, the nanoparticles still presented impurities. However, when applied to microalgae harvesting, they achieve HE%= 86% (MNPs concentration= 1,250 mg. L^{-1}; pH= 3). When functionalized with tannin, they predominantly exhibited intermolecular

interactions such as hydrogen bonding and dipole-dipole interactions. The functionalization made the particles less negatively charged, favoring their interaction with microalgae, especially at acidic pH (HE%= 77%; MNP-TANs [ ]= 1,100 mg/L; pH= 3.5) reducing the number of nanoparticles. Functionalization also contributed to particle stabilization increasing its reuse cycles from 3 to 7 cycles. At pH 10 (the final pH of the microalgae cultivation) both exhibited a similar HE% of 60%. These findings provide unpublished evidence that nanoparticles derived from particulate material, even without a high purity, can be efficiently applied to *Chlorella sp.* harvesting achieving satisfactory results during various application cycles.

5. References

AGÊNCIA NACIONAL DE MINERAÇÃO – ANM. **Brazilian mineral yearbook - main metallic substances**. [s.l: s.n.]. Disponível em: <www.anm.gov.br>.

ANDERSEN, R. A. **Algal Culturing Techniques**. [s.l: s.n.].

CARNINO, J. M.; LEE, H. Extracellular vesicles in respiratory disease. **Advances in Clinical Chemistry**, v. 108, p. 105–127, 1 jan. 2022.

CLEMONS, T. D.; KERR, R. H.; JOOS, A. Multifunctional Magnetic Nanoparticles: Design, Synthesis, and Biomedical Applications. **Comprehensive Nanoscience and Nanotechnology**, v. 1–5, p. 193–210, 1 jan. 2019.

Escória de Alto-Forno - ArcelorMittal Tubarão - Coprodutos - Produtos e Soluções - ArcelorMittal. Disponível em: <https://brasil.arcelormittal.com/produtos-solucoes/coprodutos/coprodutos/escoria-alto-forno>. Acesso em: 19 jun. 2023.

FU, Y.; HU, F.; LI, H.; CUI, L.; QIAN, G.; ZHANG, D.; XU, Y. Application and mechanisms of microalgae harvesting by magnetic nanoparticles (MNPs). **Separation and Purification Technology**, v. 265, p. 118519, 15 jun. 2021.

GALVÃO, E. S.; SANTOS, J. M.; REIS JUNIOR, N. C.; FERONI, R. DE C.; ORLANDO, M. T. D. The mineralogical composition of coarse and fine particulate material, their fate, and sources in an industrialized region of southeastern Brazil. **Environmental Monitoring and Assessment**, v. 194, n. 2, 1 fev. 2022.

GUERRIERO, E.; GUARNIERI, A.; MOSCA, S.; ROSSETTI, G.; ROTATORI, M. PCDD/Fs removal efficiency by electrostatic precipitator and wetfine scrubber in an iron ore sintering plant. **Journal of Hazardous Materials**, v. 172, n. 2–3, p. 1498–1504, 30 dez. 2009.

IBRAHIM, A.; YASER, A. Z.; LAMAMING, J. Synthesising tannin-based coagulants for water and wastewater application: A review. **Journal of Environmental Chemical Engineering**, v. 9, n. 1, p. 105007, 1 fev. 2021.

KEÇILI, R.; GHORBANI-BIDKORBEH, F.; DOLAK, İ.; CANPOLAT, G.; KARABÖRK, M.; HUSSAIN, C. M. Functionalized magnetic nanoparticles as powerful sorbents and stationary phases for the extraction and chromatographic applications. **TrAC Trends in Analytical Chemistry**, v. 143, p. 116380, 1 out. 2021.

KUFAREVA, I.; ABAGYAN, R. Methods of protein structure comparison. **Methods in molecular biology (Clifton, N.J.)**, v. 857, p. 231, 2012.

Lama de Alto Forno - ArcelorMittal Tubarão - Coprodutos - Produtos e Soluções - ArcelorMittal. Disponível em: <https://brasil.arcelormittal.com/produtos-solucoes/coprodutos/coprodutos/lama-alto-forno>. Acesso em: 19 jun. 2023.

LEE, K.; LEE, S. Y.; PRAVEENKUMAR, R.; KIM, B.; SEO, J. Y.; JEON, S. G.; NA, J. G.; PARK, J. Y.; KIM, D. M.; OH, Y. K. Repeated use of stable magnetic flocculant for efficient harvest of oleaginous Chlorella sp. **Bioresource Technology**, v. 167, p. 284–290, 1 set. 2014.

LI, X.; LIU, B.; LAO, Y.; WAN, P.; MAO, X.; CHEN, F. Efficient magnetic harvesting of microalgae enabled by surface-initiated formation of iron nanoparticles. **Chemical Engineering Journal**, v. 408, p. 127252, 15 mar. 2021.

LIMA BARIZÃO, A. C. DE; OLIVEIRA GOMES, L. E. DE; BRANDÃO, L. L.; SAMPAIO, I. C. F.; MOURA, I. V. L. DE; GONÇALVES, R. F.; OLIVEIRA, J. P. DE; CASSINI, S. T. Microalgae as tertiary wastewater treatment: Energy production, carbon neutrality, and high-value products. **Algal Research**, v. 72, p. 103113, 1 maio 2023.

MATA, T. M.; MARTINS, A. A.; CAETANO, N. S. Microalgae for biodiesel production and other applications: A review. **Renewable and Sustainable Energy Reviews**, v. 14, n. 1, p. 217–232, 1 jan. 2010.

MUNOZ, M.; PEDRO, Z. M. DE; CASAS, J. A.; RODRIGUEZ, J. J. Preparation of magnetite-based catalysts and their application in heterogeneous Fenton oxidation – A review. **Applied Catalysis B: Environmental**, v. 176–177, p. 249–265, 1 out. 2015.

NAJJAR, Y. S. H.; ABU-SHAMLEH, A. Harvesting of microalgae by centrifugation for biodiesel production: A review. **Algal Research**, v. 51, p. 102046, 1 out. 2020.

NASCIMENTO, R. F.; LIMA, A. C. A.; VIDAL, C. B.; MELO, D. Q.;; RAULINO, G. S. C. **Adsorption: Theoric aspects and environmental applications**. [s.l: s.n.].

OKORO, V.; AZIMOV, U.; MUNOZ, J.; HERNANDEZ, H. H.; PHAN, A. N. Microalgae cultivation and harvesting: Growth performance and use of flocculants - A review. **Renewable and Sustainable Energy Reviews**, v. 115, p. 109364, 1 nov. 2019.

QI, L.; HAN, T.; ZHANG, Y. Electrostatic precipitability of TiB2-Fe-Mo-Co ceramic-metal composites. **Journal of Alloys and Compounds**, v. 778, p. 507–513, 25 mar. 2019.

SALEH, T. A. Isotherm models of adsorption processes on adsorbents and nanoadsorbents. **Interface Science and Technology**, v. 34, p. 99–126, 1 jan. 2022.

SILVEIRA, C.; SHIMABUKU, L. Q.; FERNANDES, M. S.; BERGAMASCO, R. Iron-oxide Nanoparticles by Green Synthesis Method Using Moringa oleifera Leaf Extract for Fluoride Removal. **Environmental Technology**, v. 3330, n. August, p. 1–40, 2017.

TUMBELAKA, R. M.; ISTIQOMAH, N. I.; KATO, T.; OSHIMA, D.; SUHARYADI, E. High reusability of green-synthesized Fe3O4/TiO2 photocatalyst nanoparticles for efficient degradation of methylene blue dye. **Materials Today Communications**, v. 33, p. 104450, 1 dez. 2022.

UPADHYAY, K.; TAMRAKAR, R. K.; THOMAS, S.; KUMAR, M. Surface functionalized nanoparticles: A boon to biomedical science. **Chemico-Biological Interactions**, v. 380, p. 110537, 1 ago. 2023.

XU, P.; LI, J.; QIAN, J.; WANG, B.; LIU, J.; XU, R.; CHEN, P.; ZHOU, W. Recent advances in CO2 fixation by microalgae and its potential contribution to carbon neutrality. **Chemosphere**, v. 319, p. 137987, 1 abr. 2023.

YIN, S.; JIN, W.; ZHOU, X.; HAN, W.; GAO, S.; CHEN, C.; DING, W.; HE, Z.; CHEN, Y.; JIANG, G. Enhancing harvest of biodiesel-promising microalgae using Daphnia domesticated by amino acids. **Environmental Research**, v. 212, p. 113465, 1 set. 2022.

YUSUF, D.; DAVIS, A. M.; KLEYWEGT, G. J.; SCHMITT, S. An alternative method for the evaluation of docking performance: RSR vs RMSD. **Journal of Chemical Information and Modeling**, v. 48, n. 7, p. 1411–1422, 2008.

ZHAO, Y.; FAN, Q.; WANG, X.; JIANG, X.; JIAO, L.; LIANG, W. Application of Fe3O4 coated with modified plant polyphenol to harvest oleaginous microalgae. **Algal Research**, v. 38, p. 101417, 1 mar. 2019.

ZHAO, Z.; MUYLAERT, K.; VANKELECOM, I. F. J. Combining patterned membrane filtration and flocculation for economical microalgae harvesting. **Water Research**, v. 198, p. 117181, 15 jun. 2021.

3. CONCLUSIONS

This thesis concluded that the production of microalgae can yield both economic and environmental benefits throughout its production cycle. If cultivated in wastewater, these microorganisms can simultaneously enhance the quality of the effluent by incorporating nutrients, capturing high concentrations of CO2 during photosynthesis, and generating high-quality biomass rich in valuable biomolecules such as carotenoids, sterols, exopolysaccharides, and lipids. In light of these results, microalgae are a promising strategy for reducing the carbon footprint of wastewater treatment plants (WWTPs) by generating carbon credits through the reduction of greenhouse gas emissions and/or by producing bioproducts with lower climate impacts. However, to achieve this, it is necessary to make the harvesting stage feasible, which is the main limiting factor for scaling up production.

Another conclusion of this work is that the use of magnetic nanoparticles is an invaluable alternative to solve this problem by using nanoparticles with a reduced cost compared to the application of commercial nanoparticles. The use of magnetic nanoparticles from particulate material, applied for the first time for this purpose during this study, achieved harvesting efficiencies comparable to those obtained by laboratory-synthesized nanoparticles, which generally have high production costs. This is an interesting finding since the cost of the technique is no longer a limiting factor for its application. It was also possible to conclude that the use of tannin as a functionalizer for these nanoparticles was able to increase their stability, making them reusable for a greater number of cycles, in addition to maintaining the same removal efficiency. Nanoparticles functionalized with tannin from *Rhizophora mangle* reached HE% higher than those functionalized with commercial tannin, standing out as a promising alternative source of tannin to be explored.

In this way, these findings offer valuable insights for the development of more accessible and economically viable techniques for large-scale microalgae biomass harvesting. Optimal utilization of this particulate material can serve as an economically efficient solution while embracing a circular perspective by reintegrating it into the system. Nonetheless, further studies and pilot-scale applications are necessary to validate and refine these approaches on an industrial scale.

4. REFERENCES

AHMAD, A.; ASHRAF, S. S. Sustainable food and feed sources from microalgae: Food security and the circular bioeconomy. **Algal Research**, p. 103185, 30 jun. 2023.

CHEN, J.; DAI, L.; MATAYA, D.; COBB, K.; CHEN, P.; RUAN, R. Enhanced sustainable integration of CO2 utilization and wastewater treatment using microalgae in circular economy concept. **Bioresource Technology**, v. 366, p. 128188, 1 dez. 2022.

DAI, D.; QV, M.; LIU, D.; TANG, C.; WANG, W.; WU, Q.; YIN, Z.; ZHU, L. Structural insights into mechanisms of rapid harvesting of microalgae with pH regulation by magnetic chitosan composites: A study based on E-DLVO model and component fluorescence analysis. **Chemical Engineering Journal**, v. 456, p. 141071, 15 jan. 2023.

DEVI, A.; VERMA, M.; SARATALE, G. D.; SARATALE, R. G.; FERREIRA, L. F. R.; MULLA, S. I.; BHARAGAVA, R. N. Microalgae: A green eco-friendly agents for bioremediation of tannery wastewater with simultaneous production of value-added products. **Chemosphere**, v. 336, p. 139192, 1 set. 2023.

LI, P.; HUANG, Y.; XIA, A.; ZHU, XIANQING; ZHU, XUN; LIAO, Q. Bio-Decarbonization by Microalgae: A Comprehensive Analysis of CO2 Transport in Photo-Bioreactor. **De Carbon**, p. 100016, 14 jun. 2023.

LIMA BARIZÃO, A. C. DE; OLIVEIRA, J. P. DE; GONÇALVES, R. F.; CASSINI, S. T. Nanomagnetic approach applied to microalgae biomass harvesting: advances, gaps, and perspectives. **Environmental science and pollution research international**, v. 28, n. 33, p. 44795–44811, 1 set. 2021.

PARAMESWARI., R. P.; LAKSHMI, T. Microalgae as a potential therapeutic drug candidate for neurodegenerative diseases. **Journal of Biotechnology**, v. 358, p. 128–139, 10 nov. 2022.

RAZZAK, S. A.; LUCKY, R. A.; HOSSAIN, M. M.; DELASA, H. Valorization of Microalgae Biomass to Biofuel Production: A review. **Energy Nexus**, v. 7, p. 100139, 1 set. 2022.

ZHENG, Y.; ROBERTS, M.; KELLY, J.; ZHANG, N.; WALKER, T. Harvesting microalgae using the temperature-activated phase transition of thermoresponsive polymers. **Algal Research,** v. 11, p. 90–94, 1 set. 2015.

ZHUANG, D.; HE, N.; KHOO, K. S.; NG, E. P.; CHEW, K. W.; LING, T. C. Application progress of bioactive compounds in microalgae on pharmaceutical and cosmetics. **Chemosphere**, v. 291, p. 132932, 1 mar. 2022.

APPENDIX I

Table 1. ANOVA table from fractional factorial.

Factor	SS	df	MS	F	p
Microalgae [ ]	63,28	1	63,281	0,32016	0,576556
MNP-TNs [ ]	993,84	1	993,837	5,02812	0,034051
pH	4425,84	1	4425,837	22,39165	0,000075
Temperature	1,00	1	1,003	0,00508	0,943764
Agitation	111,25	1	111,253	0,56286	0,460111
Contact time	823,50	1	823,503	4,16635	0,051924
Error	4941,39	25	197,656		
Total SS	11360,11	31			

Table 2. ANOVA table from full factorial.

Factor	SS	df	MS	F	p
pH (L)	2904,000	1	2904,000	122,9364	0,000004
pH (Q)	1930,305	1	1930,305	81,7165	0,000018
MNP-TNs [ ] (L)	7,407	1	7,407	0,3136	0,590822
MNP-TNs [ ] (Q)	218,601	1	218,601	9,2541	0,016013
Error	188,976	8	23,622		
Total SS	**5035,145**	**12**			

APPENDIX II

Table 1. ANOVA table from full factorial (MNPs).

Factor	**SS**	**df**	**MS**	**F**	**p**
pH (L)	1310,296	1	1310,296	17,93734	0,002856
pH (Q)	0,003	1	0,003	0,00004	0,994814
MNPs [ ] (L)	439,185	1	439,185	6,01224	0,039813
MNPs [ ] (Q)	544,003	1	544,003	7,44715	0,025888
Error	584,388	8	73,049		
Total SS	**2971,419**	**12**			

Table 2. ANOVA table from full factorial (MNP-TANs).

Factor	SS	df	MS	F	p
pH (L)	390,4267	1	390,4267	21,66062	0,001636
pH (Q)	63,2083	1	63,2083	3,50676	0,098009
MNP-TANs [ ] (L)	160,8563	1	160,8563	8,92420	0,017404
MNP-TANs [ ] (Q)	50,6589	1	50,6589	2,81052	0,132173
Error	144,1978	8	180247		
Total SS	**778,2455**	**12**			

APPENDIX III

Article publication status

Chapter 1: published in the Algal Research Journal (FI= 5.276). Title: Microalgae as tertiary wastewater treatment: Energy production, carbon neutrality, and high-value products; **Algal Research**, Vol. 72, Page 103113 (2023). DOI: https://doi.org/10.1016/j.algal.2023.103113.).a

Chapter 2: published in the Environmental Science and Pollution Research (FI=5.190). Title: Nanomagnetic approach applied to microalgae biomass harvesting: advances, gaps, and perspectives; **Environmental Science and Pollution Research**, Vol. 28, Pages 44795 (2021). DOI: https://doi.org/10.1007/s11356-021-15260-z.).

Chapter 3: selecting suitable scientific journals for submission.

Chapter 4: selecting suitable scientific journals for submission.